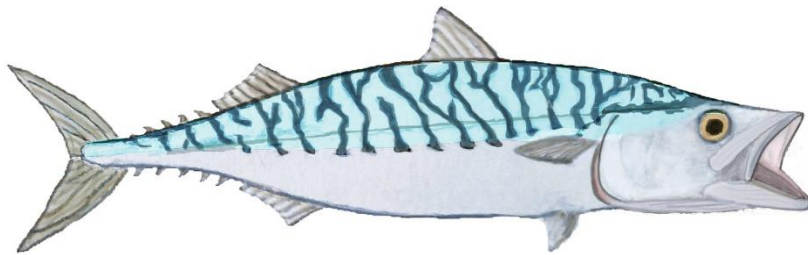


Modelling the switch between bite-feeding and filter-feeding in planktivorous fishes



Ingunn Torunnsdatter Stautland
Master of Science in Marine Biology



Department of Biological Sciences
University of Bergen

November 2019

ACKNOWLEDGEMENTS

First of all, I want to thank my supervisors Anders Frugård Opdal and Øyvind Fiksen, who have encouraged me so much and always been available for advice. Thank you for the kind support, guidance and inspiring conversations. It has been a very positive learning experience to collaborate with you.

I will also thank my fellow students for all the care, interesting discussions and fun moments. It has been so nice to get to know you, and I wish you all the best.

Last but not least, I want to thank my parents, who have always been there for me.

ABSTRACT

Many planktivorous fishes are known to switch between feeding modes in response to changing environmental conditions. According to optimal foraging theory, the preferred strategy is the one that gives the highest net energy return. Experiments report that increasing prey density and decreasing light level and prey size encourage fish to switch from visual-based bite-feeding to filter-feeding. Still, few attempts have been made to formulate combined models for bite- and filter-feeding to investigate the mechanisms regulating switching. A mechanistic, individual-based model that compares net intake rate of the alternative strategies in a multi-prey system is here proposed, and the model is parametrised for two different scenarios: 1) Atlantic mackerel (*Scomber scombrus*) feeding in the Norwegian Sea and 2) pilchard (*Sardinops sagax*) feeding in experimental tanks. Bite-feeding is more efficient at low prey densities, but the fish is predicted to switch strategy when prey density reaches above the level where filter-feeding becomes more profitable than bite-feeding, which is limited by prey handling time. Switching occurs at lower prey density if vision is reduced by low irradiance. Interestingly, increasing the proportion of large prey will benefit filter-feeding more than bite-feeding unless the prey is too evasive. Since bite-feeding fish only accept the most profitable prey, while filtration efficiency for this prey usually is low, overall diet composition and predation pressure on different prey-types vary depending on the time allocated to each feeding mode. Modelling switching dynamics is therefore important to improve our understanding of how planktivorous fishes structure prey communities.

TABLE OF CONTENTS

1 Introduction	7
2 Methods	10
2.1 Model components	16
2.2 The bite-feeding submodel	12
2.2.1 Search rate.....	12
2.2.2 Visual range.....	13
2.2.3 Encounter rate.....	15
2.2.4 Clearance rate and absolute energy intake.....	15
2.2.5 Metabolic rate and net energy intake.....	16
2.2.6 Optimal swimming speed.....	18
2.2.7 Selectivity and optimal diet breadth.....	19
2.3 The filter-feeding submodel	20
2.3.1 Filtration efficiency.....	21
2.3.2 Fraction of time spent filtering.....	22
2.3.3 Buccal flow velocity.....	22
2.3.4 Retention efficiency.....	22
2.3.5 Evasiveness of prey.....	23
2.3.6 Clearance rate and absolute energy intake.....	23
2.3.7 Metabolic rate and net energy intake.....	24
2.3.8 Optimal swimming speed.....	25
2.4 Model applications	26
2.4.1 Atlantic mackerel feeding in the Norwegian Sea.....	26
2.4.2 Pilchard feeding in experimental tanks.....	26
2.5 Sensitivity analysis	27
3 Results and discussion	28
3.1 Atlantic mackerel feeding in the Norwegian Sea	28
3.1.1 Effects of prey density and light on switching.....	28
3.1.2 Effects of prey composition on switching.....	29
3.1.3 Switching influences diet composition.....	32
3.2 Pilchard feeding in experimental tanks	34
3.2.1 Comparison of predicted and observed prey density in feeding trials.....	35

3.2.2 Comparison of predicted and observed swimming speed in feeding trials.....	37
3.3 Sensitivity analysis.....	40
4 Conclusions.....	42
References.....	43
Appendix 1 – MATLAB code for simulation of mackerel foraging.....	47
Appendix 2 – MATLAB code for simulation of pilchard foraging.....	61
Appendix 3 – References MATLAB scripts.....	77

1 INTRODUCTION

To switch or not to switch, that is the question that planktivorous fishes are continually asked, and the answer is of key importance to their own success in life as well as the survival prospects of their potential food. Many mid-trophic species of pelagic fish are able to switch adaptively between bite-feeding and filter-feeding as environmental conditions change (Lazzaro, 1987; van der Lingen, 1994). Such flexibility in feeding behaviour allows them to exploit a wide range of food resources in environments characterised by spatial and temporal variability in light regime and prey density and composition. When fish forage by bite-feeding, they pursue individual prey items that they have detected visually and singled out to capture (Macy, Sutherland and Durbin, 1998). When ram filter-feeding, they swim with their mouth agape to force water through the oral cavity, extracting plankton from the water in the process (Sanderson, S. L., Cech, J. J., Cheer, 1994). The relative profitability of each of these feeding modes varies with the external environment, and the one that results in the highest net energy gain in a given instance is expected to be the preferred strategy (Crowder, 1985). In this study, I have explored some of the underlying mechanisms regulating the switch in feeding mode.

One of the main differences between bite- and filter-feeding is how the intake rate responds to changes in prey density. As prey availability increases, bite-feeding fish will spend more time pursuing and catching prey, which means that less time is left to search for new prey (Holling, 1959; Aksnes and Giske, 1993). The intake rate of bite-feeding is therefore not proportional to prey density. Instead, the rate of increase declines until the curve reaches an asymptote at high prey densities (Fig. 1). When saturated with prey, bite-feeding fish will spend all their time handling encountered prey. Thus, bite-feeding conforms to the Type II functional response described by Holling (1959). In contrast, the intake rate of filter-feeding increases linearly with prey density, assuming that the fish do not satiate at the range of prey densities normally occurring in their natural environment (Pepin, Koslow and Pearre Jr., 1988; Macy, Sutherland and Durbin, 1998). Filter-feeding thus conforms to Holling's Type I functional response (Fig. 1, Holling, 1959).

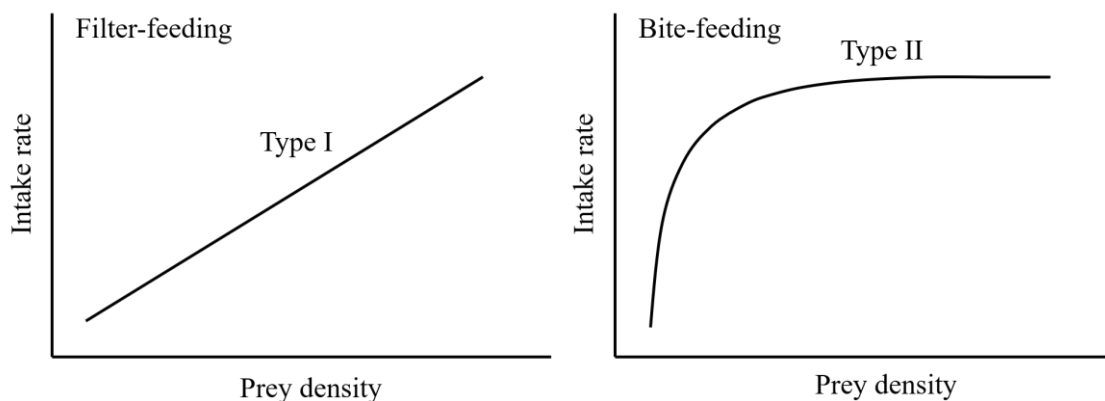


Fig. 1. Functional responses characterising the feeding modes. The intake rate from filter-feeding increases linearly with prey density (Type I functional response), whereas for bite-feeding the intake rate levels off at higher prey densities (Type II functional response).

Numerous experimental studies investigating the switching response have been conducted, and they generally report that the fish shift from bite- to filter-feeding when prey density exceeds some threshold level, or when prey-size relative to the predator is sufficiently reduced (Leong and O'Connell, 1969; O'Connell, 1972; O'Connell and Zweifel, 1972; Janssen, 1976; Gibson and Ezzi, 1985, 1992; Pepin, Koslow and Pearre Jr., 1988; James and Findlay, 1989; van der Lingen, 1994; Garrido *et al.*, 2007). Experimental studies testing the behavioural effect of changing light intensity have documented that filter-feeding becomes more common with decreasing light level (Holanov and Tash, 1978; Batty, Blaxter and Libby, 1986; Batty, Blaxter and Richard, 1990; Macy, Sutherland and Durbin, 1998). Members of the same school have been found to display some individual variation in feeding response, and the switch in strategy may also involve a transitional phase that represents an intermediate between the two distinct feeding modes (Janssen, 1976).

Crowder (1985) proposed that the choice of feeding behaviour could be predicted based on cost-benefit analyses. He demonstrated that in several experimental studies, feeding mode shifts occurred at approximately the prey densities or sizes where the two modes yielded equal energetic return per unit time (Leong and O'Connell, 1969; O'Connell, 1972; O'Connell and Zweifel, 1972; Janssen, 1976; Crowder and Binkowski, 1983; Crowder, 1985). This line of reasoning corresponds with the evolutionary logic of optimal foraging theory, which maintains that if a population exhibits variation in heritable behavioural traits influencing foraging success, traits that enhance fitness through optimisation of energy acquisition should be selected for (Emlen, 1966; MacArthur and Pianka, 1966; Pyke, 1984). It does however not imply that organisms are optimal, only that adaptive behaviours can be predicted based on optimality analyses that also consider constraints and trade-off dilemmas (Stearns and Schmid-Hempel, 2006).

Little effort has so far been made to combine formulations of bite- and filter-feeding into one coherent mechanistic model, but a few models have been developed that compare the profitability of the alternative feeding modes at varying prey densities (Crowder, 1985; Hoogenboezem *et al.*, 1992; Lovvorn, Baduini and Hunt, 2001). Of these, the model of underwater feeding in shearwaters by Lovvorn *et al.* (2001) is the most advanced, which also examines the effect of light on foraging success. Currently, no attempts have been made to formulate unified models for bite- and filter-feeding in multi-prey systems, where variations in prey composition influence feeding behaviour. Nor do existing models treat bioenergetics associated with swimming kinematics and filtering mechanics or identify optimal swimming speeds.

In this study, I have developed a mechanistic model that describes how fish capable of both bite- and filter-feeding switch strategy in response to changing environmental factors. The model explores how multiple influences and behavioural adjustments interact to determine the relative profitability of the alternative strategies when faced with different prey assemblages and light conditions. Key factors considered here are swimming behaviour, handling time, catchability, predator-prey size ratio, selectivity, filtration efficiency and energetic costs. The main objective is to improve our understanding of the processes regulating the pattern of switching observed among planktivorous fishes. The model is individual-based and deterministic, and following the example by Lovvorn *et al.* (2001), it consists of two submodels that calculate the intake rate from bite-feeding and filter-feeding, respectively. The fish feeds on a mixture of prey-types, and the effects of changing the three principal parameters ambient irradiance, total prey density and relative density of different prey-types are tested. Besides switching, two other behavioural responses intended to optimise foraging are also considered: Swimming speed is optimised for the varying conditions, and the bite-feeding fish chooses selectively the most profitable of the available prey.

To determine which feeding mode the fish will employ under different conditions, I have adhered to the optimality principle that the preferred strategy is the one that entails the greatest fitness advantage in terms of highest net specific energy intake per unit time (Crowder, 1985). This measure of fitness considers both the benefits (energy gained from food consumption) and costs (energy expended in metabolism) of the alternative strategies, and the feeding mode that maximises the difference between these represents the optimal solution. The model is intended to be generally applicable to all fishes capable of switching. In this study, the model has been parameterised to represent two different scenarios: 1) Atlantic mackerel (*Scomber scombrus*) feeding in the Norwegian Sea during summer and 2) pilchard (*Sardinops sagax*) feeding in closed tanks in experimental trials. The simulation of the field situation (1) is independent of time, while the simulation of feeding experiments (2) runs in time-steps. To evaluate the behaviour of the model, predictions are compared with data from real systems.

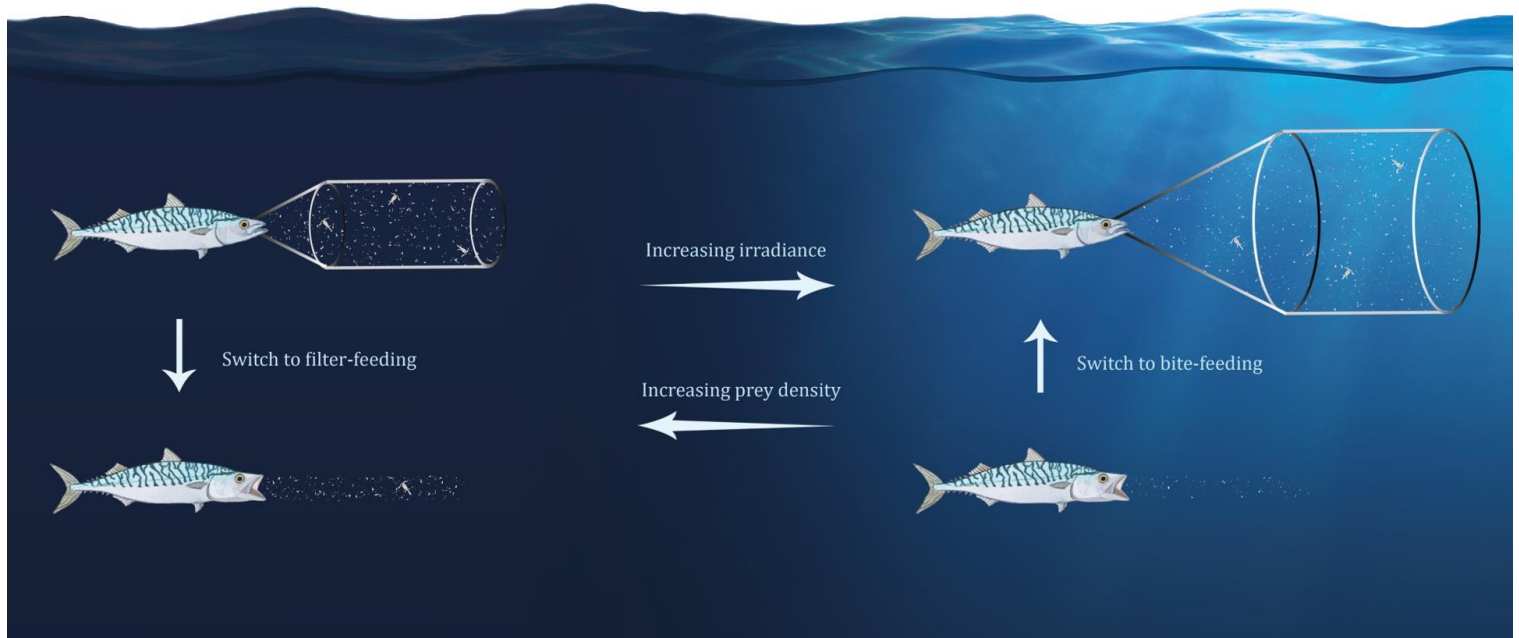


Fig. 2. Conceptual representation of the system. The fish is expected to switch from bite- to filter-feeding if the prey density increases above a threshold level, or if the irradiance decreases enough to reverse the advantage of visual predation.

2 METHODS

Net intake rates are calculated in two submodels—one for bite-feeding and one for filter-feeding. Both submodels are run under varying environmental conditions, and the fish switches strategy when the other feeding mode becomes more profitable than the one currently used. Simulations were performed in MATLAB (versions R2018b and R2019a). Complete scripts are provided as supplementary material (Appendix 1-2), where more detailed information about the model structure can be found.

2.1 MODEL COMPONENTS

Foraging efficiency depends on various predator and prey attributes as well as many environmental parameters, notably prey density and light intensity, that are beyond any direct control by the fish (Table 1). What the fish can control to some extent, though, is its behavioural responses to external influences. It can switch to the alternative feeding mode should it become more favourable, but it can also regulate its swimming speed and pattern to optimise the balance between consumption and metabolic investment. When bite-feeding, it can besides choose selectively among available prey-types. Such modifications influence the relative profitability of each feeding mode and thereby also the switching dynamic, and they are therefore accounted for in the model. Other behavioural adjustments like predator avoidance, school formation and partitioning of resources among competitors can also be important, but these factors are not part of the model.

Table 1. Some factors that determine the intake rate from aquatic feeding. The main focus is on the parameters that are highlighted, while the ones in grey are not included in the model.

Environmental factors	Behavioural factors	Predator and prey characteristics
Prey density	Feeding mode	Size
Prey composition	Swimming speed	Filtration efficiency
Light regime	Selectivity	Visibility of prey
Temperature	Schooling	Capture probability
Turbulence	When to feed	Handling time
Topography	Where to feed	Energy content of prey
Predation risk	Predator avoidance	Digestibility of prey
Competition	Niche segregation	Stomach capacity

Some of the model components are common to both submodels, whereas others are specific to either of them. An overview of all the parameters is given below (Table 2).

Table 2. Explanation of parameters used in models of bite-feeding and filter-feeding.

Symbol	Description	Unit
A_g	Gape area of fish mouth	m^2
A_p	Prey area	m^2
A_{pr}	Prey image area at retina	m^2
a_f	Activity multiplier for filter-feeding (increases the metabolic rate)	dimensionless
a_h	Activity multiplier for prey handling (increases the metabolic rate)	dimensionless
B_v	Ratio of buccal flow speed to swimming speed of fish	dimensionless
C_0	Inherent contrast of prey	dimensionless
C_r	Prey image contrast at retina	dimensionless
c	Beam attenuation coefficient	m^{-1}
E'	Visual capacity of fish (equal to $E_{max}/\Delta S_e$)	dimensionless
E_0	Irradiance just beneath water surface	$\mu E m^{-2} s^{-1}$
E_b	Background irradiance intercepted by eye lens of fish	$\mu E m^{-2} s^{-1}$
E_z	Irradiance at depth z	$\mu E m^{-2} s^{-1}$
E_{max}	Maximum processable irradiance at fish retina	$\mu E m^{-2} s^{-1}$
e_b	Rate that bite-feeding fish encounters prey	$ind. s^{-1}$
eg	Proportion of ingested energy egested by the fish (not assimilated)	dimensionless
ex	Proportion of assimilated energy excreted by the fish	dimensionless
F_b	Bite-feeding clearance rate (volume cleared for prey per unit time)	$m^3 s^{-1}$
F_f	Filter-feeding clearance rate (volume cleared for prey per unit time)	$m^3 s^{-1}$
f_i	Fraction of total filter-feeding time that fish filters prey	dimensionless
H	Handling time when capture probability P_c is 1	$s ind.^{-1}$
h	Prey-specific handling time (equal to H/P_c)	$s ind.^{-1}$
I_b	Absolute intake rate of bite-feeding	$J s^{-1}$
I_f	Absolute intake rate of filter-feeding	$J s^{-1}$
K	Coefficient for attenuation of diffuse light	m^{-1}
k_e	Half saturation constant of light processing (irradiance at fish eye lens where the retinal irradiance is half the maximum processable level)	$\mu E m^{-2} s^{-1}$
k_l	Prey length for which retention efficiency is half the maximum level	m
L	Fish length	m
l	Prey length	m
M_r	Routine metabolic rate of non-feeding fish	$J h^{-1} g^{-1}$
M_b	Metabolic rate of bite-feeding fish	$J h^{-1} g^{-1}$
M_h	Metabolic rate of fish handling prey	$J h^{-1} g^{-1}$
M_s	Metabolic rate of fish searching for prey	$J h^{-1} g^{-1}$
M_f	Metabolic rate of filter-feeding fish	$J h^{-1} g^{-1}$
N_{tot}	Total prey density	$ind. m^{-3}$
Npf	Net profitability of prey (net energy gained per handling time)	$J h^{-1} g^{-1}$
p	Proportion of prey-type to total prey density	dimensionless
P_c	Capture probability (proportion of attacked prey that the fish captures)	dimensionless
P_e	Probability that a prey will enter the oral cavity instead of escaping	dimensionless
Pf	Profitability of prey (energy gained per handling time)	$J s^{-1}$
Q_{ox}	Oxycalorific coefficient	$J (g O_2)^{-1}$
R	Visual range of fish (maximum prey detection distance)	m
r	Retention efficiency (proportion of prey retained in the oral cavity)	dimensionless
r_{max}	Maximum retention efficiency	dimensionless
s	Selectivity (proportion of encountered prey that the fish will try to capture)	dimensionless
ΔS_e	Sensitivity threshold for detection of change in irradiance at fish eye lens	$\mu E m^{-2} s^{-1}$
ΔS_r	Sensitivity threshold for detection of change in radiant flux at fish retina	$\mu E m^{-2} s^{-1}$
sda	Proportion of assimilated energy that the fish spends in processing food (specific dynamic action)	dimensionless
T	Ambient temperature	$^{\circ}C$
t_s	Time spent searching for prey	s
t_h	Time spent handling prey	s
t_{tot}	Total time spent bite-feeding	s
U	Swimming speed of fish	$m s^{-1}$

u	Proportion of ingested energy made available for use	dimensionless
v_b	Swimming speed of bite-feeding fish	m s^{-1}
v_f	Swimming speed of filter-feeding fish	m s^{-1}
v_h	Swimming speed of fish handling prey	m s^{-1}
v_r	Routine swimming speed of fish	m s^{-1}
v_s	Swimming speed of fish searching for prey	m s^{-1}
W	Wet weight of fish	g
w	Wet weight of individual prey	g ind.^{-1}
z	Depth	m
α	Intercept of metabolic function	$\text{g O}_2 \text{ day}^{-1} \text{ g}^{-1}$
β	Search rate of fish	$\text{m}^3 \text{ s}^{-1}$
δ	Coefficient for weight dependence in metabolic function	dimensionless
ε_b	Net weight-specific intake rate of bite-feeding	$\text{J h}^{-1} \text{ g}^{-1}$
ε_f	Net weight-specific intake rate of filter-feeding	$\text{J h}^{-1} \text{ g}^{-1}$
θ	Half angle of the fish's visual field	degrees
ν	Coefficient for temperature dependence in metabolic function	$^{\circ}\text{C}^{-1}$
ρ	Coefficient for swimming speed dependence in metabolic function	s m^{-1}
δ	Energy density of prey	J g^{-1}

2.2 THE BITE-FEEDING SUBMODEL

The efficiency of bite-feeding is determined by ambient irradiance (E_z , $\mu\text{E m}^{-2} \text{ s}^{-1}$), swimming speed (v_b , m s^{-1}) and visual capacity (E') of the predator, density (N_{tot} , ind. m^{-3}) and visibility of prey, predator-prey size ratio, capture probability (P_c) and the time needed to handle each prey (h , s ind^{-1}) (Aksnes and Giske, 1993; Varpe and Fiksen, 2010; Van Deurs, Jørgensen and Fiksen, 2015). The bite-feeding process comprises two main phases: a search phase where the predator actively seeks out potential prey using vision, and a handling phase where the fish attempts to capture and eat individual prey it has sighted and decided to pursue. The total time spent bite-feeding (t_{tot} , s) is therefore the sum of the time spent searching for prey (t_s , s) and the time allocated to prey handling (t_h , s):

$$t_{\text{tot}} = t_s + t_h \quad (1)$$

2.2.1 Search rate

For fish searching for prey in the pelagic realm, the visual field can be represented as a spherical sector with radius equal to the visual range (Eggers, 1977; Aksnes and Giske, 1993). The radius of the base of the spherical cap (the cone base) is thus the opposite cathetus to the half angle of the visual field (Fig. 3). The area of the cone base is also the plane area of the cylindrical volume that the fish searches through (Eggers, 1977). The volume that is scanned for prey per unit search time (β , $\text{m}^3 \text{ s}^{-1}$) is then given by the following equation (Aksnes and Giske, 1993; Huse and Fiksen, 2010):

$$\beta = v_s \pi (R \sin \theta)^2 \quad (2)$$

where v_s is the swimming speed of the fish searching for prey (m s^{-1}), R is the maximum distance from which prey can be detected (m) and θ is the half angle of the visual field (degrees). The expression $\pi(R \sin \theta)^2$ is the plane area (m^2) of the search volume, while v_s corresponds to the length of the cylindrical volume searched per unit time (m s^{-1}) (Eggers, 1977; Aksnes and Giske, 1993). The fact that the search rate increases with the square of the visual range means that light conditions greatly influence the efficiency of aquatic visual predation (Fig. 3).

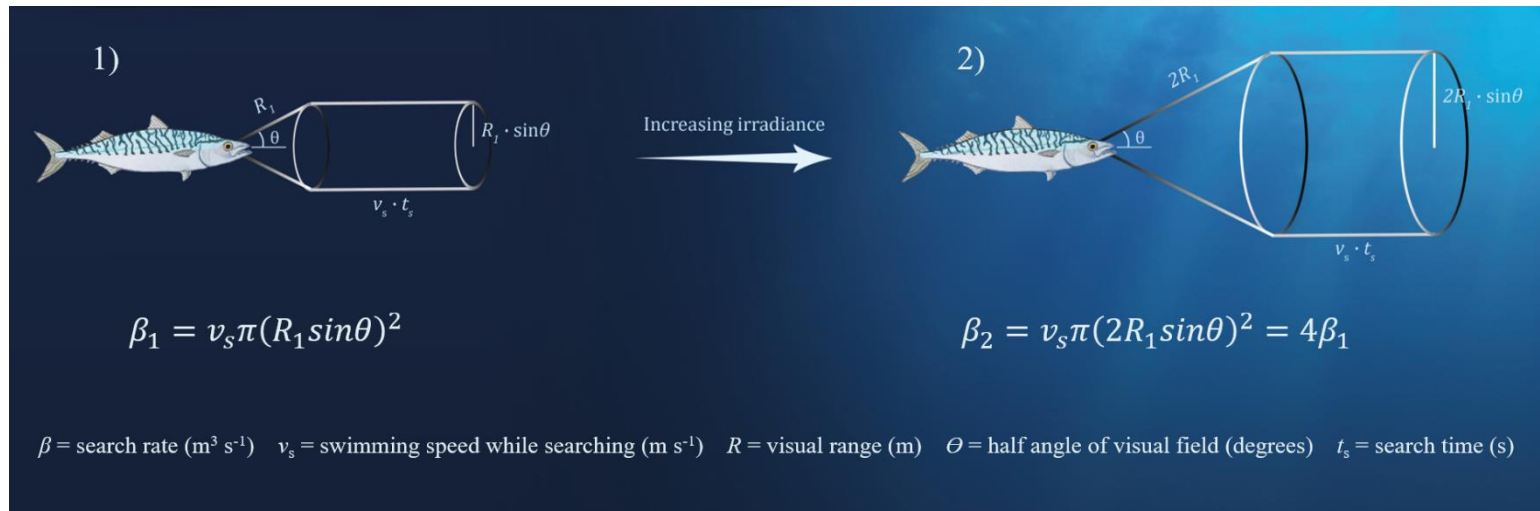


Fig. 3. The search rate β of the bite-feeding fish increases with the square of the visual range R . If the visual range doubles (situation 2), the search rate quadruples.

2.2.2 Visual range

The visual range depends on the optical environment and the visual capacity of the fish as well as prey characteristics that affect its visibility (Aksnes and Giske, 1993; Aksnes and Utne, 1997). Larger-sized prey project a larger image on the fish retina, which means that the minimum image size necessary for detection can be obtained from a greater distance. The inherent contrast of the prey (C_0) is the difference in radiance between the prey and the background, where brighter backgrounds require larger differences for a given contrast (Hester, 1968). The visual system can only discern a prey if the difference at the retina between the radiant flux conveying the prey image and the radiant flux from the background alone exceeds some threshold level (Aksnes and Giske, 1993).

In their model of aquatic visual feeding, Aksnes and Giske (1993) showed that the change in rate of photons reaching the retina can be expressed as the product of the background irradiance (E_b , $\mu\text{E m}^{-2} \text{s}^{-1}$), the prey image contrast (C_r) and the area of the prey image (A_{pr} , m^2), all as they appear at the retina. However, the neural response to changes in radiant flux is not proportional to the intensity of the incident light (Aksnes and Utne, 1997). Instead, due to various signal modifications and adaptive responses that moderate the absorption of light energy by receptors, the neural activity increases in a saturating fashion towards an asymptotic value at high irradiance levels. Increasing the light intensity above the maximum level that can be processed will therefore have no further effect on the neural activity. By including a saturation parameter that accounts for this non-linear response, Aksnes and Utne (1997) modified the model by Aksnes and Giske (1993) to arrive at following criterion for prey detection in fish:

$$|C_r|A_{pr} \left[E_{\max} \frac{E_b}{k_e + E_b} \right] \geq \Delta S_r \quad (3)$$

where E_{\max} is the maximum processable irradiance at retina ($\mu\text{E m}^{-2} \text{s}^{-1}$), k_e is the half-saturation constant (the irradiance at the eye lens where the retinal irradiance is at half the maximum processable level) ($\mu\text{E m}^{-2} \text{s}^{-1}$) and ΔS_r is the sensitivity threshold for detection of differences in radiant flux received by the retina ($\mu\text{E m}^{-2} \text{s}^{-1}$) (Aksnes and Utne, 1997). E_{\max} tends to increase with the size of the fish (Lovvorn, Baduini and Hunt, 2001; Breck and Gitter, 2008).

Light that strikes the ocean surface will be modified by absorption and scattering by water molecules and different dissolved and suspended particles along its path through the water. As a consequence, the downwelling light decreases exponentially with depth (Fig. 4).

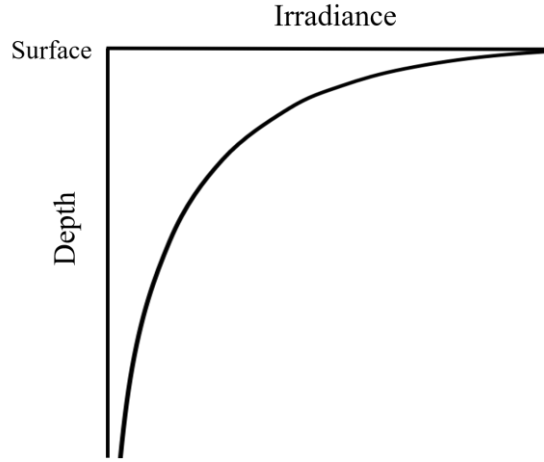


Fig. 4. Attenuation of downwelling irradiance with water depth. Light decreases more rapidly near the surface.

Beer's Law gives a quantitative description of the attenuation process:

$$E_z = E_0 e^{-Kz} \quad (4)$$

where E_z is the irradiance ($\mu\text{E m}^{-2} \text{s}^{-1}$) at a given depth (z , m), E_0 is the irradiance just beneath the water surface ($\mu\text{E m}^{-2} \text{s}^{-1}$) and K is the coefficient for attenuation of diffuse light (m^{-1}). Different wavelengths are attenuated at different rates, and the spectral composition of light consequently changes with depth.

The image transmitting ability of the light will also decrease due to beam attenuation processes (Aksnes and Giske, 1993). Accounting for these modifications, the criterion for prey detection (Eq. 3) can be translated into one that considers changes in irradiance at the eye lens when the prey is situated at a given distance away (Aksnes and Giske, 1993; Aksnes and Utne, 1997). The maximum distance R at which a prey can be detected is where the change in irradiance is equal to the sensitivity threshold:

$$R^{-2} e^{-cR} |C_0| A_p \left[E_{\max} \frac{E_z}{k_e + E_z} \right] = \Delta S_e \quad (5a)$$

or

$$R^2 e^{cR} = |C_0| A_p E' \left[\frac{E_z}{k_e + E_z} \right] \quad (5b)$$

where c is the beam attenuation coefficient (m^{-1}), C_0 is the inherent prey contrast (dimensionless), A_p is the prey area (m^2), ΔS_e is the sensitivity threshold for detection of differences in light intensity at the eye lens ($\mu\text{E m}^{-2} \text{s}^{-1}$) and E' represents the visual capacity of the fish as a dimensionless composite parameter equal to $E_{\max}/\Delta S_e$. To determine the visual range for a certain prey-type at known light conditions, Eq. 5b is solved iteratively by use of the Newton-Raphson method (Aksnes and Utne, 1997).

2.2.3 Encounter rate

Via the search rate β , the swimming speed v_s and the visual range R determine the number of prey of a given density that the fish encounters per unit time spent searching. However, to get the full picture, the time allocated to searching versus prey handling must be taken into account. As more prey are encountered, more prey must also be handled, which requires time. Hence, less time is left for searching. When the fraction of time spent handling prey becomes sufficiently high, the encounter rate no longer increases with further increase in prey density. To estimate the overall encounter rate for bite-feeding, i.e. the number of prey encountered per total time (e_b , ind. s^{-1}), the encounter rate for the search phase must be multiplied with the fraction that the search time (t_s , s) takes of the total time (t_{tot} , s):

$$e_b = \frac{t_s}{t_{tot}} N_{tot} \sum_{i=1}^n p_i \beta_i \quad (6a)$$

where n is the number of available prey-types (i), N_{tot} is the total prey density (ind. m^{-3}) and p_i is the proportion of prey-type i to total prey density. The indexed parameters are specific for prey-type i , and the weighted mean search rate β ($m^3 s^{-1}$) for all prey combined is calculated based on the proportion of each prey-type. N_{tot} corresponds to the density of prey from all prey-types included in the diet when it is at its broadest. A prey-type may be one or more taxonomic groups or different stages or size classes within groups.

Due to time restrictions, not all of the encountered prey are handled. When the fish discovers a potential prey item, it has to decide whether it should try to capture it or instead use the time to search for more profitable prey (Charnov, 2002). As the handling time becomes more limiting and the supply of prey to choose from increases, the fish should become ever more selective (Krebs *et al.*, 1977). Explicit criteria for prey selection will be derived in a later section, but for now the main point is that the fish only spends time on prey it has selected, and the time is spent whether or not it succeeds in capturing the prey. To determine the fraction of the total time that is spent searching, the denominator of the Holling disc equation can be modified by introducing a selectivity parameter s_i that either takes the value 1 (if prey-type is accepted) or 0 (if prey-type is rejected) (Holling, 1959; Charnov, 2002):

$$\frac{t_s}{t_{tot}} = \frac{1}{1 + N_{tot} \sum_{i=1}^n p_i \beta_i s_i h_i} \quad (6b)$$

where h_i is the prey-type specific time needed to handle individual prey (s ind. $^{-1}$). From Eq. 6b it becomes clear that higher prey density and also light intensity via the search rate β will increase handling time limitations so that less time is left to search for prey. When substituting this expression into Eq. 6a, we arrive at following formulation for the encounter rate (Holling, 1959; Visser and Fiksen, 2013):

$$e_b = \frac{N_{tot} \sum_{i=1}^n p_i \beta_i}{1 + N_{tot} \sum_{i=1}^n p_i \beta_i s_i h_i} \quad (6c)$$

2.2.4 Clearance rate and absolute energy intake

The clearance rate of the bite-feeding fish (F_b , $m^3 s^{-1}$) is the volume cleared for prey per unit time or the ratio between the rate of prey eaten and the total prey density:

$$F_b = \frac{\sum_{i=1}^n p_i \beta_i s_i P_{c_i}}{1 + N_{\text{tot}} \sum_{i=1}^n p_i \beta_i s_i h_i} \quad (7)$$

where P_{c_i} is the prey-type specific probability that the fish will succeed in capturing a prey it has selected (expressed as a proportion). The clearance rate is also a measure of the predation pressure. The higher the proportion of prey present in a given volume that is eaten per unit time, the higher is the risk that any individual prey will be eaten. The capture probability will be lower for prey with good escape responses, which vary between different prey-types. In general, more developed stages and larger-sized individuals have better escape ability. The handling time will also vary for different prey-types, since more evasive prey may take longer time to capture. To account for this variation, the prey-type specific handling time (h_i) is defined as being inversely proportional to the prey-type-specific capture probability ($P_{c,i}$):

$$h_i = \frac{H}{P_{c_i}} \quad (8)$$

where the constant H represents the handling time (s ind.⁻¹) when capture probability is 1. Multiplying clearance rate (F_b) with total prey density (N_{tot}) gives the number of individuals eaten per unit time, and multiplying again with the energy content of individual prey (the product of weight (w , g ind.⁻¹) and energy density (∂ , J g⁻¹)) gives the rate of energy intake (Visser and Fiksen, 2013):

$$I_b = \frac{N_{\text{tot}} \sum_{i=1}^n p_i \beta_i s_i P_{c_i} w_i \partial_i}{1 + N_{\text{tot}} \sum_{i=1}^n p_i \beta_i s_i h_i} \quad (9)$$

where I_b is the absolute intake rate of bite-feeding for all prey combined (J s⁻¹). It is uncertain whether or to what extent planktivorous fish become satiated in their natural environment, as piscivorous fish do. Piscivorous fish eat much larger prey that takes longer time to digest, and their feeding is therefore gut-limited (Fall and Fiksen, in press; Breck, 1993). In this model, the stomach capacity is not assumed to place any limits on the intake rate of adult planktivorous fish (Pepin, Koslow and Pearre Jr., 1988). Instead, handling time limits ingestion to a level below the full capacity.

2.2.5 Metabolic rate and net energy intake

To determine net rate of energy intake, several forms of energy loss must be subtracted from the absolute intake rate (Kitchell, Stewart and Weininger, 1977; Stewart *et al.*, 1983; Bachiller *et al.*, 2018). Organisms are not able to exploit all energy consumed, and some of the energy made available will be spent in cellular respiration. The remaining energy can be invested in biomass accumulation in the form of growth, energy storage or reproduction. The proportion u of ingested energy that is available for use in metabolism or bioaccumulation can be expressed as follows:

$$u = (1 - eg)(1 - sda - ex) \quad (10)$$

where eg is the proportion of ingested energy that is egested instead of assimilated, sda is the coefficient of specific dynamic action (proportion of assimilated energy expended in processing food) and ex is the proportion of assimilated energy that is excreted (Bachiller *et al.*, 2018). The weight-specific metabolic rate (M , J h⁻¹ g⁻¹) decreases with the weight of the fish (W , g) and increases with ambient temperature (T , °C) and swimming speed (U , m s⁻¹) in the following relationship (Stewart *et al.*, 1983):

$$M = \alpha Q_{\text{ox}} W^{\delta-1} e^{\rho T} e^{100\nu U} \frac{1}{24} \quad (11)$$

A factor of 100 is applied to convert swimming speed from metres per second to centimetres per second (the unit used by Stewart *et al.* (1983)), and the model is divided by 24 to convert from a daily to an hourly rate. α , δ , ρ and ν are constants estimated empirically by use of multiple linear regression of log-transformed data, where the metabolic rate is measured as total oxygen consumption by the fish. In order to convert to weight-specific energy expenditure, the intercept α ($\text{g O}_2 \text{ day}^{-1} \text{ g}^{-1}$) of the model is multiplied by an oxycalorific coefficient Q_{ox} ($\text{J (g O}_2)^{-1}$) (Elliott and Davison, 1975), and the model is divided by the fish weight. Accordingly, the value of 1 is subtracted from the coefficient of weight-dependence δ , making the exponent negative (Stewart *et al.*, 1983).

In the model, metabolic rates are calculated for each of the different activity modes (non-, bite- and filter-feeding). To save energy, the non-feeding fish employs routine swimming, where the speed v_r (m s^{-1}) is adjusted to let the fish cover sufficient distances with minimum investment. The routine metabolic rate M_r ($\text{J h}^{-1} \text{ g}^{-1}$) is consequently lower than the metabolic rate of feeding fish. When bite-feeding, the fish engages in two distinct activity states with different associated metabolic rates. The total metabolic rate of the bite-feeding fish (M_b , $\text{J h}^{-1} \text{ g}^{-1}$) can hence be decomposed into a search component (M_s , $\text{J h}^{-1} \text{ g}^{-1}$) and a handling component (M_h , $\text{J h}^{-1} \text{ g}^{-1}$), the relative contribution of each depending on how much of the time is allocated to searching versus handling:

$$M_b = \frac{t_s}{t_{\text{tot}}} M_s + \frac{t_h}{t_{\text{tot}}} M_h \quad (12a)$$

$$M_b = \frac{1}{1 + N_{\text{tot}} \sum_{i=1}^n p_i \beta_i s_i h_i} M_s + \left(1 - \frac{1}{1 + N_{\text{tot}} \sum_{i=1}^n p_i \beta_i s_i h_i} \right) M_h \quad (12b)$$

$$M_b = \frac{M_s - M_h}{1 + N_{\text{tot}} \sum_{i=1}^n p_i \beta_i s_i h_i} + M_h \quad (12c)$$

In Eq. 11 the swimming velocity is assumed to be rather stable, which as an approximation can hold for the search phase of bite-feeding. During the handling phase, however, the fish often changes speed and direction in order to capture prey (van der Lingen, 1994). To account for the higher energetic costs associated with such frequent accelerations (Boisclair and Tang, 1993), an activity multiplier a_h for prey handling is applied to the equation for the metabolic rate (Eq. 11):

$$M_h = a_h M \quad (13)$$

The value of a_h is always higher than 1, but how much depends on the swimming behaviour of the species in question. When the metabolic rate has been quantified, the net specific energy intake rate (ε_b , $\text{J h}^{-1} \text{ g}^{-1}$), which is the energy available for biomass production per unit fish weight, can be calculated in this way:

$$\varepsilon_b = \frac{u I_b}{W} 3600 - M_b \quad (14)$$

A factor of 3600 is applied to convert the intake per second to an hourly rate. Because net energy intake from feeding (ε_b) can be negative, it follows from Eq. 14 that fish can lose biomass at a higher rate while feeding than while fasting. This is contradictory to the purpose of feeding, and a threshold for the initiation of bite-feeding is therefore defined:

$$\varepsilon_b > -M_r \quad (15)$$

2.2.6 Optimal swimming speed

The fish can regulate its swimming speed in order to maximise energy gain, and the optimal speed is identified as the speed that results in the highest net energy intake (Ware, 1975). The absolute speed that is optimal for foraging increases with body length, but the optimal relative speed (in body lengths per second) is lower for larger fish. In situations with low prey densities, the optimal swimming speed will increase with the supply of prey, but at higher densities more of the time will be spent handling prey. It is therefore commonly presumed that the fish should save energy by reducing swimming speed at high prey densities (Ware, 1978). This model however distinguishes between the swimming behaviours associated with each of the two different phases of bite-feeding.

The fish is only able to handle one prey at a time, and it should do so in the most efficient way to increase the possibility of successful capture without expending too much time and energy. Efficient capture means that more time can be spent searching for additional prey to eat, or if saturated with prey, more of the available prey can be procured. In other words, the optimal swimming behaviour should ensure a high ratio between the capture probability P_c and the handling time h , and ideally, it should be specific to each prey-type (i).

The benefit of increasing this ratio is highest when the encounter rate is at its maximum (handling time limits the consumption), but as an approximation, the mean swimming speed v_h during the handling phase is assumed to be independent of prey density and light intensity. The swimming speed varies highly in the course of each handling event, and sharp manoeuvres and fast accelerations are probably more important for the outcome than what the mean speed is. For a given size and species of fish, a single value for v_h that is constant across all prey-types and environmental conditions is therefore chosen based on swimming speeds reported in the literature.

The swimming pattern is more stable during the search phase, and although the search rate varies between prey-types due to different visual ranges, the search swimming speed v_s is the same for all prey. It can hence be factored out of the expression for the weighted mean search rate so that the equation for the encounter rate (Eq. 6c) becomes:

$$e_b = \frac{N_{\text{tot}} v_s \sum_{i=1}^n p_i (R_i \sin \theta)^2}{1 + N_{\text{tot}} v_s \sum_{i=1}^n p_i (R_i \sin \theta)^2 s_i h_i} \quad (16)$$

From Eq. 16 it follows that the encounter rate (e_b) and thereby the intake rate (ε_b) will increase with the search swimming speed v_s , but that the rate of increase will decline at higher prey densities (N_{tot}) and/or light intensities (directly influencing visual range R). The encounter rate then approaches its maximum. Higher v_s will itself also increase handling time limitations, and the intake rate will consequently respond more to changes in v_s when the speed is low. When nearly all of the time is spent handling prey rather than searching for them, the value of v_s does not matter anymore.

The metabolic rate (M_b , Eq. 12c) will also increase with the swimming speed, and the fish is therefore expected to save energy by slowing down at very low encounter rates when there is little to gain from the investment. The optimal search swimming speed v_s can be determined for each of the different light intensities and prey densities and compositions by choosing among a realistic spectre of swimming speeds the one that gives the highest net energy intake. The weighted mean swimming speed v_b during bite-feeding can be calculated in the same way as done for the metabolic rate (Eq.

12c), by taking into account the fraction of the total time that is spent on searching (t_s) and handling (t_h):

$$v_b = \frac{v_s - v_h}{1 + N_{\text{tot}} \sum_{i=1}^n p_i \beta_i s_i h_i} + v_h \quad (17)$$

As handling time becomes more limiting, the overall swimming speed v_b will change from being most similar to v_s to become nearly equal to v_h .

2.2.7 Selectivity and optimal diet breadth

Traditionally, the concept of selectivity in foraging fish has been applied as a general term for the discrepancy between the prey composition found in fish stomachs and the prey composition observed in their environment (Luo, Brandt and Klebasko, 1996). Much of this discrepancy can however be ascribed to differential encounter rates for prey of different sizes and contrasts, or differential capture rates for prey with different escape abilities (Drenner, Strickler and O'Brien, 1978; Holzman and Genin, 2005). These are both forms of passive selection and do not reflect real preferences in the fish. To determine patterns of active prey choice, the prey community must be viewed from the fish's perspective, that is, the prey composition observed by the fish (Luo, Brandt and Klebasko, 1996).

Several forms of active selection have been proposed, for example specialisation on the most common prey-type (Murdoch *et al.*, 1975), but here preferences are based on the profitability of prey, which is consistent with the intake maximation principle (Visser and Fiksen, 2013). The profitability pf_i (J s^{-1}) of prey of a given type (i) can be defined as the ratio between the energy gained from handling the prey and the time it takes to handle it (Charnov, 2002):

$$pf_i = \frac{P_{c_i} w_i \partial_i}{h_i} \quad (18a)$$

where w_i and ∂_i is the wet weight (g ind.^{-1}) and energy density (J g^{-1}) of prey-type i , respectively. The net profitability can be determined by multiplying the energy consumed with the proportion that becomes available for use per unit fish weight and then subtracting the metabolic cost of handling:

$$Npf_i = \frac{upf_i}{W} 3600 - M_h \quad (18b)$$

where Npf_i is the net profitability or the net weight-specific energy intake during handling of the prey ($\text{J h}^{-1} \text{g}^{-1}$). For fish foraging on a mixture of prey-types, which differ in catchability, size and energy density, it is only worth to invest time in trying to capture a prey from category i if it meets the criterion (Charnov, 2002; Visser and Fiksen, 2013):

$$Npf_i \geq \varepsilon_b \quad (19)$$

The value of the selectivity parameter s becomes 1 if the criterion is met, or 0 if it is not met (Charnov, 2002). If the net energy gained per handling time is lower than the overall net intake rate, the fish should ignore the prey. This inclusion criterion is independent of the density and search rate for the prey-type in question, since only the intake rate during the handling of the prey determines whether the total intake rate will change by including it, and if so, in what direction it will change. What the density and search rate influence, though, is *how much* the intake rate will change. If the prey-type constitutes a large proportion of the total prey density, or if the prey can be detected from a long

distance compared to other members of the diet, more individuals of this prey-type will be handled per unit time. This increases the significance of including the prey-type. Also, if it takes long time to handle it, more of the total time will be spent on this prey-type.

The selectivity values for each prey-type is decided by first ranking them according to profitability, and then testing one diet at a time, beginning with the most profitable prey-type and then adding the next in the rank (Visser and Fiksen, 2013) (Appendix 1). To determine the maximum potential diet breadth, each prey-type can be tested to decide if it is profitable to handle it if it was the only food available:

$$Npf_i > -M_r \quad (20)$$

If net rate of energy intake during handling is more negative than the routine metabolism, the fish will lose biomass feeding on the prey and should therefore reject it, even if it is the only available prey-type. The maximum potential diet breadth will be equal to the number of prey-types (n) that fulfil the criterion set in Eq. 20. Under most circumstances, the optimal diet will only constitute a fraction of this theoretical diet. The optimal diet becomes narrower as the intake rate increases and unprofitable prey-types are excluded, until eventually only the most valuable of the potential prey are accepted at saturating conditions (Charnov, 2002; Visser and Fiksen, 2013). The optimal diet breadth will vary as total prey density, relative densities of different prey-types and light conditions change.

2.3 THE FILTER-FEEDING SUBMODEL

Filtration or suspension-feeding is a foraging mode where the fish extracts small prey items from the water as it flows through the oral cavity, passes laterally through the gills and exits behind the opercula where the pressure is lower (Sanderson, S. L., Cech, J. J., Cheer, 1994; Sanderson *et al.*, 2001, 2016). Several mechanisms have traditionally been proposed to explain how particles are retained in the fish mouth. One common supposition has been that the gill rakers protruding from the branchial arches form a mesh that functions as a dead-end sieve through which water flows perpendicularly (Sanderson *et al.*, 2001). Only particles that are larger than the pore sizes in the filter are retained, while the smaller ones escape through as part of the filtrate. Another suggested mechanism is that particles are entrapped by adhering to mucus-covered surfaces on the filter (Sanderson *et al.*, 2001).

More recent studies that employ video endoscopy and numerical simulations of hydrodynamic flow patterns have revealed that fish instead capture particles by means of cross-flow filtration, where the water flows parallel to the filter surface (Sanderson *et al.*, 2001, 2016; Cheer *et al.*, 2012; Brooks *et al.*, 2018). Some of the water separates from the parallel flow and exits through the pores, while the majority of particles follow the main flow towards the posterior oral cavity, where they are concentrated. This enables the fish to retain particles that are much smaller than the mesh size of the gill raker filter, as has been observed in several species (Lazzaro, 1987; van der Lingen, 1994; Langeland and Nøst, 1995).

Through endoscopic documentation of particle trajectories in mouths of filter-feeding fish, Sanderson *et al.* (2001) discovered that about 95% of the food particles present in the water never actually come into contact with any oral surface during their transport. Furthermore, surgical removal of gill rakers in tilapia did not result in any substantial impairment of the ability to retain small particles, as would be expected if the gap between the rakers determined the threshold size of retainable particles (Drenner *et al.*, 2004; Smith and Sanderson, 2013).

The fact that particles do not accumulate on the gill rakers means that the fish avoids clogging of the filtering apparatus, but the mechanisms by which particles remain suspended in the flow have only

recently been elucidated. When Sanderson *et al.* (2016) investigated the filtration process in physical models of paddlefish and basking shark, they noticed that the branchial arches and the slots between them form a series of ribs with small ratio between groove width and rib height (Sanderson *et al.*, 2016). These ribs act as backward-facing steps along the wall of the oral cavity, and the gill rakers form a porous outer surface that is separated from the main flow by the slots. When the cross-flow passes a rib, a vortex is generated that covers the whole slot between the two neighbouring ribs, with the effect that particles are transported back into the oral cavity and transferred further posterior towards the oesophageal opening. This filtration principle, termed vortical cross-step filtration, appears to be a convergent phenomenon found in both baleen whales and filter-feeding birds as well as planktivorous fish (Sanderson *et al.*, 2016).

2.3.1 Filtration efficiency

The maximum clearance rate (F_{\max} , $\text{m}^3 \text{s}^{-1}$) is the theoretical maximum volume that the fish can clear for prey per unit time. For ram filter-feeding, this rate is determined by the swimming speed (v_f , m s^{-1}) and the gape area of the fish mouth (A_g , m^2) in the following relationship (Fig. 5, Durbin and Durbin, 1975; van der Lingen, 1994):

$$F_{\max} = v_f A_g \quad (21)$$

In reality the clearance rate is always some fraction of this theoretical rate. Some of the feeding time is used to handle the filtered prey (van der Lingen, 1994; Sims, 1999; Garrido *et al.*, 2007), the intra-oral flow speed is lower than the swimming speed (Sanderson, S. L., Cech, J. J., Cheer, 1994), and not all of the particles that enter the oral cavity are retained (Friedland, Haas and Merriner, 1984; Langeland and Nøst, 1995; Mummert and Drenner, 2004). Also, some of the prey that would otherwise have entered the oral cavity manage to evade the fish gape due to escape responses (Drenner, Strickler and O'Brien, 1978; Kiørboe and Visser, 1999; Heuch, Doall and Yen, 2007). The clearance rate of filter-feeding fish F_{\max} can thus be compared to the search rate β of the bite-feeding fish—both are measures of the volume of water processed in a given time, but not all of the prey present in this volume can be exploited.

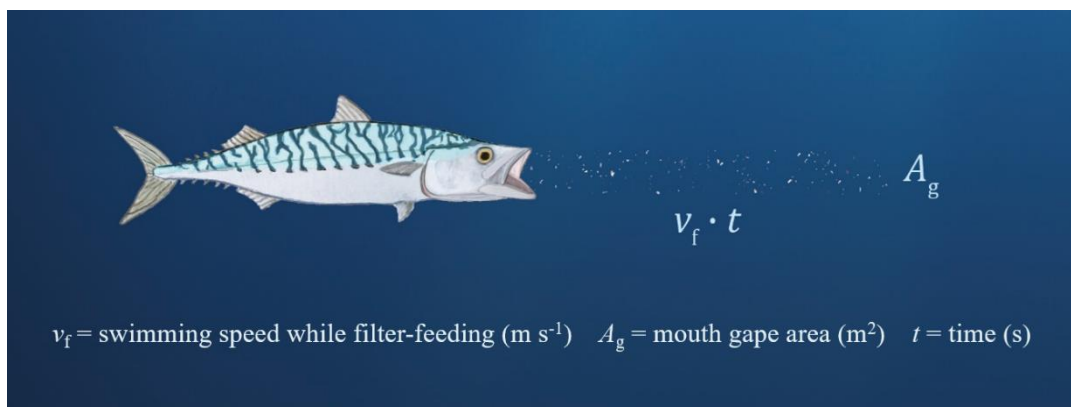


Fig. 5. The theoretical maximum clearance rate F_{\max} of the filter-feeding fish is the product of the swimming speed v_f and the mouth gape area A_g .

The actual volume cleared by a filter-feeding fish per time-unit can be estimated empirically by measuring the difference in prey concentration at the start and end of a feeding trial (Harvey, 1937;

Friedland, Haas and Merriner, 1984; van der Lingen, 1994). The ratio of this experimental rate to the maximum clearance rate gives a measure of the filtration efficiency (Durbin and Durbin, 1975), but it does not tell us how this fraction can be attributed to the different components of the filtration process.

2.3.2 Fraction of time spent filtering

Filter-feeding fish are observed to periodically close their mouth and opercula for a brief time before they resume filtering, supposedly because they need to swallow the filtered prey (Ehlinger, 1989; Sanderson, Cech and Patterson, 1991; Sanderson, S. L., Cech, J. J., Cheer, 1994; van der Lingen, 1994; Garrido *et al.*, 2007). The duration of each filtering bout times the frequency gives the fraction of the total time that the fish spends filtering. In a feeding experiment with *Sardinops sagax*, the filtering bout duration was on average 1.3 s, and they filtered 85% of the time (van der Lingen, 1994). In an experiment with *Sardina pilchardus*, the fish were observed to swim with their mouth open 52% of the time, each bout lasting around 0.5 s (Garrido *et al.*, 2007). Others have reported feeding bout durations ranging from 0.2 to 4.4 s (Leong and O'Connell, 1969; Janssen, 1976; Gibson and Ezzi, 1985; James and Findlay, 1989).

2.3.3 Buccal flow velocity

In a study on American paddlefish (*Polyodon spathula*) where they simultaneously measured the buccal flow speed with a thermistor probe and the swimming speed using videotapes, Sanderson *et al.* (1994) found that the intra-oral flow speed during ram filter-feeding was 60% of the swimming speed (Sanderson, S. L., Cech, J. J., Cheer, 1994). They hypothesised that this reduction in speed might be due to the resistance exerted by the oral surfaces. Higher resistance will cause more water to be displaced in front of the mouth instead of entering and therefore lower the filtering rate (Sanderson, S. L., Cech, J. J., Cheer, 1994). It is possible that the buccal flow fraction will *decrease* at high swimming speeds, since then the filtering apparatus might function more as a solid surface than a filter, but whether the fish swims at high enough speeds to significantly impede the functioning of the filtering system is uncertain (Carey and Goldbogen, 2017).

If the oral cavity widens posterior to the mouth opening, this expansion in “pipe” diameter will also cause the flow to slow down (Sanderson, S. L., Cech, J. J., Cheer, 1994), but without changing the volume of water passing through the mouth per unit time. The buccal flow speed is still important for the filtration efficiency, though, since the Reynolds number (the ratio of inertial forces to viscous forces) increases with the flow velocity. This again affects the particle encounter rate and retention efficiency (Siddiqui and Banerjee, 1975), but for simplicity, only reduction in buccal flow speed that affects the volumetric rate of the flow is considered in this model.

2.3.4 Retention efficiency

Although there seems to be no clear general correspondence between the gill raker gap and minimum size of retainable prey (Gibson, 1988; Langeland and Nøst, 1995; Drenner *et al.*, 2004; Smith and Sanderson, 2013), some studies have nevertheless reported a correlation between gill raker gap and retention efficiency for different prey-types. The common bream (*Abramis brama*) is for example known to adjust the gill raker gaps to feed selectively on different size classes of prey (Hoogenboezem *et al.*, 2008). It is also unable to retain *Daphnia* that are much wider than the smallest retainable copepods, which proposedly is due to the more flattened shape of *Daphnia* which allows it to pass between the rakers (Van den Berg *et al.*, 1993). Moreover, as the Pacific mackerel (*Scomber japonicus*) grows larger and employs filter-feeding more frequently, the gill raker gaps narrow

(Molina, Manrique and Velasco, 1996). Since dead-end sieving in fish is refuted, it is possible that the gill rakers more indirectly influence particle retention through their effect on hydrodynamic flow patterns (Cheer *et al.*, 2012).

It is widely observed that the retention efficiency increases with the size of the food particles until the maximum retainability is reached at a given size, which varies between species and different stages within species (Friedland, Haas and Merriner, 1984; van der Lingen, 1994; Langeland and Nøst, 1995; Mummert and Drenner, 2004). A possible reason for this size-specific retention efficiency is that drag forces and inertial forces are greater for larger particles, which cause them to deviate from the streamlines that pass through the gill raker gaps (Cheer *et al.*, 2012). Instead, they adhere to the main flow pattern of recirculating vortices and cross-flow (Sanderson *et al.*, 2016; Brooks *et al.*, 2018).

Presuming that the retention efficiency does not change considerably with the length of the fish once it has reached adult size, but that the retainability of prey increases with prey length before it gradually levels off, the retention efficiency for prey-type i (r_i) can be described with a Michaelis-Menten equation:

$$r_i = r_{\max} \frac{l_i}{k_1 + l_i} \quad (22)$$

where r_{\max} is the maximum retention efficiency (value near 1), k_1 is a species-specific parameter representing the prey length for which retention efficiency is half the maximum value (m) and l is the length of the prey (m). The retention efficiency represents the proportion of incoming prey that are retained in the oral cavity and is thus a dimensionless quantity. If all prey-types included in the specified diet have mean sizes above the level where maximum retention efficiency is reached, r is equal to r_{\max} for all prey.

2.3.5 Evasiveness of prey

When the fish makes its way through the water, it generates hydrodynamic signals that can be detected by nearby prey, eliciting escape responses. When bite-feeding, the fish aligns itself to seize particular prey, guided by vision, but when filter-feeding, the fish does not specifically target individual prey. The behaviour of the fish is more predictable during filter-feeding, which makes it easier for prey to evade. In the model, the probability that a prey positioned in the trajectory of the fish will enter the oral cavity instead of escaping is therefore set lower than the probability that similar prey will be captured during the handling phase of bite-feeding. Prey from some taxonomic groups and size classes are more evasive than others, which causes differential feeding rates on different prey-types also for filter-feeding, even though the fish is not selective in a behavioural sense.

2.3.6 Clearance rate and absolute energy intake

The clearance rate of the filter-feeding fish can be modelled by adding to Eq. 20 the different components that determine the filtration efficiency (Lovvorn, Baduini and Hunt, 2001). The clearance rate or filtration rate (F_f , $\text{m}^3 \text{s}^{-1}$) is then expressed as a fraction of the theoretical maximum rate:

$$F_f = v_f A_g f_t B_v \sum_{i=1}^n p_i P_{ei} r_i \quad (23)$$

where f_t is the fraction of the total filter-feeding time that the fish actually filters prey, B_v is the fraction that the buccal flow speed takes of the swimming speed, P_{ei} is the probability that a prey will enter the fish mouth and r_i is the probability that the prey will be retained in the oral cavity once it has entered. Similar to the bite-feeding intake (Eq. 9), the absolute intake rate I_f of filter-feeding ($J s^{-1}$) is calculated by multiplying the clearance rate (F_f) with the total prey density (N_{tot}) and the energy content of prey ($w_i \partial_i$):

$$I_f = v_f A_g f_t B_v N_{tot} \sum_{i=1}^n p_i P_{ei} r_i w_i \partial_i \quad (24)$$

2.3.7 Metabolic rate and net energy intake

The metabolic rate of filter-feeding differs from that of bite-feeding due to different swimming patterns and body shapes (James and Probyn, 1989; van der Lingen, 1995; Carey and Goldbogen, 2017). When filtering, the fish flares its opercula and opens the mouth wide. Hence, the body becomes less streamlined, and the fish experiences higher drag (Durbin and Durbin, 1983; James and Probyn, 1989; Sanderson and Cech, 1992; Macy, Durbin and Durbin, 1999).

The fish can compensate for this increased cost of locomotion by moderating its swimming behaviour. For northern anchovy (*Engraulis mordax*), Carey and Goldbogen (2017) found that kinematic parameters were much less variable during filter-feeding than during routine swimming, which is characterised by alternating phases of acceleration and gliding (beat-glide swimming) (Carey and Goldbogen, 2017). When the body is held straight, the drag imposed on it is much lower than when it flexes, leading the fish to adopt a more stable swimming pattern with reduced lateral movements while filter-feeding. They also speculated that filtration may be more efficient if the filtering apparatus is kept steady, or that filtering mechanics impede movement of anterior body (Carey and Goldbogen, 2017).

Studies that have measured respiration rate of fish in relation to feeding mode report different relative costs of bite- and filter-feeding for different species and size classes within species (James and Probyn, 1989; Yowell and Vinyard, 1993; van der Lingen, 1995). The slope of the relationship between respiration rate and swimming speed during filter-feeding is found to be much steeper for Cape anchovy (*Engraulis capensis*) than it is for pilchard (*Sardinops sagax*) and Atlantic menhaden (*Brevoortia tyrannus*) with size almost 2.8 times the length of anchovy (James and Probyn, 1989; van der Lingen, 1995). For the small-sized anchovy, filter-feeding is more energetically expensive than bite-feeding (James and Probyn, 1989), whereas the opposite is observed for pilchard (van der Lingen, 1995).

The reason for this discrepancy is probably that while viscous forces are negligible compared to inertial forces for pilchard, the Reynolds number for anchovy is low enough to make viscous forces count. The importance of skin friction is thereby increased, which is higher when filter-feeding than when bite-feeding (James and Probyn, 1989; Vogel, 1994; van der Lingen, 1995). In contrast, the untidy swimming pattern of bite-feeding is more energy demanding for the larger pilchard. This corresponds with the fact that bite-feeding is the principal foraging mode of anchovies (James, 1987; James and Findlay, 1989), while adult pilchards are mainly filter-feeders that can switch to bite-feeding if presented with larger food items (van der Lingen, 1994). Similarly, for blue tilapia (*Tilapia aurea*) the weight-specific cost of filter-feeding is reported to decrease with size, whilst for bite-feeding it increases (Yowell and Vinyard, 1993). It is also generally observed that fish capable of filtering change feeding behaviour throughout ontogeny from employing bite-feeding only to engage

more in filter-feeding when they reach a threshold size (Janssen, 1976; Drenner, de Noyelles and Kettle, 1982; Sanderson and Cech, 1992; Yowell and Vinyard, 1993).

In summary, the metabolic rate is higher for filter-feeding than for non-feeding activity (Hettler, 1976; James and Probyn, 1989; van der Lingen, 1995), but how much higher depends partly on the fish size. To account for this, Eq. 11 is multiplied with a size-specific activity coefficient a_f , which gives the following equation for the metabolic rate M_f of filter-feeding ($\text{J h}^{-1} \text{g}^{-1}$):

$$M_f = a_f M \quad (25)$$

Once the absolute energy intake and metabolic rate have been determined, the net weight-specific intake rate ε_f of filter-feeding ($\text{J h}^{-1} \text{g}^{-1}$) can be calculated in the same way as done for bite-feeding (Eq. 14):

$$\varepsilon_f = \frac{uI_f}{W} 3600 - M_f \quad (26)$$

Similar to the bite-feeding criterion (Eq. 15), the fish will not initiate filter-feeding unless the net energy intake (ε_f) exceeds the threshold level corresponding to the non-feeding routine metabolic rate (M_r):

$$\varepsilon_f > -M_r \quad (27)$$

2.3.8 Optimal swimming speed

It is uncertain to which extent filter-feeding fish are able to regulate their swimming speed to maximise net energy return, but basking sharks (*Cetorhinus maximus*) have been shown to change swimming speed according to prey availability (Sims, 1999). Carey and Goldbogen (2017) observed that the northern anchovy lowers its speed during filter-feeding compared to routine swimming, which has also been documented for filtering sharks and bowhead whales (Sims, 1999; Heyman *et al.*, 2001; Simon *et al.*, 2009). This probably reflects the high cost of filter-feeding, but it is also possible that the filtering process is hampered if the speed becomes too high (Carey and Goldbogen, 2017). In contrast, other studies have found that the fish increases its swimming speed during filter-feeding (Pepin, Koslow and Pearre Jr., 1988; James and Probyn, 1989), but some of these cases might represent initial “feeding frenzy” of the fish when prey is introduced rather than normal filter-feeding activity (James and Probyn, 1989; Carey and Goldbogen, 2017).

The results of studies comparing swimming speeds for the two feeding modes are also variable. Some report that the fish swims faster while filter-feeding than while bite-feeding (Gibson and Ezzi, 1985; Pepin, Koslow and Pearre Jr., 1988), whereas others report the opposite (James and Findlay, 1989; Batty, Blaxter and Richard, 1990). In any case, since the energy return increases with prey density, the filter-feeding fish is expected to increase its swimming speed in response to higher prey availability before levelling off when the costs become too high compared to the intake (Ware, 1978). Similar to the swimming speed during the search phase of bite-feeding, the swimming speed chosen in the filter-feeding model is the one that maximises net energy return.

2.4 MODEL APPLICATIONS

In order to examine the behaviour of the model, it is applied on two different species of fish known to alternate between bite- and filter-feeding, and for which relevant field or experimental data are available. These applications can serve as examples of how the model can be adapted to simulate systems in the real world. The first example is of Northeast Atlantic mackerel (*Scomber scombrus*) feeding in Atlantic waters in the Norwegian Sea during its summer migration (Langøy *et al.*, 2006). The second represents feeding trials where pilchards (*Sardinops sagax*) forage in closed experimental tanks (van der Lingen, 1994). The model is calibrated to make it suitable for the particular species by adjusting the parameter values according to data found in scientific literature and comparing model results with observations from the real systems. The simulation experiments do however not establish the predictive ability of the model, which would require data sets independent of the ones used to calibrate the model.

2.4.1 Atlantic mackerel feeding in the Norwegian Sea

The feeding of mackerel is simulated without any time dimension, instead feeding rates and behaviours are modelled as functions of light intensity and prey density and composition independent of time. The adaptation is based mainly on a field study conducted by Langøy *et al.* (2006), where the prey community observed in samples from WP2 plankton nets are compared to the diet composition found in stomach samples from mackerel caught in the same area. In the model, the prey community is divided into different categories, each with its own set of parameter values, so that it accords with the prey composition in the environment as observed in the study. To investigate the correspondence between model results and observed data, the diet composition predicted from submodels of bite- and filter-feeding at a fixed set of parameter values is compared to the diet observed in stomach samples. Details on how this comparison was performed are given in the code for the simulation (Appendix 1).

2.4.2 Pilchard feeding in experimental tanks

For pilchard experimental studies of bite- and filter-feeding have been performed were results can readily be compared with model projections (van der Lingen, 1994, 1995). In a laboratory experiment, schools of fish were held in closed tanks and fed different types of prey, and water samples were taken at regular time intervals to determine the change in prey density during the course of a feeding trial (van der Lingen, 1994). In addition, feeding mode, swimming speed and feeding intensity (proportion of school feeding) were monitored using video camera. To make the model applicable to this experimental situation, it was converted to a simulation model for single-prey systems where the prey density is updated over time for each of the feeding-modes. The prey assemblages confined in the tank can be regarded as closed populations, and the decrease in prey density with time accordingly is the result of the feeding activity of the fish (natural mortality is ignored since the trials are of a relatively short duration). The number of prey subtracted from the population at a given time-step equals the total number of prey eaten by the fish in the tank during that time. In addition to prey densities, simulated and observed swimming speeds are also compared. For details on the procedure, the code can be consulted (Appendix 2).

A problem that arose when planning this simulation was that not all members of the school were actually feeding at the various timepoints, and the proportion that were feeding decreased considerably as prey density declined (van der Lingen, 1994). The model is individual-based, though, and it is not obvious whether the modelled fish should represent the average of the whole school or only the feeding members of the school. Both variants are included when comparing model results with experimental data. While the simulation model for mackerel uses the regression equations for

metabolic rate presented earlier (Eqs. 11-13 and 25), other metabolic equations are chosen in the case of pilchard. The reason for this deviation is that it was difficult to find species specific values for all the constants needed, and when using the values that apply to mackerel, the metabolic rates became much lower than estimations based on an experiment with pilchards (van der Lingen, 1995). In this study, which was performed under similar laboratory conditions as the feeding experiment, the metabolic rate is given as a linear function of the swimming speed both for bite-, filter- and non-feeding activity. These regression equations were used instead. In the experiments, no distinction is made between the search phase and the handling phase of bite-feeding. Only a single optimised swimming speed v_b for bite-feeding is therefore determined in the simulation model for pilchard.

2.5 SENSITIVITY ANALYSIS

The model output is strongly dependent on the value of the different parameters, and some of them have greater impact than others. Uncertainties regarding parameter estimations will therefore be of little concern for some parameters, while for others it can greatly influence results. To evaluate the significance of some of the parameters involved, the sensitivity of the model to variations over realistic ranges was analysed using the simulation model for mackerel. The relative importance of varying handling time, fish length, ambient temperature, capture/enter probability, swimming speed and the proportion of ingested energy made available for use was examined by calculating percent change in net intake rate e_b and e_f as a function of percent change in parameter value. When testing a parameter, the others were held constant at their default values, while the same fixed values for light intensity and prey density and composition were chosen as those used when estimating the diet composition of mackerel. For bite-feeding, only the swimming speed v_s for the search phase was tested, since only this was optimised in the simulations.

3 RESULTS AND DISCUSSION

3.1 ATLANTIC MACKEREL FEEDING IN THE NORWEGIAN SEA

The general behaviour of the model was explored by simulating Atlantic Mackerel foraging in the Norwegian Sea during summer. The diets predicted by the bite- and filter-feeding submodels differ both from each other and from the prey compositions observed in the environment by Langøy *et al.* (2006). Prey compositions observed in stomach samples represent an intermediate between the bite- and filter-feeding diets.

3.1.1 Effects of prey density and light on switching

When light is not limiting, net intake rate ϵ_b from bite-feeding increases rapidly with total prey density due to high encounter rate, but levels off abruptly when prey density is still very low (N_{tot} approximately 1×10^3 ind. m^{-3} , Fig. 6). Contrary, when ambient irradiance E_z is low enough to considerably limit the neural activity of the visual system, the intake rate increases more gradually with prey density. The more limiting the light is, the more does the response in intake to changes in prey density decline. Consequently, the intake rate reaches its maximum at much higher prey densities under poor light conditions than in full light. However, as long as irradiance is above zero, the theoretical intake rate will eventually stabilise at the same asymptotic value if only the prey density becomes sufficiently high. When this stage is reached, neither prey density nor light place any limits on the intake anymore. The maximum absolute intake rate I_b is determined solely by the relative densities of the different prey-types and of the prey-type specific values of handling time, prey area and contrast, capture probability and energy content of prey.

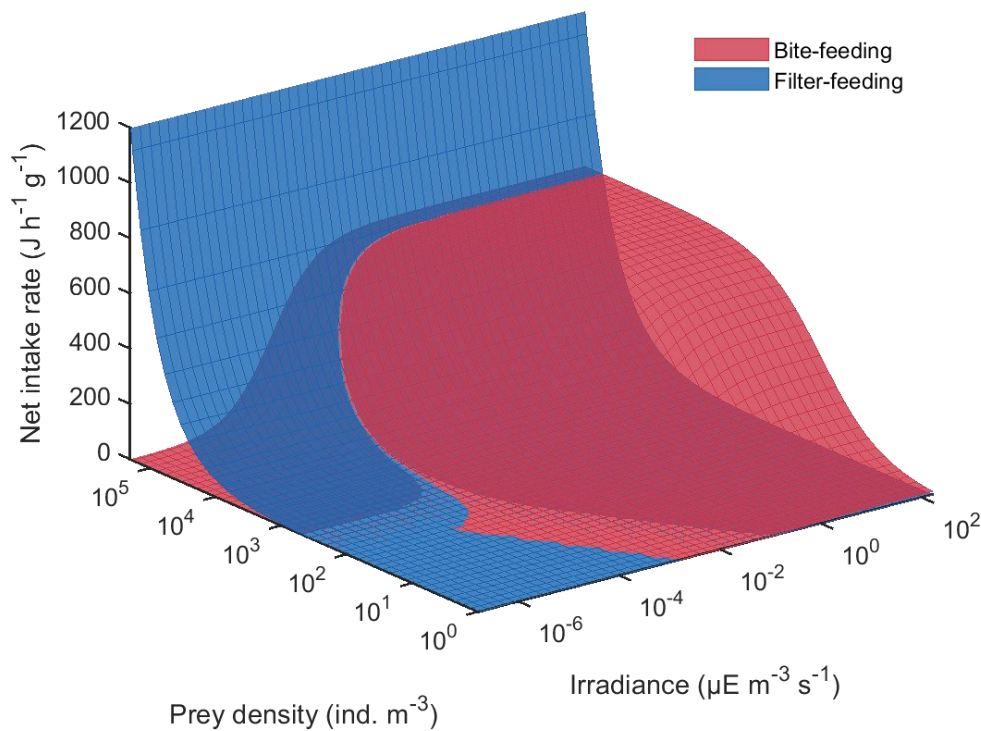


Fig. 6. Predicted net weight-specific energy intake ϵ_b and ϵ_f for mackerel bite- and filter-feeding in the Norwegian Sea at various prey densities N_{tot} and ambient irradiances E_z . In the simulation, 0.1% of the prey were krill and amphipods.

At satiating conditions, the metabolic cost of bite-feeding only depends on the handling component and is therefore at its highest ($M_b = 1.6 \text{ J h}^{-1} \text{ g}^{-1}$). This is insignificant compared to the maximum net intake rate ($\epsilon_b = 638.7 \text{ J h}^{-1} \text{ g}^{-1}$). When prey density limits the intake, some of the feeding time is allocated to searching, which is less energy demanding than handling due to a more stable swimming pattern. Only at very low prey densities and light intensities is the energy gained from feeding reduced enough to let the metabolic rate influence the efficiency of bite-feeding to any appreciable extent.

Net intake rate ϵ_f from filter-feeding is independent of light and increases linearly and unabated with prey density (Fig. 6). This may appear counterintuitive, since the fish repeatedly has to interrupt the filtering activity in order to swallow prey retained in the oral cavity. However, the time needed to handle incoming prey is the same regardless of the influx, resulting in the observed linear response. At low prey densities, intake rate from filter-feeding is considerably lower than for bite-feeding, unless irradiance is reduced to very low levels (E_z approximately $1.0 \times 10^{-4} \mu\text{E m}^{-2} \text{ s}^{-1}$). This is because the bite-feeding intake initially responds more to changes in prey density. The metabolic rate is usually minor compared to the intake rate also for filter-feeding ($M_f = 1.5$ and $1.7 \text{ J h}^{-1} \text{ g}^{-1}$ at low and high prey densities, respectively), but at very low prey densities, net intake rate becomes negative.

As prey density increases and handling time limitations cause the bite-feeding intake rate to level off, it is eventually exceeded by the intake rate from filter-feeding, encouraging the fish to switch feeding mode from bite- to filter-feeding (Fig. 6). In full light, the switching occurs at a relatively high prey density ($N_{\text{tot}} = 1.0 \times 10^5 \text{ ind. m}^{-3}$), but when irradiance is low enough to significantly limit the bite-feeding intake (E_z approximately $2.0 \times 10^{-3} \mu\text{E m}^{-2} \text{ s}^{-1}$), switching occurs at lower prey density. The more limiting light becomes, the less efficient bite-feeding is, favouring filter-feeding with progressively less prey available.

This main pattern of switching is reversed at extremely low prey densities (N_{tot} below 100 ind. m^{-3}), where switching instead occurs at higher prey densities when irradiance decreases (Fig. 6). Here, the switching points coincide with the set of prey densities and light intensities where the optimal diet breadth of bite-feeding is expanded to include 4 prey-types after only comprising krill and amphipods. Lower light intensities require higher prey densities for the additional prey-types to be included. The intake rate from bite-feeding therefore accelerates at these points, surpassing the intake rate from filter-feeding and causing the fish to switch feeding mode along the same pattern, until prey density is high enough to favour filter-feeding despite the broadening of the diet.

3.1.2 Effects of prey composition on switching

At relatively high ambient irradiance ($E_z = 8.1 \times 10^{-2} \mu\text{E m}^{-2} \text{ s}^{-1}$), increasing the proportion of krill and amphipods—the largest and most profitable prey-type—from 0.1 to 0.3% slightly enhances the intake rate from bite-feeding only when total prey density is very low (Fig. 7, scenario 1). At higher prey densities, the fish spends nearly all the time handling krill and amphipods, and increasing the supply of these prey has no additional effect. In lower light ($E_z = 1.2 \times 10^{-3} \mu\text{E m}^{-2} \text{ s}^{-1}$), more of the time is spent searching for prey. The effect of increasing the proportion of the preferred prey-type is accordingly much greater, and prey density is higher before the effect is abated (Fig. 7, scenario 2).

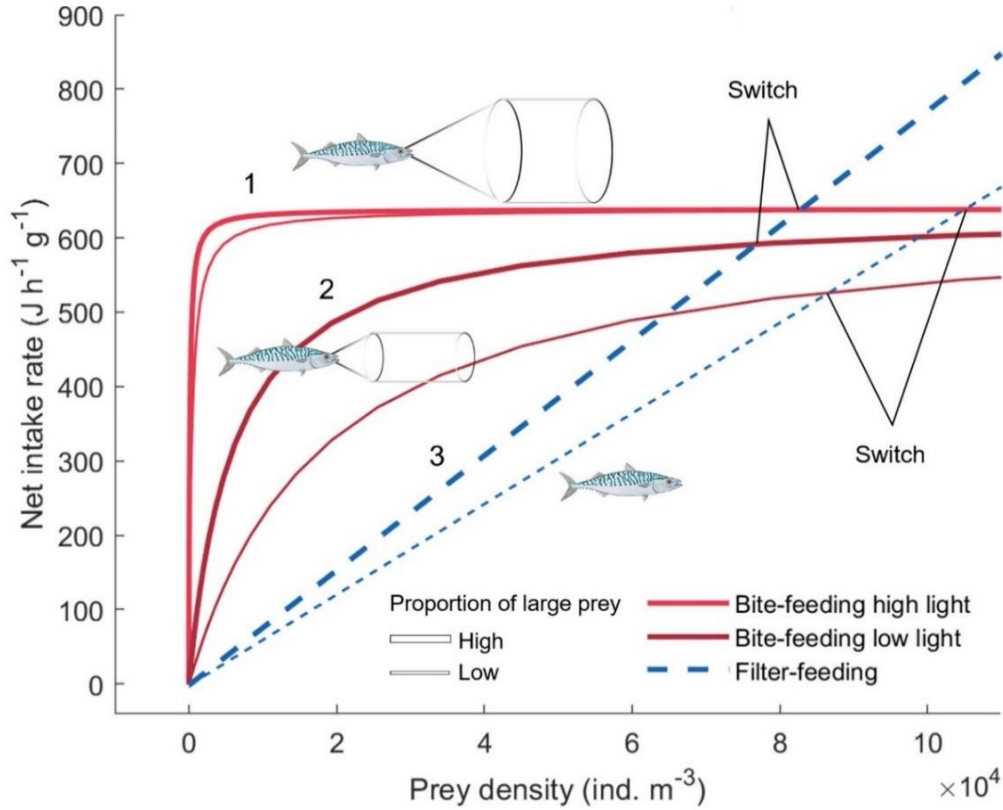


Fig. 7. Predicted net weight-specific energy intake ϵ_b and ϵ_f as a function of prey density N_{tot} for mackerel bite- and filter-feeding in the Norwegian Sea at different ambient irradiances ($E_z = 1.2 \times 10^{-3}$ and $8.1 \times 10^{-2} \mu\text{E m}^{-2} \text{s}^{-1}$) and proportions of large prey (0.1 and 0.3% krill and amphipods). The switch between feeding modes occurs at lower prey density if the light intensity decreases or if the relative density of large prey increases. 1) In high light, nearly all the time is spent handling krill and amphipods unless prey density is very low, and only then does the intake rate from bite-feeding increase with the proportion of the preferred prey-type. 2) In lower light, more of the time is spent searching for prey, and the intake rate from bite-feeding therefore responds more to increased access to krill and amphipods. 3) The intake rate from filter-feeding is not limited by handling time. Thus, it increases persistently with the proportion of krill and amphipods.

The intake rate from filter-feeding, on the other hand, increases linearly and persistently with the proportion of krill and amphipods, and the response is independent of total prey density (Fig. 7, scenario 3). The reason for the increase is that the product of the prey-type specific parameters in the equation for the absolute intake rate I_f (Eq. 24) is greater for krill and amphipods (category 1) than the weighted mean of the products is for the remaining prey-types:

$$P_{e1}r_1w_1\partial_1 > \sum_{i=2}^n \frac{p_i P_{ei}r_iw_i\partial_i}{1-p_1} \quad (28)$$

Had the inequality been the opposite, the intake rate would instead have decreased with the proportion of the prey-type. Since more prey are encountered by the filter-feeding fish at high prey densities, the absolute difference between the intake rates at different proportions of krill and amphipods consistently becomes larger as total prey density increases. For bite-feeding, the corresponding difference in intake rates eventually diminishes—soon in high light conditions and more gradually if light is limiting—and the switch from bite- to filter-feeding hence occurs at a lower total prey density if the proportion of large prey is higher (Figure 7, switching points marked). However, if irradiance is decreased to very low levels (not shown), higher proportions of large prey benefit bite-feeding more

than filter-feeding at the prey densities where switching occurs, causing the fish to instead switch strategy at higher prey densities with higher proportions of large prey.

These results demonstrate that prey size is important for switching. Experimental studies that have tested the effect of varying the size of prey in single-prey systems have documented that fish shift from filter- to bite-feeding when the prey exceeds a given size (Leong and O'Connell, 1969; James and Findlay, 1989; van der Lingen, 1994; Macy, Sutherland and Durbin, 1998). This threshold size increases if the prey has low escape ability, as for example is the case for cultivated individuals compared to wild members of the same taxonomic group (van der Lingen, 1994).

When filter-feeding, the number of prey that can be handled per unit time is in principle unlimited. As long as the prey can be retained and density is sufficiently high, the fish meets its energy demands by filter-feeding even if each individual prey has a low energy content. As prey become larger and more evasive, the probability that they will enter the fish mouth instead of escaping decreases considerably. The spectre of prey lengths that a filter-feeding fish is capable of exploiting is thus demarcated by a lower limit determined by retainability of prey and an upper limit which depends on their escape ability (Fig. 8). The upper limit is extended if the fish feeds on cultivated prey with reduced escape reaction (van der Lingen, 1994).

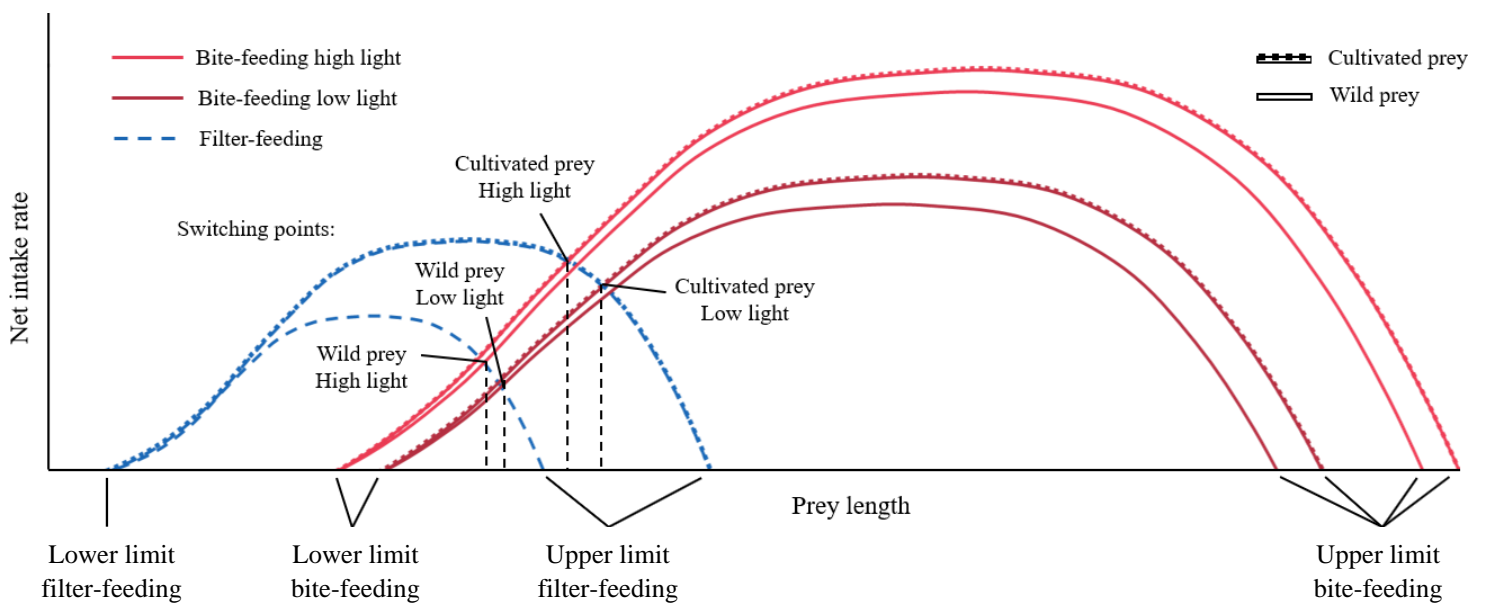


Fig. 8. Conceptual representation of how the net intake rate from bite- and filter-feeding is assumed to vary with length of wild and cultivated prey at high and low light intensity. The energy content of the prey increases with length, but the capture/enter probability decreases, and it decreases more for filter- than bite-feeding and more for wild than cultivated prey due to better escape ability. These variations lead to the differences in switching points and spectres of exploitable prey lengths illustrated in the diagram.

The spectre of exploitable prey is shifted towards larger prey when fish are bite-feeding. For small prey, net energy gained per handling time is too low to make them profitable to feed on (Eq. 20), while the pursuit of selected individuals makes it possible to capture larger prey that are too evasive for filter-feeding. The spectre becomes light contracted when irradiance decreases, while larger sizes can be exploited if the prey is cultivated in labs and therefore easier to catch. If the predator-prey size ratio is reduced due to larger fish size, the upper limit of filterable prey is extended because bigger mouth gape increases the probability that prey will be engulfed. Very large filter-feeders like rorqual whales

(Balaenopteridae) and whale sharks (*Rhincodon typus*) do for example include small fish in their diet (Potvin, Goldbogen and Shadwick, 2010; Rohner *et al.*, 2013). For bite-feeding the whole spectre shifts towards larger prey when the predator gets bigger. The net profitability of prey of a given length is lower for larger-sized fish (Eq. 18b), increasing the threshold size for initiation of bite-feeding. At the same time, better swimming capability makes the fish able to capture larger prey.

The exact mechanisms by which prey length affects the intake rate from each feeding mode is somewhat complicated. As prey grow longer, the weight increases, and for a given energy density, the energy content of individual prey increases accordingly. For both feeding modes, the intake rate is proportional to both prey weight and capture/enter probability (Eqs. 9 and 23). If the factor that the prey weight increases with is greater than the factor with which the capture or enter probability decreases, intake rate will increase with prey length. If it does so for both strategies, the positive effect of increasing prey length will eventually be greater for filter-feeding if only prey density becomes sufficiently high, despite the fact that enter probability of filter-feeding decreases more than capture probability of bite-feeding does. Even if the intake rate from filter-feeding decreases with prey length, this can in theory be compensated for by increasing prey density. The fish accordingly shifts from filter- to bite-feeding at larger prey lengths if density is increased. However, in addition to being more evasive, larger prey tends to occur in lower densities, which both negatively affect filter-feeding much more than bite-feeding. Increasing the prey length therefore generally favours bite-feeding over filter-feeding (Leong and O’Connell, 1969; James and Findlay, 1989; van der Lingen, 1994; Macy, Sutherland and Durbin, 1998).

Whether the larger energy content outweighs the negative effect of reduced filtration efficiency for krill and amphipods, as assumed in the simulation model for mackerel, is an open question. As emphasised, the effect of prey length on intake rates very much depends on the negatively correlated capture and enter probabilities. The values chosen in the simulations are merely tentative. Ideally these probabilities should be determined mechanistically for each prey-type by modelling the attack or engulfment success, as has been done for zooplankton exposed to planktonic predators, where deformation rates, avoidance behaviour and attack kinematics determine the outcome (Kjørboe and Visser, 1999; Caparroy, Thygesen and Visser, 2000; Visser, 2001; Kjørboe, 2008). Kjørboe and Visser (1999) meant that their “considerations are robust up to at least Re of the order of 10”. The Reynolds number is however much larger for adult fish than for planktonic larvae (Vogel, 1994), and due to uncertainties regarding how this affects small-scale hydrodynamic patterns in the model, I abandoned an initial attempt to model capture success. Future developments of foraging models for fishes should strive to incorporate mechanistic formulations of the attack or engulfment process, since this would greatly improve our understanding of how predator-prey size ratios and inherent escape abilities affect the probability of obtaining prey of different types and densities. The effects of prey composition on switching would then emerge from first principles, improving the predictive abilities of the models.

3.1.3 Switching influences diet composition

When relative intake rates and corresponding biomass consumption for different prey-types by bite- and filter-feeding fish were compared, it became clear that the diet composition of mackerel feeding in the Norwegian Sea will differ much depending on which feeding mode the fish mainly employs (Fig. 9). When bite-feeding, the model predicts that the fish will forage only on krill and amphipods if prey density and irradiance are both very low—presumably because the visual range R for the smaller prey-types are too short to let the fish spot them, unless they occur in high densities. As light conditions improve, the visual range increases relatively more for small than for large prey, and the fish expands its diet to include all prey-types except for the smallest copepods (mostly *Oithona*), which are too minute to be worth handling. At this point the optimal diet corresponds to the broadest potential diet

comprising all prey that “pass the test” of net profitability (Eq. 19). When further increasing irradiance, prey handling soon occupies so much of the feeding time that the fish becomes choosy, eventually rejecting all prey except for the most valuable category of krill and amphipods. At moderate to high irradiance, the fish feeds exclusively on krill and amphipods regardless of prey density, while at lower irradiances the fish supplements its diet with smaller prey when density is low, save in very dim light when they again are excluded.

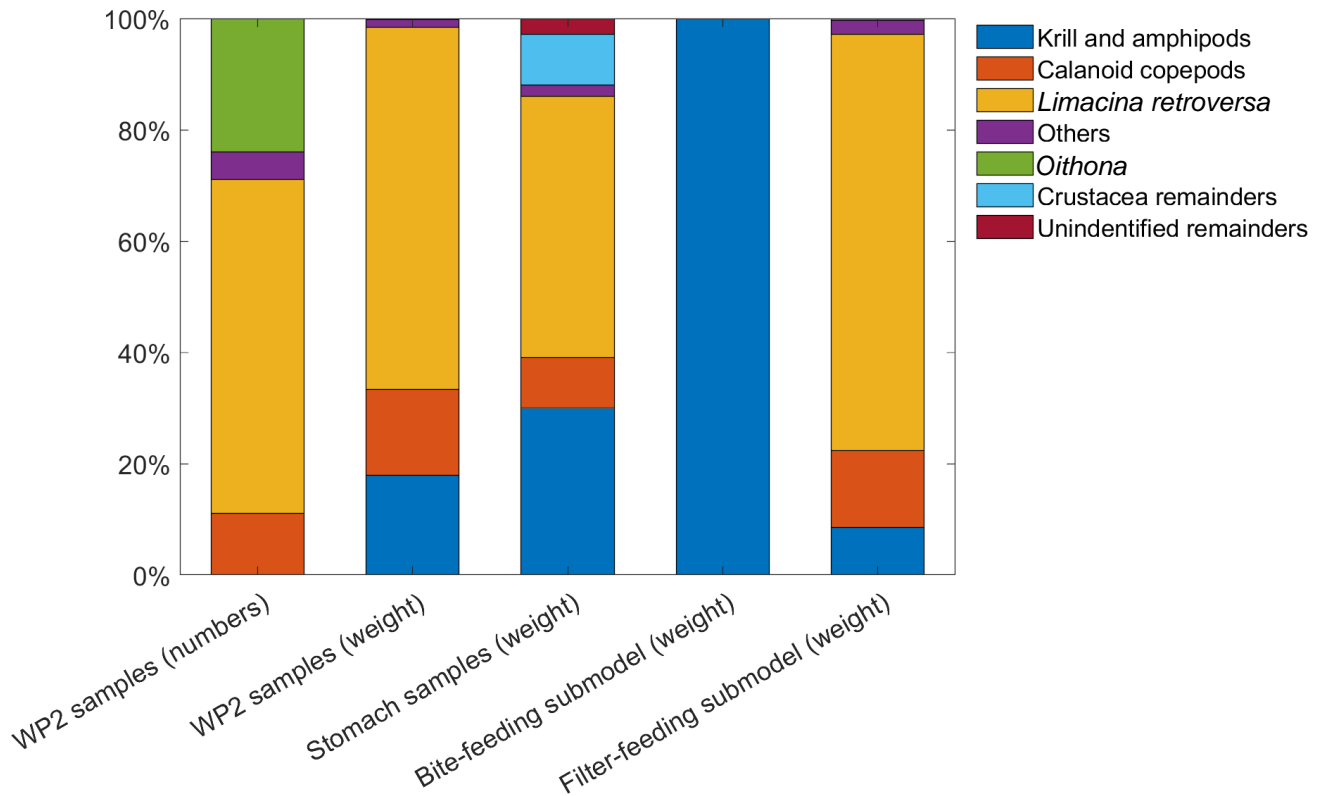


Fig. 9. Percentage of each prey-type in WP2 samples (numbers and wet weight), stomach samples from mackerel (dry weight) and in the diet predicted by bite- and filter-feeding submodels (wet weight). Samples were collected in Atlantic waters in the Norwegian Sea during summer by Langøy *et al.* (2006). A fixed set of parameter values were chosen for the simulation ($E_z = 1.2 \times 10^{-3} \mu\text{E m}^{-2} \text{s}^{-1}$, $N_{\text{tot}} = 1.9 \times 10^4 \text{ ind. m}^{-3}$, and 0.1% of the prey were krill and amphipods). Predicted net intake rate was then higher for bite-feeding ($\epsilon_b = 328 \text{ J h}^{-1} \text{ g}^{-1}$) than filter-feeding ($\epsilon_f = 116 \times 10^3 \text{ J h}^{-1} \text{ g}^{-1}$).

When the fish is filter-feeding, the predicted diet reflects the prey composition observed in the ambient environment by Langøy *et al.* (2006) to a larger extent than when it is bite-feeding. Still, varying escape abilities among the prey do result in somewhat altered wet weight percentages in the diet compared to WP2 samples (Fig. 9). In particular, the percentage of krill and amphipods—the most evasive prey-type—is significantly reduced, while the percentage of the more inert *Limacina retroversa* is correspondingly increased. The wet weight percentage of calanoid copepods is only slightly lower in the filter-feeding diet than in the environment, since the enter probability for this prey-type almost equals the fraction of the total prey biomass concentration that the fish is capable of exploiting by filter-feeding. Although numerous both in the environment and in the stomach of the filter-feeding fish, the individual weight of the smallest prey-type in the diet, *Oithona*, is too low to let them constitute any noticeable fraction of the total prey weight. In contrast, only 0.1% of the members

of the prey community were krill and amphipods, but their contribution in weight is still significant both in the environment and in the diet.

In the simulation, temporal and spatial variations in prey occurrence were not accounted for, while in reality, prey distributions are often patchy and vary during a diel cycle (Pinel-Alloul, 1995; Langøy *et al.*, 2012). Krill do for example form dense aggregations in some places at some times, but may be absent in other instances (Kaartvedt *et al.*, 2005; Eriksen *et al.*, 2016). During daylight hours when conditions are optimal for bite-feeding, krill and amphipods have mostly migrated to deeper waters to take refuge from visual predators (Falk-Petersen *et al.*, 2008; Kaartvedt, 2010), while mackerel stay near the surface all day (Godø *et al.*, 2004; Nøttestad *et al.*, 2016). In comparison, blue whiting (*Micromesistius poutassou*) generally occur in deeper water than mackerel in the same feeding area of the Norwegian Sea, and they forage mainly on krill and amphipods (Huse, Utne and Fernö, 2012; Langøy *et al.*, 2012; Bachiller *et al.*, 2016). The prediction that bite-feeding mackerel would exclude all other prey-types from their diet unless conditions are very unfavourable is probably not valid as a general statement, but if swarms or even loose aggregations of krill or amphipods are encountered, the fish are expected to specialise on these prey.

The prey composition observed in stomach samples from mackerel in the area is more similar to the diet predicted for filter- than for bite-feeding, but the observed weight percentage of krill and amphipods is considerably higher than predicted for filter-feeding, while the percentages of the remaining prey-types are lower (Fig. 9). The contribution of krill and amphipods in the observed diet also clearly exceeded the weight percentage in the ambient environment, implying that the fish spent enough time bite-feeding to more than outweigh the decrease in predation pressure on this prey-type associated with filter-feeding. The observed diet thus resembles a combination of the diets predicted for each of the two feeding modes, but exactly how much of the total feeding time the fish would allocate to either of them is difficult to ascertain, since predictions are uncertain. It should also be noted that the observed weights were dry while the predicted ones were wet, and the ratios between these weight measures are quite variable. Still, the model results clearly demonstrate that the overall predation pressure on different segments of the prey community and the resulting diet composition are highly dependent on how the fish switches between bite- and filter-feeding in the course of a day. Under conditions favouring filter-feeding, small prey-types with weak escape reactions are most vulnerable, whereas larger, energy rich prey-types are most at risk when adequate light and scarcity of prey encourage bite-feeding.

In species alternating between feeding-modes, the relative contribution of each prey-type may vary predictively across their geographical distribution. Maybe Atlantic mackerel inhabiting crystal-clear waters of the oligotrophic Mediterranean Sea spend relatively more of their time bite-feeding than conspecifics located in turbid and nutrient-rich waters such as the North Sea. Moreover, coastal areas at high latitudes are subject to climate-driven water darkening due to increased runoff of dissolved organic matter (DOM) from terrestrial sources (Opdal, Lindemann and Aksnes, 2019), which may cause the fish to resort more to filter-feeding, relieving some of the pressure on large prey. To better evaluate how planktivorous fishes regulate prey populations and structure zooplankton communities in different regions and changing environments, it is thus important to understand the switching dynamics of the species.

3.2 PILCHARD FEEDING IN EXPERIMENTAL TANKS

When simulating experiments conducted by van der Lingen (1994), where schools of pilchard were fed prey of different size and density and the resulting feeding activity monitored, predicted results vary depending on how the fish in the individual-based model is assumed to represent the multiple fish in the tank.

3.2.1 Comparison of predicted and observed prey density in feeding trials

When the individual fish represents the average of the whole observed school of pilchard bite-feeding on wild *Calanus agulhensis* adults (version 1 of the simulation), the prey density N_{tot} in the tank is predicted to decrease more slowly than observed in the experiment (Fig. 10). Even so, the predicted change in prey density with time corresponds far better with observed values than what is the case if the individual fish is assumed to only represent feeding members of the school (version 2). According to this alternative simulation, the modelled fish will only manage to consume 12% of the prey present in the tank before the feeding trial is over, while in the experiment about 98% of the prey were eaten when averaged over several replicated trials (van der Lingen, 1994). In contrast, total prey consumption predicted in version 1 nearly equals the observed percentage, and the fish terminate feeding almost halfway through the trial, shortly after all the 15 fish in the school had ceased feeding in most of the experimental replicates.

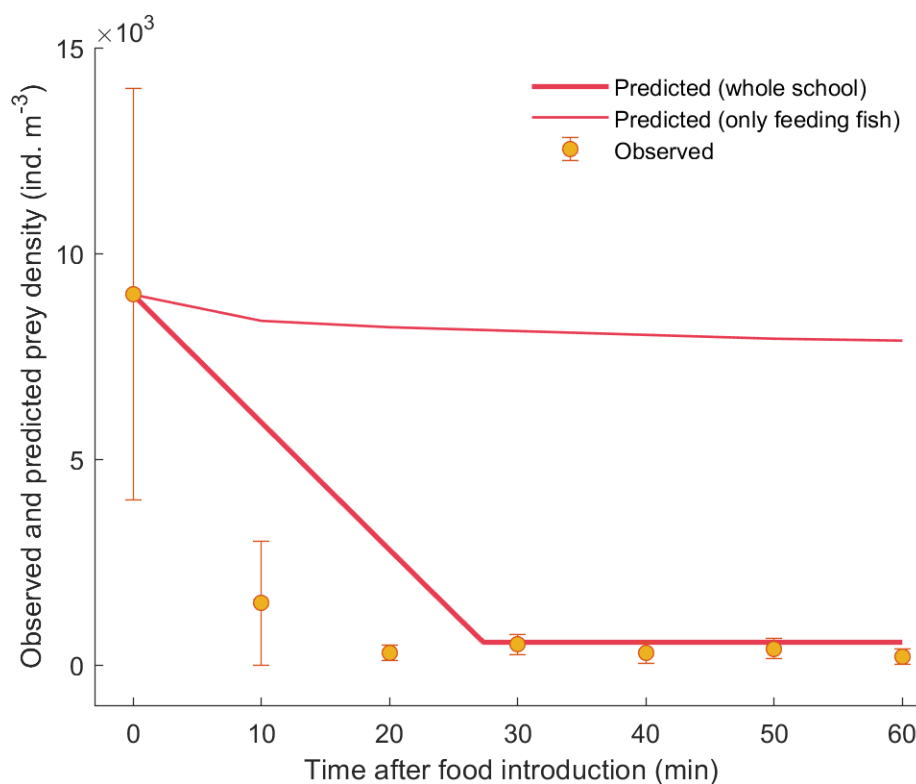


Fig. 10. Observed and predicted prey density at different times after food introduction in feeding trials with pilchard bite-feeding on wild *Calanus agulhensis* adults (van der Lingen, 1994). Means \pm 2 SD for the observations are shown.

The observed feeding intensity was not very high at the start of the feeding trial either—the percentage of school feeding decreased from 35 to 5% already during the first 10 min (van der Lingen, 1994). The low feeding intensity explains the large difference between results from the two simulation versions, but it is not straightforward to explain why the predicted prey densities fit observations best if the feeding rate of the ideal fish is multiplied with the total number of fish in the tank. Even then, the predicted consumption rate is lower than observed, although only a minority of the fish were actually feeding in the experiment. Underestimation of the search rate is probably not the cause for this disparity, for as the linear decrease in prey density reveals, the simulated fish spend almost all their

time handling prey as long as they are feeding (Fig. 10). It is possible that the capture probability P_c is underestimated and the handling time h overestimated, but still it is difficult to comprehend the very large discrepancy between observed and predicted results when only feeding fish are included in the calculations.

Maybe the key to the conundrum is to appreciate the role that schooling behaviour might have in shaping the feeding process. When fish are bite-feeding, the pattern of schooling is less rigid than when they are filter-feeding, since individual fish often must alter speed and direction to pursue selected prey (van der Lingen, 1995). Still, the fish form an aggregation that may allow them to function as a coherent whole, and the chance that any individual prey will be attacked and captured is perhaps higher if it is approached by a shoal than if it is subject to randomly spaced fish feeding wholly independently of each other. It is hard to circumvent multiple possible attackers at once, and if a prey survives an initial attack from one fish, it might be easier for a neighbouring fish to capture it subsequently. Furthermore, it is not given that non-feeding fish were so locked in this state that they would not occasionally snatch easy prey when given the opportunity, and the high capture probability for such attacks would increase the consumption rate above the predicted level. Whatever the explanation may be, the initial prey density in the experimental replicates besides varied highly (Fig. 10, van der Lingen, 1994), which makes the comparison between model and experimental results uncertain. Another source of uncertainty is that the number of fish feeding during a time interval was calculated in the simulation as the average between the observations at two consecutive timepoints, while in reality the decline in feeding intensity could have been nonlinear.

When the fish filter-feed on *Artemia franciscana* nauplii, which are too small for bite-feeding, the predicted prey densities correspond well with observations (Fig. 11). For the first 10 min of the feeding trial, the fit is closest if only feeding fish are included in the simulation, while for the rest of the trial, predictions agree better with observations if the fish instead represent the average of the whole school. The difference between the two set of predictions is however very small, which can be attributed to the relatively high feeding intensity in the first part of the trial (van der Lingen, 1994). About 85% of the school members were initially feeding, but the percentage dropped to well below 10% midway through when few prey were left, increasing the difference between predictions slightly for the second half. It would therefore be premature to conclude that the predictive ability of the model is better for filter-feeding than for bite-feeding, even though the results from the filter-feeding submodel are more in accordance with observations. Moreover, the enter probability in the filter-feeding simulation was adjusted to make the model predictions conform with observations, and although the prey are very small (mean length 47.87×10^{-4} m) and have reduced escape ability because they are cultivated, it could have been set too high ($P_e = 0.9$). Besides, the much higher prey densities in the filter-feeding experiment reduced the influence of variation (van der Lingen, 1994), which partly obscured the results for bite-feeding.

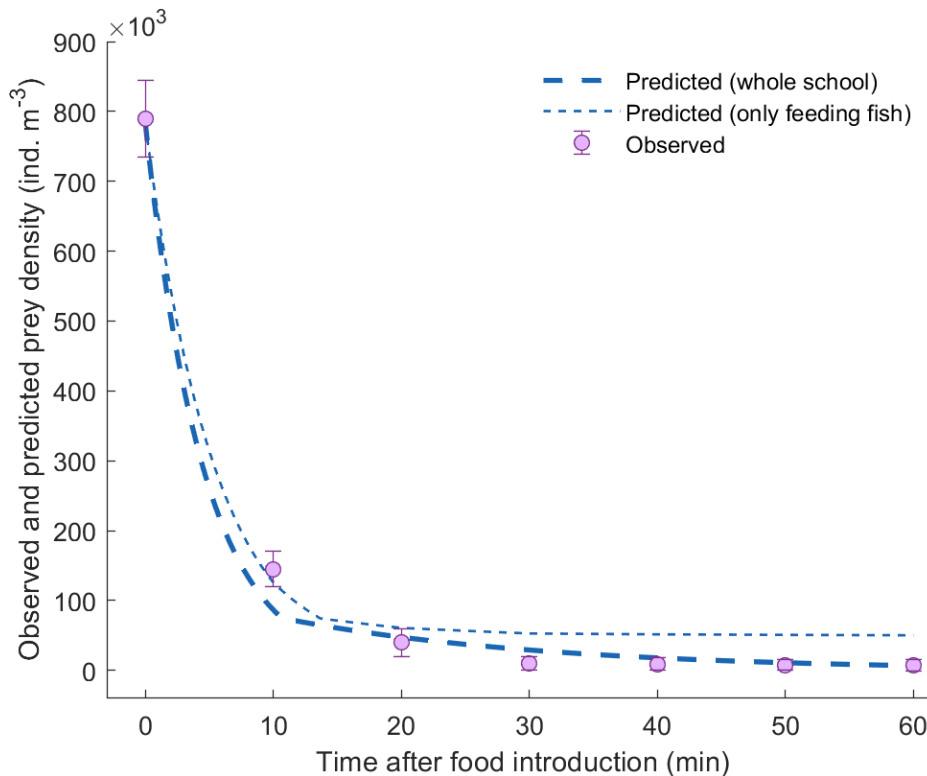


Fig. 11. Observed and predicted prey density at different times after food introduction in feeding trials with pilchard filter-feeding on cultivated *Artemia franciscana* nauplii (van der Lingen, 1994). Means \pm 2 SD for the observations are shown.

To save energy, schooling fish form a hydrodynamically advantageous configuration where individuals are positioned diagonally to each other (Weihs, 1973; van der Lingen, 1995). This formation, which is denser during filter-feeding than bite-feeding, probably facilitates the engulfment of encountered prey, but it is also conceivable that the prey density will be higher at the front than at the rear of the school as a result of the feeding activity (O’Connell, 1972). The rearmost fish would then be at a disadvantage to those located at the front, which besides have better overview of the prey field. Whether total consumption rate for the school as a whole is higher or lower than it would have been were the fish feeding independently as assumed in the model, is difficult to say. Schooling may perhaps involve a trade-off between feeding opportunity and predator defence (Partridge, 1982), since centrally positioned school members have reduced access to prey. Reduced feeding opportunity might also partly be the reason why only some of the fish were feeding, even when prey density was very high.

3.2.2 Comparison of predicted and observed swimming speed in feeding trials

For the whole duration of the feeding trial, the optimal swimming speed v_b for pilchard bite-feeding on *Calanus agulhensis* is predicted to be the lowest alternative in the predetermined set of possible speeds (Fig. 12), which were chosen based on experimental data (van der Lingen, 1995). This is true whether the individual fish is considered the average of the whole school or only feeding fish. The reason why the fish are swimming so slowly is that the net rate of energy N_{pf} gained from handling the prey is very low—negative in fact—and just barely exceeding the negative of the routine metabolic rate M_r (Eq. 20). For the fish to even initiate feeding, the capture probability was set higher ($P_c = 0.72$) than it was for copepods of similar length (2.5×10^{-3} m) in the simulation model for mackerel ($P_c = 0.5$). To

save energy, the simulated pilchard reduce their swimming speed, which in contrast to the optimised speed for mackerel is not composed of distinct speeds v_s and v_h for the search and handling phases of bite-feeding. Had the swimming speed instead been constant for the handling phase and only optimised for the search phase, the overall speed would have been higher (assuming higher speed for handling than the lowest possible for searching), as the fish spent most of their feeding time handling prey. In this particular case of bite-feeding pilchard, the metabolic rate M_b would then have been too high compared to the intake rate I_b to allow feeding (Eq. 15).

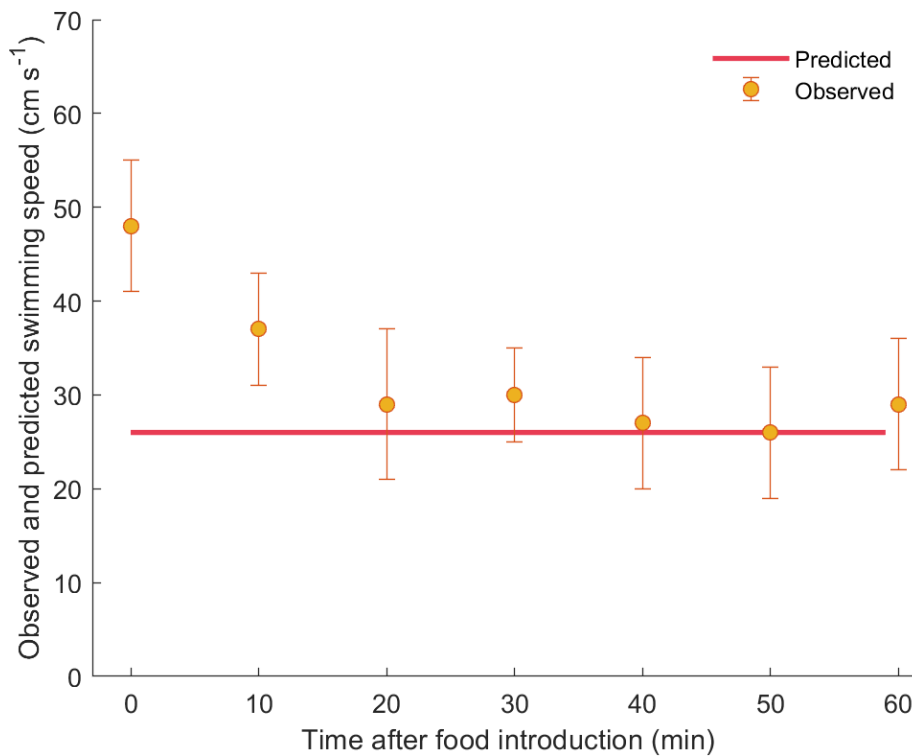


Fig. 12. Observed and predicted swimming speed at different times after food introduction in feeding trials with pilchard bite-feeding on wild *Calanus agulhensis* adults (van der Lingen, 1994). Means \pm 2 SD for the observations are shown.

The observed mean swimming speed of all the fish in the tank was higher than predicted for the first part of the feeding trial, but it decreased towards predicted levels as prey density declined (Fig. 12). The main reason for the decrease in swimming speed is probably that the relatively high prey density early in the trial encouraged more of the fish to feed actively (van der Lingen, 1994). Since swimming speed is higher for feeding than non-feeding activity, decline in feeding intensity would reduce the mean speed. This does however not explain why the feeding members of the school were swimming at a much higher speed than predicted, but it is likely a consequence of both the underestimated intake rate and the lack of distinction between the search and the handling phase when optimising swimming speed. Besides too low rate of prey intake (Fig. 11), the net intake rate ϵ_b , which is the parameter to be maximised by the optimal foraging fish, could also have been underestimated if the proportion of the consumed energy made available for use was set too low (Eq. 14). The metabolic rate however is probably not decisive, as special regression equations for pilchard were used (van der Lingen, 1995).

When pilchard filter-feed on *Artemia franciscana* nauplii, net intake rate is higher than when they bite-feed on *Calanus agulhensis*, and they can thus afford to spend more energy. High prey density in the

beginning of the feeding trial makes it profitable to invest more in faster swimming and thereby higher prey consumption (Fig. 13). Since intake rate from filter-feeding does not affect handling time, it increases linearly with swimming speed. Measured in absolute rate of energy intake, the fish thus have more to gain from increasing swimming speed when they are filter-feeding than when they are bite-feeding, unless searching occupies most of the bite-feeding time. For pilchard the metabolic rate besides increases less with swimming speed for filter- than for bite-feeding (van der Lingen, 1995), and net rate of energy intake therefore also responds more to changes in swimming speed when the fish are filter-feeding. This is reflected by higher observed and simulated difference between swimming speeds early and late in the feeding trial for filter- than for bite-feeding (Figs. 12-13).

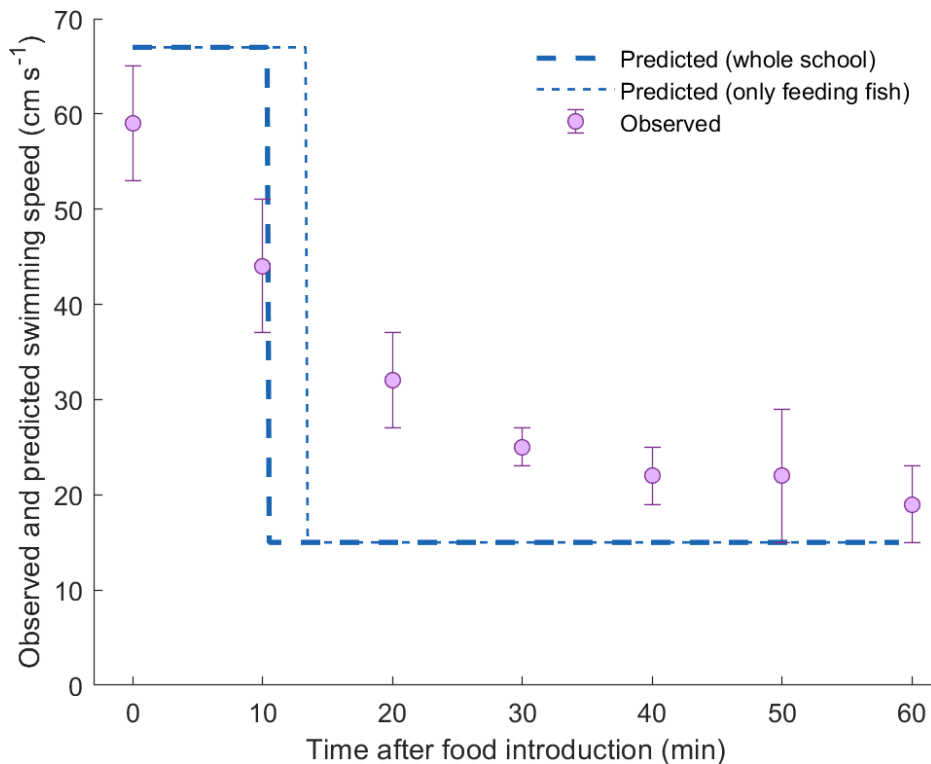


Fig. 13. Observed and predicted swimming speed at different times after food introduction in feeding trials with pilchard filter-feeding on cultivated *Artemia franciscana* nauplii (van der Lingen, 1994). Means \pm 2 SD for the observations are shown.

Predicted swimming speeds for filter-feeding agree better with observations than the speeds predicted for bite-feeding do, probably because there is no need to distinguish between different phases of the feeding process, as ideally should have been done when optimising the bite-feeding swimming speed. Still, the predicted swimming speed does not decrease gradually as the observed mean speed does (Fig. 13). According to the simulation model, where linear respiration equations were used instead of exponential, the fish should swim as fast as possible as long as net intake rate increases with swimming speed, and as slowly as possible when it decreases with speed. The predicted swimming speed therefore drops momentarily from highest to lowest possible value when prey density becomes so low that net intake rate starts to decrease with swimming speed. At this timepoint the rate of prey consumption decreases abruptly (Fig. 12). The drop in swimming speed occurs later when the individual fish represents the average of only feeding fish instead of the whole school (Fig. 13), since prey density then increases more slowly due to lower consumption rate.

3.3 SENSITIVITY ANALYSIS

The bite- and filter-feeding submodels differ in their sensitivity to variations in most of the parameters tested (Fig. 14). In both submodels, percent change in net weight-specific intake rate e_b or e_f as a function of percent change in parameter value is highest when varying the fish length L , but the response to changing length is greatest for bite-feeding. Since larger fish are heavier, weight-specific intake rate is negatively correlated with length. However, both the visual capacity E' and the mouth gape area A_g increase nonlinearly with length, and the response in intake to increasing length is therefore less negative for larger fish. At the fixed parameter values chosen for the simulation ($E_z = 1.2 \times 10^{-3} \mu\text{E m}^{-2} \text{s}^{-1}$, $N_{\text{tot}} = 1.9 \times 10^4 \text{ ind. m}^{-3}$, 0.1% krill and amphipods), mouth area limits intake from filter-feeding more than visual capacity limits intake from bite-feeding, which may explain why the filter-feeding intake rate decreases less with length. The sharp decline in intake rate with length is probably not realistic, for larger fish have better swimming abilities. Higher capture probability and lower handling time for larger fish would benefit bite-feeding, and higher maximum swimming speed would increase absolute intake rate from filter-feeding.

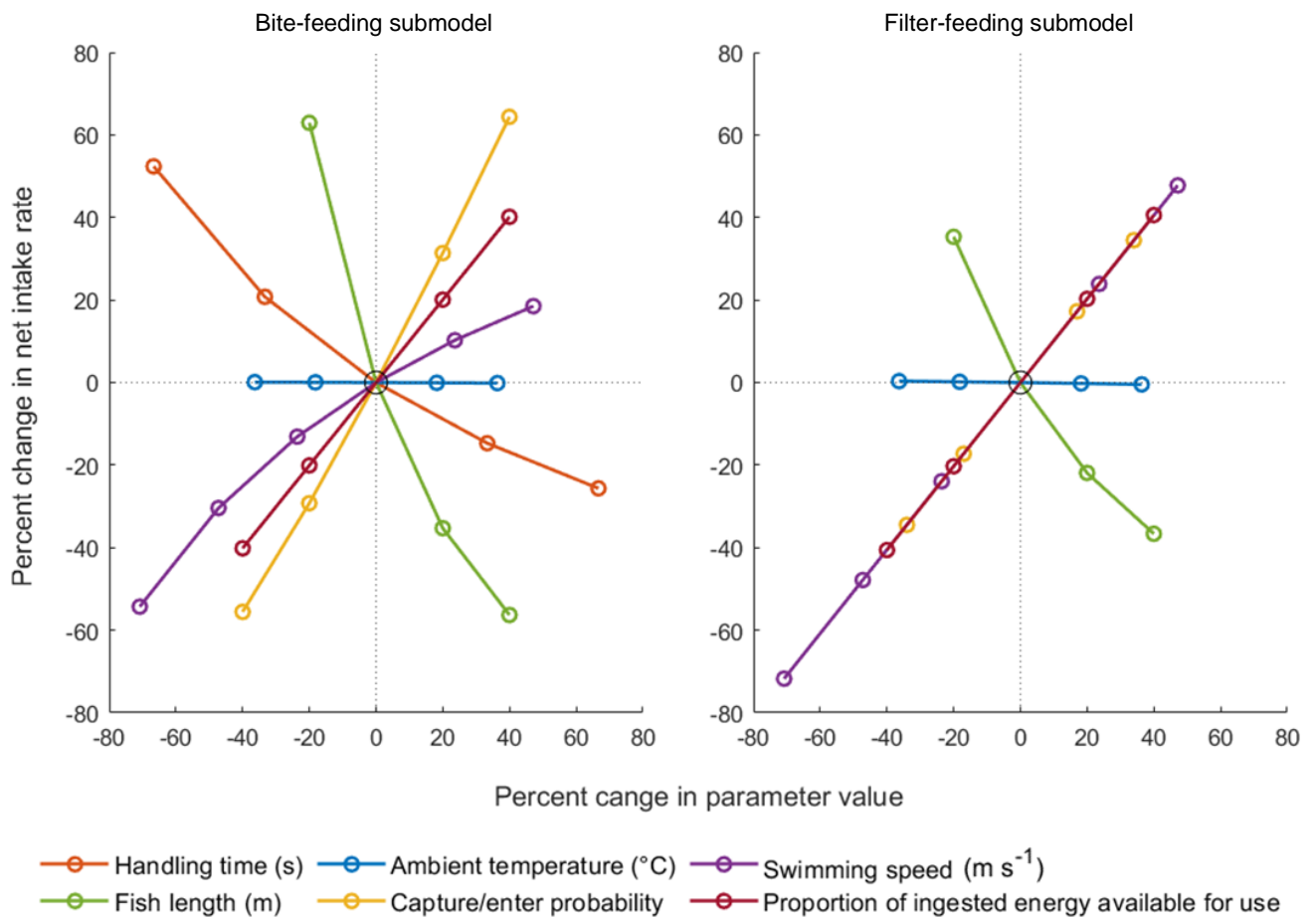


Fig. 14. Sensitivity of bite- and filter-feeding submodels to variations in selected parameter values over realistic ranges. Analyses were performed using simulation model for mackerel with fixed values for irradiance and prey density and composition ($E_z = 1.2 \times 10^{-3} \mu\text{E m}^{-2} \text{s}^{-1}$, $N_{\text{tot}} = 1.9 \times 10^4 \text{ ind. m}^{-3}$, and 0.1% of the prey were krill and amphipods). When testing a parameter, the others were held constant at their default values. Only the swimming speed v_s for the search phase was tested for the bite-feeding model.

Changes in temperature T have no appreciable effect on net intake rate in either of the submodels (Fig. 14). The metabolic rate M increases exponentially with temperature (Eq. 11), but at the parameter values chosen in the simulation, metabolic rate is too small compared to the intake rate to matter. In reality, however, it is possible that net intake rate could slightly increase with temperature. Although higher temperature leads to higher metabolic rate, the optimal swimming speed rises exponentially with temperature at low values (Ware, 1978; Stewart *et al.*, 1983). The density and viscosity of the water decreases with temperature, hence the drag imparted on the fish declines, allowing higher swimming speeds and thereby higher intake rates for a given metabolic rate. These relationships are not accounted for in the model.

The filter-feeding submodel is equally sensitive to changes in swimming speed v_f , enter probability P_e and the proportion u of ingested energy made available for use (Fig. 14). Net intake rate from filter-feeding increases linearly with all these parameters at the chosen prey density and composition (Eqs. 24 and 26). If prey density and the proportion of krill and amphipods had been low enough, net intake rate would instead have decreased with swimming speed. Net intake rate from bite-feeding increases linearly with capture probability P_c and the proportion of ingested energy available for use, but the positive response to increasing search swimming speed v_s declines at higher speeds due to increasing handling time limitations (Eqs. 9 and 14). The bite-feeding submodel is more sensitive to variations in capture probability than the filter-feeding submodel is to variations in enter probability, for the prey-specific handling time h is inversely related to capture probability (Eq. 8).

The bite-feeding submodel is most sensitive to variations in handling time when it is low (Fig. 14). Searching then occupies so much of the time that the rate of prey encountered is significantly reduced when handling time increases (Eq. 6c). When it takes long time to handle prey, little time is left for searching, and the encounter rate does not respond much to increases in handling time. Still, net intake rate declines since fewer prey can be handled and eaten per unit time spent handling prey.

4 CONCLUSIONS

The ability to switch between bite- and filter-feeding is an important behavioural adaptation that combined with prey selection and regulation of swimming speed allow planktivorous fishes to more optimally exploit available prey as environmental conditions change. According to model predictions, bite-feeding is the most efficient feeding mode at low prey densities unless ambient irradiance limits vision too much. However, as more prey are encountered, the fish soon spends so much of the time handling prey that intake rate levels off. Conversely, intake rate from filter-feeding increases unabated with prey density and will eventually surpass the bite-feeding intake rate, encouraging switching. This happens at lower prey density if irradiance decreases enough to significantly limit visual foraging or if the proportion of valuable prey increases. Filter-feeding persistently increases with the proportion of large prey unless filtration efficiency is too low, but for bite-feeding the response is limited by handling time. Since bite-feeding fish only select the most valuable prey, which often are too evasive to constitute much of the filter-feeding diet, overall diet composition of the fish largely depends on how much of the time the fish spends on each feeding mode.

Metabolic rate is usually too low compared to net intake rate to significantly influence switching, but it is important in determining which prey-types bite-feeding fish will forage on. Nor do the proportion of ingested energy made available for use affect switching points much, for net intake rate of both feeding modes increases linearly with this parameter. Assuming that mean swimming speed during prey handling does not vary with environmental conditions, optimising swimming speed will benefit filter-feeding more than bite-feeding. Evasiveness of prey greatly influences intake rate from both feeding modes, but bite-feeding is especially sensitive to variations in capture probability. When comparing model results with experimental observations, it became clear that schooling behaviour must play a central role in determining foraging efficiency. For both feeding-modes, predicted prey consumption fit observations best if the individual fish represented the average of the whole school, even though only some of the fish were actively feeding. We know that schooling fish do not feed independently of each other, but the mechanisms by which schooling affects intake rate of individual fish are poorly understood. If effects of schooling behaviour could be incorporated into mechanistic formulations that also include the attack or engulfment process of foraging, we would further improve our understanding of the mechanisms regulating intake rates and switching dynamics.

REFERENCES

- Aksnes, D. L. and Giske, J. (1993) 'A theoretical model of aquatic visual feeding', *Ecological Modelling*. doi: 10.1016/0304-3800(93)90007-F.
- Aksnes, D. L. and Utne, A. C. W. (1997) 'A revised model of visual range in fish', *Sarsia*. doi:10.1080/00364827.1997.10413647.
- Bachiller, E. *et al.* (2016) 'Feeding ecology of Northeast Atlantic Mackerel, Norwegian spring-spawning herring and blue whiting in the Norwegian Sea', *PLoS ONE*. doi: 10.1371/journal.pone.0149238.
- Bachiller, E. *et al.* (2018) 'Bioenergetics modeling of the annual consumption of zooplankton by pelagic fish feeding in the Northeast Atlantic', *PLoS ONE*. doi: 10.1371/journal.pone.0190345.
- Batty, R. S., Blaxter, J. H. S. and Libby, D. A. (1986) 'Herring (*Clupea harengus*) filter-feeding in the dark', *Marine Biology*. doi: 10.1007/BF00428631.
- Batty, R. S., Blaxter, J. H. S. and Richard, J. M. (1990) 'Light intensity and the feeding behaviour of herring, *Clupea harengus*', *Marine Biology*. doi: 10.1007/BF01313419.
- Van den Berg, C. *et al.* (1993) 'Shape of zooplankton and retention in filter-feeding - a quantitative comparison between industrial sieves and the branchial sieves of common bream (*Abramis brama*) and white bream (*Blicca bjoerkna*)', *Canadian Journal of Fisheries and Aquatic Sciences*.
- Boisclair, D. and Tang, M. (1993) 'Empirical analysis of the influence of swimming pattern on the net energetic cost of swimming in fishes', *Journal of Fish Biology*. doi: 10.1111/j.1095-8649.1993.tb00319.x.
- Breck, J. E. (1993) 'Foraging Theory and Piscivorous Fish: Are Forage Fish Just Big Zooplankton?', *Transactions of the American Fisheries Society*. doi: 10.1577/15488659(1993)122<0902:FTAPF A>2.3.CO;2.
- Breck, J. E. and Gitter, M. J. (2008) 'Effect of Fish Size on the Reactive Distance of Bluegill (*Lepomis macrochirus*) Sunfish', *Canadian Journal of Fisheries and Aquatic Sciences*. doi: 10.1139/f83-026.
- Brooks, H. *et al.* (2018) 'Physical modeling of vortical cross-step flow in the American paddlefish, *Polyodon spathula*', *PLoS ONE*. doi: 10.1371/journal.pone.0193874.
- Caparroy, P., Thygesen, U. H. and Visser, A. W. (2000) 'Modelling the attack success of planktonic predators: patterns and mechanisms of prey size selectivity', *Journal of Plankton Research*. doi: 10.1093/plankt/22.10.1871.
- Carey, N. and Goldbogen, J. A. (2017) 'Kinematics of ram filter feeding and beat-glide swimming in the northern anchovy *Engraulis mordax*', *The Journal of Experimental Biology*. doi: 10.1242/jeb.158337.
- Charnov, E. L. (2002) 'Optimal Foraging: Attack Strategy of a Mantis', *The American Naturalist*. doi: 10.1086/283054.
- Cheer, A. *et al.* (2012) 'Computational Fluid Dynamics of Fish Gill Rakers During Crossflow Filtration', *Bulletin of Mathematical Biology*. doi: 10.1007/s11538-011-9709-6.
- Crowder, L. B. (1985) 'Optimal foraging and feeding mode shifts in fishes', *Environmental Biology of Fishes*. doi: 10.1007/BF00007710.
- Crowder, L. B. and Binkowski, F. P. (1983) 'Foraging behaviors and the interaction of alewife, *Alosa pseudoharengus*, and bloater, *Coregonus hoyi*', *Environmental Biology of Fishes*. doi: 10.1007/BF00005177.
- Van Deurs, M., Jørgensen, C. and Fiksen, O. (2015) 'Effects of copepod size on fish growth: A model based on data for North Sea sandeel', *Marine Ecology Progress Series*. doi: 10.3354/meps11092.
- Drenner, R. W. *et al.* (2004) 'Particle Ingestion by *Tilapia galilaea* is Not Affected by Removal of Gill Rakers and Microbranchiospines', *Transactions of the American Fisheries Society*. doi: 10.1577/1548-8659(1987)116<272:pibtgi>2.0.co;2.
- Drenner, R. W., de Noyelles, F. and Kettle, D. (1982) 'Selective impact of filter-feeding gizzard shad on zooplankton community structure', *Limnology and Oceanography*. doi: 10.4319/lo.1982.27.5.0965.
- Drenner, R. W., Strickler, J. R. and O'Brien, W. J. (1978) 'Capture Probability: The Role of Zooplankton Escape in the Selective Feeding of Planktivorous Fish', *Journal of the Fisheries Research Board of Canada*. doi: 10.1139/f78-215.
- Durbin, A. G. and Durbin, E. G. (1975) 'Grazing rates of the Atlantic menhaden *Brevoortia tyrannus* as a function of particle size and concentration', *Marine Biology*. doi: 10.1007/BF00390931.
- Durbin, E. G. and Durbin, A. G. (1983) 'Energy and nitrogen budgets for the Atlantic menhaden, *Brevoortia tyrannus* (Pisces: Clupeidae), a filter-feeding planktivore.', *Fishery Bulletin*.
- Eggers, D. M. (1977) 'The Nature of Prey Selection by Planktivorous Fish', *Ecology*. doi: 10.2307/1935107.
- Ehlinger, T. J. (1989) 'Foraging mode switches in the golden shiner (*Notemigonus crysoleucas*)', *Canadian Journal of Fisheries and Aquatic Sciences*. doi: 10.1093/annonc/mdr384.
- Elliott, J. M. and Davison, W. (1975) 'Energy equivalents of oxygen consumption in animal energetics', *Oecologia*. doi: 10.1007/BF00345305.

- Emlen, J. M. (1966) 'The Role of Time and Energy in Food Preference', *The American Naturalist*. doi: 10.1086/282455.
- Eriksen, E. *et al.* (2016) 'The Barents Sea euphausiids: Methodological aspects of monitoring and estimation of abundance and biomass', *ICES Journal of Marine Science*. doi: 10.1093/icesjms/fsw022.
- Falk-Petersen, S. *et al.* (2008) 'Vertical migration in high Arctic waters during autumn 2004', *Deep-Sea Research Part II: Topical Studies in Oceanography*. doi: 10.1016/j.dsr2.2008.05.010.
- Fall, J. and Fiksen, Ø. (in press) 'No room for dessert: A mechanistic model of prey selection in gut-limited predatory fish', *Fish and Fisheries*. doi: 10.1093/icesjms/fsr036.
- Friedland, K. D., Haas, L. W. and Merriner, J. V. (1984) 'Filtering rates of the juvenile Atlantic menhaden *Brevoortia tyrannus* (Pisces: Clupeidae), with consideration of the effects of detritus and swimming speed', *Marine Biology*. doi: 10.1007/BF00392994.
- Garrido, S. *et al.* (2007) 'Laboratory investigations on the effect of prey size and concentration on the feeding behaviour of *Sardina pilchardus*', *Marine Ecology Progress Series*. doi: 10.3354/meps330189.
- Gibson, R. N. (1988) 'Development, morphometry and particle retention capability of the gill rakers in the herring, *Clupea harengus L.*', *Journal of Fish Biology*. doi: 10.1111/j.1095-8649.1988.tb05438.x.
- Gibson, R. N. and Ezzi, I. A. (1985) 'Effect of particle concentration on filter- and particulate-feeding in the herring *Clupea harengus*', *Marine Biology*. doi: 10.1007/BF00397157.
- Gibson, R. N. and Ezzi, I. A. (1992) 'The relative profitability of particulate- and filter-feeding in the herring, *Clupea harengus L.*', *Journal of Fish Biology*. doi: 10.1111/j.1095-8649.1992.tb02607.x.
- Godø, O. R. *et al.* (2004) 'Behaviour of mackerel schools during summer feeding migration in the Norwegian Sea, as observed from fishing vessel sonars', in *ICES Journal of Marine Science*. doi: 10.1016/j.icesjms.2004.06.009.
- Harvey, H. W. (1937) 'Note on Selective Feeding by *Calanus*', *Journal of the Marine Biological Association of the United Kingdom*. doi: 10.1017/S0025315400011899.
- Hester, F. J. (1968) 'Visual contrast thresholds of the goldfish (*Carassius auratus*)', *Vision Research*. doi: 10.1016/0042-6989(68)90053-9.
- Hettler, W. F. (1976) 'Influence of temperature and salinity on routine metabolic rate and growth of young Atlantic menhaden', *Journal of Fish Biology*. doi: 10.1111/j.1095-8649.1976.tb03907.x.
- Heuch, P. A., Doall, M. H. and Yen, J. (2007) 'Water flow around a fish mimic attracts a parasitic and deters a planktonic copepod', in *Journal of Plankton Research*. doi: 10.1093/plankt/fbl060.
- Heyman, W. D. *et al.* (2001) 'Whale sharks *Rhincodon typus* aggregate to feed on fish spawn in Belize', *Marine Ecology Progress Series*. doi: 10.3354/meps215275.
- Holanov, S. H. and Tash, J. C. (1978) 'Particulate and filter feeding in threadfin shad, *Dorosoma petenense*, at different light intensities', *Journal of Fish Biology*. doi: 10.1111/j.1095-8649.1978.tb03475.x.
- Holling, C. S. (1959) 'Some Characteristics of Simple Types of Predation and Parasitism', *The Canadian Entomologist*. doi: 10.4039/Ent91385-7.
- Holzman, R. and Genin, A. (2005) 'Mechanisms of selectivity in a nocturnal fish: A lack of active prey choice', *Oecologia*. doi: 10.1007/s00442-005-0205-2.
- Hoogenboezem, W. *et al.* (1992) 'A model for switching between particulate-feeding and filter-feeding in the common bream, *Abramis brama*', *Environmental Biology of Fishes*. doi: 10.1007/BF00002549.
- Hoogenboezem, W. *et al.* (2008) 'Prey Retention and Sieve Adjustment in Filter-Feeding Bream (*Abramis brama*) (Cyprinidae)', *Canadian Journal of Fisheries and Aquatic Sciences*. doi: 10.1139/f93-054.
- Huse, G. and Fiksen, Ø. (2010) 'Modelling encounter rates and distribution of mobile predators and prey', *Progress in Oceanography*. doi: 10.1016/j.pocean.2009.09.011.
- Huse, G., Utne, K. R. and Fernö, A. (2012) 'Vertical distribution of herring and blue whiting in the Norwegian Sea', *Marine Biology Research*. doi: 10.1080/17451000.2011.639779.
- James, A. and Findlay, K. (1989) 'Effect of particle size and concentration on feeding behaviour, selectivity and rates of food ingestion by the Cape anchovy *Engraulis capensis*', *Marine Ecology Progress Series*. doi: 10.3354/meps050275.
- James, A. G. (1987) 'Feeding ecology, diet and field-based studies on feeding selectivity of the cape anchovy *Engraulis capensis Gilchrist*', *South African Journal of Marine Science*. doi: 10.2989/025776187784522784.
- James, A. G. and Probyn, T. (1989) 'The relationship between respiration rate, swimming speed and feeding behaviour in the cape anchovy *Engraulis capensis Gilchrist*', *Journal of Experimental Marine Biology and Ecology*. doi: 10.1016/0022-0981(89)90001-4.
- Janssen, J. (1976) 'Feeding modes and prey size selection in the alewife (*Alosa pseudoharengus*)', *Journal of Fisheries Research Board Canada*. doi: 10.1139/f76-251.
- Kaartvedt, S. *et al.* (2005) 'Piscivorous fish patrol krill swarms', *Marine Ecology Progress Series*. doi: 10.3354/meps299001.
- Kaartvedt, S. (2010) Diel Vertical Migration Behaviour of the Northern Krill (*Meganyctiphanes norvegica Sars*), *Advances in Marine Biology*. doi: 10.1016/B978-0-12-381308-4.00009-1.

- Kjørboe, T. (2008) *'A Mechanistic Approach to Plankton Ecology'*. Princeton University Press.
- Kjørboe, T. and Visser, A. W. (1999) 'Predator and prey perception in copepods due to hydromechanical signals', *Marine Ecology Progress Series*. doi: 10.3354/meps179081.
- Kitchell, J. F., Stewart, D. J. and Weininger, D. (1977) 'Applications of a Bioenergetics Model to Yellow Perch (*Perca flavescens*) and Walleye (*Stizostedion vitreum vitreum*)', *Journal of the Fisheries Research Board of Canada*. doi: 10.1139/f77-258.
- Krebs, J. R. *et al.* (1977) 'Optimal prey selection in the great tit (*Parus major*)', *Animal Behaviour*. doi: 10.1016/0003-3472(77)90064-1.
- Langeland, A. and Nøst, T. (1995) 'Gill raker structure and selective predation on zooplankton by particulate feeding fish', *Journal of Fish Biology*. doi: 10.1111/j.1095-8649.1995.tb01937.x.
- Langøy, H. *et al.* (2006) 'Feeding Ecology of Atlantic Mackerel (*Scomber scombrus*) in the Norwegian Sea: Diet, Prey Selection and Possible Food Competition with Herring (*Clupea harengus*) in different Water Masses', *ICES CM 2006/F:12*.
- Langøy, H. *et al.* (2012) 'Overlap in distribution and diets of Atlantic mackerel (*Scomber scombrus*), Norwegian spring-spawning herring (*Clupea harengus*) and blue whiting (*Micromesistius poutassou*) in the Norwegian Sea during late summer', *Marine Biology Research*. doi: 10.1080/17451000.2011.642803.
- Lazzaro, X. (1987) 'A review of planktivorous fishes: Their evolution, feeding behaviours, selectivities, and impacts', *Hydrobiologia*. doi: 10.1007/BF00008764.
- Leong, R. J. H. and O'Connell, C. P. (1969) 'A Laboratory Study of Particulate and Filter Feeding of the Northern Anchovy (*Engraulis mordax*)', *Journal of the Fisheries Research Board of Canada*. doi: 10.1139/f69-053.
- van der Lingen, C. D. (1994) 'Effect of particle size and concentration on the feeding behaviour of adult pilchard *Sardinops sagax*', *Marine Ecology Progress Series*. doi: 10.3354/meps109001.
- van der Lingen, C. D. (1995) 'Respiration rate of adult pilchard *Sardinops sagax* in relation to temperature, voluntary swimming speed and feeding behaviour', *Marine Ecology Progress Series*. doi: 10.3354/meps129041.
- Lovvorn, J. R., Baduini, C. L. and Hunt, G. L. (2001) 'Modeling underwater visual and filter feeding by planktivorous shearwaters in unusual sea conditions', *Ecology*. doi: 10.1890/0012-9658(2001)082[2342:MUVAFF]2.0.CO;2.
- Luo, J., Brandt, S. B. and Klebasko, M. J. (1996) 'Virtual reality of planktivores: A fish's perspective of prey size selection', *Marine Ecology Progress Series*. doi: 10.3354/meps140271.
- MacArthur, R. H. and Pianka, E. R. (1966) 'On Optimal Use of a Patchy Environment', *The American Naturalist*. doi: 10.1086/282454.
- Macy, W. K., Durbin, A. G. and Durbin, E. G. (1999) 'Metabolic rate in relation to temperature and swimming speed, and the cost of filter feeding in Atlantic menhaden, *Brevoortia tyrannus*', *Fishery Bulletin*.
- Macy, W. K., Sutherland, S. J. and Durbin, E. G. (1998) 'Effects of zooplankton size and concentration and light intensity on the feeding behavior of Atlantic mackerel *Scomber scombrus*', *Marine Ecology Progress Series*. doi: 10.3354/meps172089.
- Molina, R. E., Manrique, F. A. and Velasco, H. E. (1996) 'Filtering apparatus and feeding of the pacific mackerel (*Scomber japonicus*) in the Gulf of California', *California Cooperative Oceanic Fisheries Investigations Reports*.
- Mummert, J. R. and Drenner, R. W. (2004) 'Effect of Fish Size on the Filtering Efficiency and Selective Particle Ingestion of a Filter-Feeding Clupeid', *Transactions of the American Fisheries Society*. doi: 10.1577/1548-8659(1986)115<522:eofsot>2.0.co;2.
- Murdoch, W. W. *et al.* (1975) 'Switching in Predatory Fish', *Ecology*.
- Nøttestad, L. *et al.* (2016) 'Feeding strategy of mackerel in the Norwegian Sea relative to currents, temperature, and prey', *ICES Journal of Marine Science*. doi: 10.1093/icesjms/fsv239.
- O'Connell, C. P. (1972) 'The Interrelation of Biting and Filtering in the Feeding Activity of the Northern Anchovy (*Engraulis mordax*)', *Journal of the Fisheries Research Board of Canada*. doi: 10.1139/f72-047.
- O'Connell, C. P. and Zweifel, J. R. (1972) 'A laboratory study of particulate and filter feeding of the pacific mackerel, *Scomber japonicus*', *Fishery Bulletin*. doi: 10.1006/jfbi.1999.1222.
- Opdal, A. F., Lindemann, C. and Aksnes, D. L. (2019) 'Centennial decline in North Sea water clarity causes strong delay in phytoplankton bloom timing', *Global Change Biology*. doi: 10.1111/gcb.14810.
- Partridge, B. L. (1982) 'The structure and function of fish schools', *Scientific American*. doi: 10.1038/scientificamerican0682-114.
- Pepin, P., Koslow, J. A. and Pearre Jr., S. (1988) 'Laboratory Study of Foraging by Atlantic Mackerel, *Scomber scombrus*, on Natural Zooplankton Assemblages', *Canadian Journal of Fisheries and Aquatic Sciences*. doi: 10.1139/f88-106.
- Pinel-Alloul, P. (1995) 'Spatial heterogeneity as a multiscale characteristic of zooplankton community', *Hydrobiologia*. doi: 10.1007/BF00024445.

- Potvin, J., Goldbogen, J. A. and Shadwick, R. E. (2010) 'Scaling of lunge feeding in rorqual whales: An integrated model of engulfment duration', *Journal of Theoretical Biology*. doi: 10.1016/j.jtbi.2010.08.026.
- Pyke, G. H. (1984) 'Optimal Foraging Theory: A Critical Review', *Annual Review of Ecology and Systematics*. doi: 10.1146/annurev.es.15.110184.002515.
- Rohner, C. A. *et al.* (2013) 'Diet of whale sharks *Rhincodon typus* inferred from stomach content and signature fatty acid analyses', *Marine Ecology Progress Series*. doi: 10.3354/meps10500.
- Sanderson, S. L., Cech, J. J., Cheer, A. Y. (1994) 'Paddlefish buccal flow velocity during ram suspension feeding and ram ventilation', *The Journal of experimental biology*.
- Sanderson, S. L. *et al.* (2001) 'Crossflow filtration in suspension-feeding fishes', *Nature*. doi: 10.1038/35086574.
- Sanderson, S. L. *et al.* (2016) 'Fish mouths as engineering structures for vortical cross-step filtration', *Nature Communications*. doi: 10.1038/ncomms11092.
- Sanderson, S. L. and Cech, J. J. (1992) 'Energetic Cost of Suspension Feeding versus Particulate Feeding by Juvenile Sacramento Blackfish', *Transactions of the American Fisheries Society*. doi: 10.1577/1548-8659(1992)121<0149:ECOSFV>2.3.CO;2.
- Sanderson, S. L., Cech, J. J. and Patterson, M. R. (1991) 'Fluid dynamics in suspension-feeding blackfish', *Science*. doi: 10.1126/science.251.4999.1346.
- Siddiqui, K. A. and Banerjee, A. K. (1975) 'Physical mechanisms and rates of particle capture by suspension-feeders', *Folia microbiologica*.
- Simon, M. *et al.* (2009) 'Behaviour and kinematics of continuous ram filtration in bowhead whales (*Balaena mysticetus*)', *Proceedings of the Royal Society B: Biological Sciences*. doi: 10.1098/rspb.2009.1135.
- Sims, D. W. (1999) 'Threshold foraging behaviour of basking sharks on zooplankton: Life on an energetic knife-edge?', *Proceedings of the Royal Society B: Biological Sciences*. doi: 10.1098/rspb.1999.0798.
- Smith, J. C. and Sanderson, S. L. (2013) 'Particle retention in suspension-feeding fish after removal of filtration structures', *Zoology*. doi: 10.1016/j.zool.2013.08.008.
- Stearns, S. C. and Schmid-Hempel, P. (2006) 'Evolutionary Insights Should Not Be Wasted', *Oikos*. doi: 10.2307/3565561.
- Stewart, D. J. *et al.* (1983) 'An Energetics Model for Lake Trout, *Salvelinus namaycush* : Application to the Lake Michigan Population', *Canadian Journal of Fisheries and Aquatic Sciences*. doi: 10.1139/f83-091.
- Varpe, Ø. and Fiksen, Ø. (2010) 'Seasonal plankton-fish interactions: Light regime, prey phenology, and herring foraging', *Ecology*. doi: 10.1890/08-1817.1.
- Visser, A. W. (2001) 'Hydromechanical signals in the plankton', *Marine Ecology Progress Series*. doi: 10.3354/meps222001.
- Visser, A. W. and Fiksen, O. (2013) 'Optimal foraging in marine ecosystem models: Selectivity, profitability and switching', *Marine Ecology Progress Series*. doi: 10.3354/meps10079.
- Vogel, S. (1994) *Life in moving fluids: The physical biology of flow, Second edition, Life in moving fluids: The physical biology of flow, Second edition*. Princeton University Press.
- Ware, D. M. (1975) 'Growth, Metabolism, and Optimal Swimming Speed of a Pelagic Fish', *Journal of the Fisheries Research Board of Canada*. doi: 10.1139/f75-005.
- Ware, D. M. (1978) 'Bioenergetics of Pelagic Fish: Theoretical Change in Swimming Speed and Ration with Body Size', *Journal of the Fisheries Research Board of Canada*. doi: 10.1139/f78-036.
- Weihs, D. (1973) 'Hydromechanics of fish schooling', *Nature*. doi: 10.1038/241290a0.
- Yowell, D. W. and Vinyard, G. L. (1993) 'An energy-based analysis of particulate-feeding and filter-feeding by blue tilapia, *Tilapia aurea*', *Environmental Biology of Fishes*. doi: 10.1007/BF00005980.

APPENDIX 1 – MATLAB code for simulation of mackerel foraging

```
%% BITE-FEEDING AND FILTER-FEEDING
%*****

% The model compares net specific energy intake for fish bite-feeding and filter-feeding
% at varying light conditions and prey densities and compositions. Irradiance is modelled
% as a function of depth, surface irradiance and chlorophyll concentration. The prey is
% divided into individual categories with different sets of parameter values, and diet
% breadth and swimming speeds are optimised to maximise net energy return. The model also
% explores the effect of temperature, fish size and handling time. Values of R, which is
% the detection range of a visual predator, are calculated separately in Fortran and read
% from R-tables into Matlab. The model is parametrised for Atlantic mackerel (Scomber
% scombrus) feeding in Atlantic waters in the Norwegian Sea during summer.

close all;
clear all;

%% PARAMETERS

%% Parameters for environment

Z = 10; % depth (m) where the fish is located (Nøttestad et al., 2016; Bachiller et al., 2018)
Chla = 1; % concentration of chl a (mg/m^3) (Bagøien, Melle and Kaartvedt, 2012)
BeamAtt = 0.066 + 0.39*Chla^0.57*0.93; % beam attenuation coefficient (m^-1) (Mobley, 1994)
DiffAtt = 0.125 + Chla*(0.0506*exp(-0.606*Chla) + 0.0285); % diffuse attenuation coefficient (m^-1) (Mobley, 1994)
E0 = logspace(-6,3,50); % range of surface irradiances (μE/m^2/s)
Ez = E0*exp(-DiffAtt*Z); % irradiance at depth Z (μE/m^2/s) (Aksnes and Utne, 1997)
T = 11; % either: default ambient temperature (°C) (Bagøien, Melle and Kaartvedt, 2012)
%T = 7:2:13; % or: range of temperatures (°C) (for sensitivity analysis)

%% Parameters for prey

PreyC = 1:5; % prey categories
```

```

Ntot = logspace(0,6,50); % range of total prey concentrations (ind./m^3)
Ctr = 0.3; % inherent contrast of prey (Utne-Palm, 1999)
pi = 4*atan(1); % value of pi
Fc = 0.8; % fraction of plan area of prey that is visible core area
Apscale = (pi/8)*(1.5*10^-3)^2*Fc; % image area of small prey (m^2) (for scaling)
p1 = [0.001,0.003]; % range of proportions of prey category 1 (krill and amphipods) to total number of prey
vp = 1:length(p1); % elements in p1 vector
dfvp = 1; % element in p1 vector that gives default value (0.001)

% Parameters for prey category 1 (krill and amphipods)

l(1) = 0.025; % length of prey (m) approximated from data on different species (Agersted and Nielsen, 2014; Sirenko
et al., 2019)
d(1) = 4700; % energy density of prey (J/(g wet weight)) approximated from data on different species and assuming
that dry weight is 24% of wet weight (Percy and Fife, 1981; Kulka and Corey, 1982; Schaafsma et al., 2018)
p(1,vp) = p1(vp); % proportion of prey category to total number of prey (only fractional)
Pc(1) = 0.29; % capture probability (fraction of attacked prey that fish succeeds in capturing)
Pe(1) = 0.09; % enter probability (probability that prey on the trajectory of the fish will enter the mouth)
wpctEmp(1) = 30; % observed dry weight percentage of prey category in stomach samples (Langøyet al., 2006)

% Parameters for prey category 2 (calanoid copepods (mostly Calanus finmarchicus))

l(2) = 2.5*10^-3; % length of prey (prosoma length (m)) (Hirche et al., 1994; Choquet et al., 2018)
d(2) = 4500; % energy density of prey (J/(g wet weight)) assuming that dry weight is 16% of wet weight (Davies,
Ryan and Taggart, 2012; Davis, 1993)
p(2,vp) = 0.11*(1 - p1(vp)); % proportion of prey category to total number of prey (Langøyet al., 2006)
Pc(2) = 0.5; % capture probability (fraction of attacked prey that fish succeeds in capturing)
Pe(2) = 0.17; % enter probability (probability that prey on the trajectory of the fish will enter the mouth)
wpctEmp(2) = 9; % observed dry weight percentage of prey category in stomach samples (Langøyet al., 2006)

% Parameters for prey category 3 (Limacina retroversa)

l(3) = 2.0*10^-3; % length of prey (shell diameter (m)) (Sirenko et al., 2019)
d(3) = 2700; % energy density of prey (J/(g wet weight)) (Davis et al., 1998)
p(3,vp) = 0.6*(1 - p1(vp)); % proportion of prey category to total number of prey (Langøyet al., 2006)
Pc(3) = 0.6; % capture probability (fraction of attacked prey that fish succeeds in capturing)
Pe(3) = 0.2; % enter probability (probability that prey on the trajectory of the fish will enter the mouth)
wpctEmp(3) = 47; % observed dry weight percentage of prey category in stomach samples (Langøyet al., 2006)

```



```

% Parameters for prey category 4 ("others" (miscellaneous zooplankton))

l(4) = 1.5*10^-3;           % length of prey (m)
d(4) = 3800;              % energy density of prey (J/(g wet weight))
p(4, vp) = 0.05*(1 - p1(vp)); % proportion of prey category to total number of prey
Pc(4) = 0.8;              % capture probability (fraction of attacked prey that fish succeeds in capturing)
Pe(4) = 0.3;              % enter probability (probability that prey on the trajectory of the fish will enter the mouth)
wpctEmp(4) = 2;           % observed dry weight percentage of prey category in stomach samples (Langøy et al., 2006)

% Parameters for prey category 5 (small copepods (mostly Oithona and some Microcalanus))

l(5) = 5.0*10^-4;         % mean length of prey (prosome length (m)) (Sirenko et al., 2019)
d(5) = 4300;              % energy density of prey (J/(g wet weight)) (assumed to be somewhat lower than for C. finmarchicus)
p(5, vp) = 0.24*(1 - p1(vp)); % proportion of prey category to total number of prey (Langøy et al., 2006)
Pc(5) = 0.8;              % capture probability (fraction of attacked prey that fish succeeds in capturing)
Pe(5) = 0.3;              % enter probability (probability that prey on the trajectory of the fish will enter the mouth)
wpctEmp(5) = 0.1;         % observed dry weight percentage of prey category in stomach samples (only fractional)

wpctEmp(6) = 9;           % observed dry weight percentage of Crustacea remainders in stomach samples (Langøy et al., 2006)
wpctEmp(7) = 2.9;         % observed dry weight percentage of unidentified remainders in stomach samples (Langøy et al., 2006)

% Initialising matrices

w = zeros(1, length(PreyC)); % prey weight ((g wet weight)/ind.)
Ar = zeros(1, length(PreyC)); % plan area of prey (m^2)
Ap = zeros(1, length(PreyC)); % image area of prey (m^2)
pw = zeros(length(PreyC), length(p1)); % weight of each prey category per total prey abundance ((g wet weight)/ind.)
pwSum = zeros(1, length(p1)); % weight of all prey combined per total prey abundance ((g wet weight)/ind.)
wpct = zeros(length(PreyC), length(p1)); % wet weight percentage of prey category in field samples

for vp = 1:length(p1) % loop over different proportions of prey category 1 (krill and amphipods)
    for preyC = 1:length(PreyC) % loop over different prey categories

        w(prexC) = 6.25*(10.^(3.13*log10(10.^6*1(prexC))-8.18)/10.^6); % weight of copepods and "others" ((g wet weight)/ind.)
        assuming that dry weight is 16% of wet weight (Uye, 1982)
        w(1) = (10.^((log10((10.^3*1(1) - 9.331)/1.832) - 0.0682)/0.3662))/10.^3; % weight of krill and amphipods ((g wet
        weight)/ind.) (from data on Meganycitiphanes norvegica) (Kulka and Corey, 1982)
    end
end

```

```

w(3) = 3.57*1.37*10^-4*(10^3*1(3))^1.5005; % weight of Limacina retroversa ((g wet weight)/ind.) assuming that dry weight
is 28% of wet weight (Davis and Wiebe, 1985; Bednaršek et al., 2012)
Ar(preyc) = (pi/8)*l(preyc).^2; % plan area of prey (m^2) calculated as an ellipse with length l and width l/2 (Van Deurs,
Jørgensen and Fiksen, 2015)
Ar(1) = (pi/20)*l(1).^2; % plan area of krill and amphipods (m^2) calculated as an ellipse with length l and width l/5
Ap(preyc) = Ar(preyc)*Fc; % image area of prey (m^2)
pw(preyc, vp) = p(preyc, vp)*w(preyc); % weight of each prey category per total prey abundance ((g wet weight)/ind.)
pwSum(vp) = sum(pw(:, vp), 1); % weight of all prey combined per total prey abundance ((g wet weight)/ind.)

end % prey categories

for preyc = 1:length(Preyc) % loop over different prey categories

    wpct(preyc, vp) = pw(preyc, vp)/pwSum(vp)*100; % wet weight percentage of prey category in field samples

end % prey categories
end % proportions of prey category 1

%% Parameters for fish predator

L = 0.3; % either: default fish length (m) (Collette and Nauen, 1983)
%L = 0.1:0.1:0.6; % or: range of fish lengths (m) (for sensitivity analysis) (Muus, B.J. and J.G. Nielsen, 1999)
dfvL = 3; % element in L vector that gives default value

%vSearch = 0.50; % swimming speed of fish searching for prey (m/s)
vSearch = linspace(0.35,1.2,10); % range of swimming speeds of fish searching for prey (m/s) (Pepin, Koslow and Pearre Jr.,
1988; Macy, Sutherland and Durbin, 1998; Nøttestad et al., 2016)
vHandling = 0.50; % mean swimming speed of fish handling prey (m/s)
H = 1.5; % either: default handling time when capture probability is 1 (s/ind.)
%H = 1:6; % or: range of handling time values (s/ind.) (for sensitivity analysis)
Theta = 30; % half angle of reavtive field (degrees) (Dunbrack and Dill, 1984; Giske and Aksnes, 1992)
Ke = 1; % half-saturation constant (irradiance at half the maximum processable level) ( $\mu\text{E}/\text{m}^2/\text{s}$ )
RsmallPrey = 1; % detection distance in body lengths for small prey when light is not limiting (Varpe and Fiksen,
2010; Blaxter, 1966)

%vFilter = 0.50; % swimming speed of filter-feeding fish (m/s)
vFilter = linspace(0.35,1.2,10); % range of swimming speeds of filter-feeding fish (m/s) (Pepin, Koslow and Pearre Jr., 1988;
Macy, Sutherland and Durbin, 1998; Nøttestad et al., 2016)

```

```

ft = 0.85; % fraction of time spent filtering (assumed to be similar to pilchard (Sardinops sagax)) (van der
Lingen, 1994)
Bf = 0.95; % buccal flow as fraction of swimming speed
r = 0.99; % retention efficiency (maximum reached for prey classes) (Molina, Manrique and Velasco, 1996)

vRoutine = 0.18; % routine swimming speed of non-feeding fish (m/s) (Johnstone, Wardle and Almatar, 1993)
eg = 0.16; % proportion of ingested energy egested (not assimilated) (Bachiller et al., 2018)
ex = 0.10; % proportion of assimilated energy excreted (Bachiller et al., 2018)
sda = 0.172; % proportion of assimilated energy expended in processing food (Bachiller et al., 2018)

% Initialising matrices

W = zeros(1,length(L)); % fish weight (g wet weight)
h = zeros(length(PreyC),length(H)); % handling time for each prey category (s/ind.)
prof = zeros(length(PreyC),length(H)); % profitability of prey (J/s)
EM = zeros(1,length(L)); % visual capacity of fish scaled such that the detection distance in body lengths for small prey is 1
when light is not limiting (Varpe and Fiksen, 2010; Blaxter, 1966)
gAr = zeros(1,length(L)); % mouth gape area of fish (m^2)
Mroutine = zeros(length(T),length(L)); % metabolic rate of fish swimming at routine speed (J/h/(g fish))
Msearch = zeros(length(T),length(L),length(vSearch)); % metabolic rate of fish searching for prey (J/h/(g fish))
Mhandling = zeros(length(T),length(L)); % metabolic rate of fish handling prey (J/h/(g fish))
fM = zeros(length(L),length(vFilter),length(T)); % metabolic rate of filter-feeding fish (J/h/(g fish))

for vT = 1:length(T) % loop over different temperatures (°C)
    for vL = 1:length(L) % loop over different fish lengths (m)
        for vS = 1:length(vSearch) % loop over different swimming speeds for searching (m/s)
            for vF = 1:length(vFilter) % loop over different swimming speeds for filter-feeding (m/s)
                for vH = 1:length(H) % loop over different handling time values (s/ind.)
                    for preyC = 1:length(PreyC) % loop over different prey categories

                        W(vL) = 0.00338*(100*L(vL))^3.241; % fish weight (g wet weight) (Bachiller et al., 2018)
                        h(preyc,vH) = H(vH)/Pc(preyc); % handling time for each prey category (s/ind.)
                        prof(preyc,vH) = Pc(preyc)*w(preyc)*d(preyc)/H(vH); % profitability of prey (energy gained per handling time) (J/s)
                        (Visser and Fiksen, 2013)
                        EM(vL) = (L(vL)*RsmallPrey)^2/(Ctr*Apscale); % visual capacity of fish eye (Varpe and Fiksen, 2010; Blaxter, 1966)
                        gAr(vL) = 1.32*10^-6*(100*L(vL))^1.895; % mouth gape area of fish (m^2) (MacKay, 1979)
                        Mroutine(vT,vL) = 0.00264*13560*W(vL)^-0.217*exp(0.06818*T(vT))*exp(0.0234*vRoutine/0.23)/24; % metabolic rate of fish
                        swimming at routine speed (J/h/(g fish)) (Elliott and Davison, 1975; Stewart et al., 1983; Bachiller et al., 2018)
                    end
                end
            end
        end
    end
end

```

```

Msearch(vT,vL,vS) = 0.00264*13560*W(vL)^-0.217*exp(0.06818*T(vT))*exp(0.0234*vSearch(vS)/0.23)/24; % metabolic rate of
fish searching for prey (J/h/(g fish))
Mhandling(vT,vL) = 0.00264*13560*W(vL)^-0.217*exp(0.06818*T(vT))*exp(0.0234*vHandling/0.23)*1.5/24; % metabolic rate of
fish handling prey (J/h/(g fish))
fM(vT,vL,vF) = 0.00264*13560*W(vL)^-0.217*exp(0.06818*T(vT))*exp(0.0234*vFilter(vF)/0.23)*1.5/24; % metabolic rate of
filter-feeding fish (J/h/(g fish))

    end % prey categories
    end % handling time
    end % swimming speeds filter-feeding
    end % swimming speeds searching
    end % fish lengths
end % temperatures

%% BITE-FEEDING MODEL

% Initialising matrices

R = zeros(length(PreyC),length(Ez),length(L)); % visual range of fish (m)
B = zeros(length(PreyC),length(Ez),length(L),length(vSearch)); % search rate of fish (m^3/s)
EtSearch = zeros(length(Ntot),length(Ez),length(PreyC),length(p1),length(L),length(vSearch)); % energy intake per search time
for each prey category (J/s)
tHandlingtSearch = zeros(length(Ntot),length(Ez),length(PreyC),length(p1),length(L),length(vSearch),length(H)); % ratio of
handling time to search time for each prey category
bNIDiet = zeros(length(Ntot),length(Ez),length(PreyC),length(T),length(p1),length(L),length(vSearch),length(H)); % net specific
energy intake for all prey in potential diet (J/h/(g fish))
bNI = zeros(length(Ntot),length(Ez),length(T),length(p1),length(L),length(vSearch),length(H)); % net specific energy intake for
all prey combined (J/h/(g fish))
odb = zeros(length(Ntot),length(Ez),length(T),length(p1),length(L),length(vSearch),length(H)); % optimal diet breadth (number of
categories)
bNIOpt = zeros(length(Ntot),length(Ez),length(T),length(p1),length(L),length(H)); % net specific energy intake at optimal
swimming speed (J/h/(g fish))
vSind = zeros(length(Ntot),length(Ez),length(T),length(p1),length(L),length(H)); % index for optimal speed

vSearchOpt = zeros(length(Ntot),length(Ez),length(T),length(p1),length(L),length(H)); % optimal swimming speed of fish searching
for prey (m/s)

```

```

BOpt = zeros(length(Ntot),length(Ez),length(PreyC),length(T),length(p1),length(L),length(H)); % search rate of fish swimming at
optimal speed (m3/s)
ODB = zeros(length(Ntot),length(Ez),length(T),length(p1),length(L),length(H)); % optimal diet breadth at optimal swimming speed
Nprof = zeros(length(PreyC),length(T),length(L),length(H)); % net profitability of prey (net energy gained per handling time)
(J/h/(g fish))
Nproftest = zeros(length(PreyC),length(T),length(L),length(H)); % testing if it is profitable to handle prey from category if it
is the only food available. Value either 0 or 1
minDB = zeros(length(T),length(L),length(H)); % minimum potential diet breadth
maxDB = zeros(length(T),length(L),length(H)); % maximum potential diet breadth
ODBminSize = zeros(length(Ntot),length(Ez),length(T),length(p1),length(L),length(vSearch),length(H)); % minimum size of prey in
optimal diet
ODBmaxSize = zeros(length(T),length(L),length(H)); % maximum size of prey in optimal diet (m)
S = zeros(length(Ntot),length(Ez),length(PreyC),length(T),length(p1),length(L),length(vSearch),length(H)); % selectivity
(fraction of encountered prey that the fish will attack). Value either 0 or 1
bin = zeros(length(Ntot),length(Ez),length(PreyC),length(T),length(p1),length(L),length(vSearch),length(H)); % individuals from
prey category eaten by each fish during timestep
bIn = zeros(length(Ntot),length(Ez),length(T),length(p1),length(L),length(vSearch),length(H)); % total number of individuals
eaten by each fish during timestep
bi = zeros(length(Ntot),length(Ez),length(PreyC),length(T),length(p1),length(L),length(vSearch),length(H)); % absolute intake
rate for each prey category (J/s)
bI = zeros(length(Ntot),length(Ez),length(T),length(p1),length(L),length(vSearch),length(H)); % absolute intake rate for all
prey combined (J/s)
bIOpt = zeros(length(Ntot),length(Ez),length(T),length(p1),length(L),length(H)); % absolute intake rate at optimal swimming
speed (J/s)
tSearcht = zeros(length(Ntot),length(Ez),length(T),length(p1),length(L),length(vSearch),length(H)); % ratio of search time to
total time
bMsearch = zeros(length(Ntot),length(Ez),length(T),length(p1),length(L),length(vSearch),length(H)); % metabolic rate of bite-
feeding fish (search component) (J/h/(g fish))
bMhandling = zeros(length(Ntot),length(Ez),length(T),length(p1),length(L),length(vSearch),length(H)); % metabolic rate of bite-
feeding fish (handling component) (J/h/(g fish))
bM = zeros(length(Ntot),length(Ez),length(T),length(p1),length(L),length(vSearch),length(H)); % total metabolic rate of bite-
feeding fish (J/h/(g fish))
bMOpt = zeros(length(Ntot),length(Ez),length(T),length(p1),length(L),length(H)); % total metabolic rate of fish bite-feeding at
optimal swimming speed (J/h/(g fish))
bNiOpt = zeros(length(Ntot),length(Ez),length(PreyC),length(T),length(p1),length(L),length(H)); % net specific energy intake for
each prey category at optimal swimming speed (J/h/(g fish))
bfOpt = zeros(length(Ntot),length(Ez),length(PreyC),length(T),length(p1),length(L),length(H)); % volume cleared for prey
category by fish swimming at optimal speed (m3/min)
bFOpt = zeros(length(Ntot),length(Ez),length(T),length(p1),length(L),length(H)); % volume cleared for all prey by fish swimming
at optimal speed (m3/min)

```

```

bwiOpt = zeros(length(Ntot),length(Ez),length(PreyC),length(T),length(p1),length(L),length(H)); % daily consumption rate in
weight of each prey category by fish swimming at optimal speed (g/day/(g fish))
bwIOpt = zeros(length(Ntot),length(Ez),length(T),length(p1),length(L),length(H)); % daily consumption rate in weight by fish
swimming at optimal speed (g/day/(g fish))
bwpctOpt = zeros(length(Ntot),length(Ez),length(PreyC),length(T),length(p1),length(L),length(H)); % relative consumption of each
prey category by fish swimming at optimal speed (wet weight percentage)

% Loops

for N = 1:length(Ntot) % loop over different total prey densities (ind./m^3)
  for E = 1:length(Ez) % loop over different light intensities ( $\mu\text{E}/\text{m}^2/\text{s}$ )
    for vT = 1:length(T) % loop over different temperatures ( $^{\circ}\text{C}$ )
      for vp = 1:length(p1) % loop over different proportions of prey category 1 (krill and amphipods)
        for vL = 1:length(L) % loop over different fish lengths (m)
          for vS = 1:length(vSearch) % loop over different swimming speeds (m/s)
            for vH = 1:length(H) % loop over different handling time values (s/ind.)
              for preyC = 1:length(PreyC) % loop over different prey categories

                R(preyC,E,vL) = getr(BeamAtt,Ctr,Ap(preyC),EM(vL),Ke,Ez(E)); % visual range of fish (m), call SUBROUTINE GETR()
(Aksnes and Utne, 1997)
                B(preyC,E,vL,vS) = vSearch(vS)*pi*(R(preyC,E,vL)*sind(Theta))^2; % search rate of fish ( $\text{m}^3/\text{s}$ ) (Huse and Fiksen,
2010)
                EtSearch(N,E,preyC,vp,vL,vS) = Ntot(N)*p(preyC,vp)*B(preyC,E,vL,vS)*Pc(preyC)*w(preyC)*d(preyC); % energy intake per
search time for each prey category (numerator) (J/s);
                EtSearchDiet = cumsum(EtSearch,3); % total energy intake per search time (numerator) (J/s);
                tHandlingtSearch(N,E,preyC,vp,vL,vS,vH) = Ntot(N)*p(preyC,vp)*B(preyC,E,vL,vS)*h(preyC,vH); % ratio of handling time
to search time for each prey category
                tHandlingtSearchDiet = cumsum(tHandlingtSearch,3); % ratio of total handling time to search time (in denominator)
                tSearchtDiet = 1/(1 + tHandlingtSearchDiet(N,E,preyC,vp,vL,vS,vH)); % ratio of search time to total time (inverse of
denominator)
                bIDiet = EtSearchDiet(N,E,preyC,vp,vL,vS)/(1 + tHandlingtSearchDiet(N,E,preyC,vp,vL,vS,vH)); % absolute intake rate
for all prey in potential diet (J/s);
                bUDiet = bIDiet*3600/W(vL)*(1 - eg)*(1 - ex - sda); % mass-specific surplus energy intake (assimilated energy minus
excretion and specific dynamic action) (J/h/(g fish)) (Bachiller et al., 2018)
                bMsearchDiet = Msearch(vT,vL,vS)*tSearchtDiet; % metabolic rate of bite-feeding fish (search component) (J/h/(g
fish))
                bMhandlingDiet = Mhandling(vT,vL)*(1 - tSearchtDiet); % metabolic rate of bite-feeding fish (handling component)
(J/h/(g fish))
            end
          end
        end
      end
    end
  end
end

```

```

    bNIDiet(N,E,preyC,vT,vp,vL,vS,vH) = max((bUDiet - bMsearchDiet - bMhandlingDiet), - Mroutine(vT,vL)); % net specific
energy intake for all prey in potential diet (J/h/(g fish)). If net intake rate is more negative than routine metabolism, the
fish will not feed.
    [bNI(N,E,vT,vp,vL,vS,vH), odb(N,E,vT,vp,vL,vS,vH)] = max(bNIDiet(N,E, :, vT, vp, vL, vS, vH), [], 3); % net specific energy
intake for all prey in optimal diet (J/h/(g fish)); optimal diet breadth (number of categories)
    [bNIOpt(N,E,vT,vp,vL,vH), vSind(N,E,vT,vp,vL,vH)] = max(bNI(N,E,vT,vp,vL, :, vH), [], 6); % net specific energy intake at
optimal swimming speed (J/h/(g fish)); index for optimal speed

    vSearchOpt(N,E,vT,vp,vL,vH) = vSearch(vSind(N,E,vT,vp,vL,vH)); % optimal swimming speed of fish searching for prey
(m/s)
    BOpt(N,E,preyC,vT,vp,vL,vH) = B(preyc,E,vL,vSind(N,E,vT,vp,vL,vH)); % search rate of fish swimming at optimal speed
(m^3/s)
    ODB(N,E,vT,vp,vL,vH) = odb(N,E,vT,vp,vL,vSind(N,E,vT,vp,vL,vH),vH); % optimal diet breadth at optimal swimming speed
Nprof(preyc,vT,vL,vH) = prof(preyc,vH)*3600/W(vL)*(1 - eg)*(1 - ex - sda) - Mhandling(vT,vL); % net profitability of
prey (net energy gained per handling time) (J/h/(g fish))
    Nproftest(preyc,vT,vL,vH) = Nprof(preyc,vT,vL,vH) > - Mroutine(vT,vL); % testing if it is profitable to handle prey
from category if it is the only food available. Value either 0 or 1
    minDB(vT,vL,vH) = min(Preyc(Nproftest(:,vT,vL,vH) == 1)); % minimum potential diet breadth (only the most profitable
category is accepted (if it passed the above test))
    maxDB(vT,vL,vH) = max(Preyc(Nproftest(:,vT,vL,vH) == 1)); % maximum potential diet breadth (all categories that
passed the test are accepted)
    ODBminSize(N,E,vT,vp,vL,vS,vH) = l(odb(N,E,vT,vp,vL,vS,vH)); % minimum size of prey in optimal diet (m)
    ODBmaxSize(vT,vL,vH) = l(minDB(vT,vL,vH)); % maximum size of prey in optimal diet (m)
    S(N,E,preyc,vT,vp,vL,vS,vH) = Nprof(preyc,vT,vL,vH) >= bNI(N,E,vT,vp,vL,vS,vH); % selectivity (fraction of
encountered prey that the fish will attack). Value either 0 or 1
    bin(N,E,preyc,vT,vp,vL,vS,vH) = Ntot(N)*p(preyc,vp)*B(preyc,E,vL,vS)*S(N,E,preyc,vT,vp,vL,vS,vH)*Pc(preyc)/(1 +
tHandlingtSearchDiet(N,E,odb(N,E,vT,vp,vL,vS,vH),vp,vL,vS,vH)); % individuals from prey category eaten by each fish (ind./s)
    bIn(N,E,vT,vp,vL,vS,vH) = sum(bin(N,E, :, vT, vp, vL, vS, vH), 3); % individuals from all categories eaten by the fish
(ind./s)
    bi(N,E,preyc,vT,vp,vL,vS,vH) = bin(N,E,preyc,vT,vp,vL,vS,vH)*w(preyc)*d(preyc); % absolute intake rate for each prey
category (J/s)
    bI(N,E,vT,vp,vL,vS,vH) = sum(bi(N,E, :, vT, vp, vL, vS, vH), 3); % absolute intake rate for all prey (J/s)
    bIOpt(N,E,vT,vp,vL,vH) = bI(N,E,vT,vp,vL,vSind(N,E,vT,vp,vL,vH),vH); % absolute intake rate at optimal swimming speed
(J/s)
    tSearcht(N,E,vT,vp,vL,vS,vH) = 1/(1 + tHandlingtSearchDiet(N,E,odb(N,E,vT,vp,vL,vS,vH),vp,vL,vS,vH)); % ratio of
search time to total time
    bMsearch(N,E,vT,vp,vL,vS,vH) = Msearch(vT,vL,vS)*tSearcht(N,E,vT,vp,vL,vS,vH); % metabolic rate of bite-feeding fish
(search component) (J/h/(g fish))

```

```

    bMhandling(N,E,vT,vp,vL,vS,vH) = Mhandling(vT,vL)*(1 - tSearcht(N,E,vT,vp,vL,vS,vH)); % metabolic rate of bite-
feeding fish (handling component) (J/h/(g fish))
    bM(N,E,vT,vp,vL,vS,vH) = bMsearch(N,E,vT,vp,vL,vS,vH) + bMhandling(N,E,vT,vp,vL,vS,vH); % total metabolic rate of
bite-feeding fish (J/h/(g fish))
    bMOpt(N,E,vT,vp,vL,vH) = bM(N,E,vT,vp,vL,vSind(N,E,vT,vp,vL,vH),vH); % total metabolic rate of fish bite-feeding at
optimal swimming speed (J/h/(g fish))
    bNiOpt(N,E,preyC,vT,vp,vL,vH) = bi(N,E,preyC,vT,vp,vL,vSind(N,E,vT,vp,vL,vH),vH)*3600/W(vL)*(1 - eg)*(1 - ex - sda) -
bMOpt(N,E,vT,vp,vL,vH); % net specific energy intake for each prey category (J/h/(g fish))
    bfOpt(N,E,preyC,vT,vp,vL,vH) = bin(N,E,preyC,vT,vp,vL,vSind(N,E,vT,vp,vL,vH),vH)/(Ntot(N)*p(prexC,vp)); % volume
cleared for prey category by fish swimming at optimal speed (m^3/s)
    bFOpt(N,E,vT,vp,vL,vH) = bIn(N,E,vT,vp,vL,vSind(N,E,vT,vp,vL,vH),vH)/Ntot(N); % volume cleared for all prey by fish
swimming at optimal speed (m^3/s)
    bwiOpt(N,E,preyC,vT,vp,vL,vH) = bi(N,E,preyC,vT,vp,vL,vSind(N,E,vT,vp,vL,vH),vH)*3600*24/d(prexC)/W(vL); % daily
consumption rate in weight of each prey category by fish swimming at optimal speed (g/day/(g fish))
    bwIOpt(N,E,vT,vp,vL,vH) = sum(bwiOpt(N,E,:,vT,vp,vL,vH),3); % daily consumption rate in weight by fish swimming at
optimal speed (g/day/(g fish))

end

for preyC = 1:length(PrexC) % loop over different prey categories

    bwpctOpt(N,E,preyC,vT,vp,vL,vH) = bwIOpt(N,E,preyC,vT,vp,vL,vH)/bwIOpt(N,E,vT,vp,vL,vH)*100; % relative consumption
of each prey category by fish swimming at optimal speed (wet weight percentage)

    end % prey categories
end % handling time
end % swimming speeds
end % fish lengths
end % proportions of prey category 1
end % temperatures
end % light intensities
end % prey densities

%% FILTER-FEEDING MODEL

% Initialising matrices

```



```

fin = zeros(length(Ntot),length(Ez),length(PreyC),length(p1),length(L),length(vFilter)); % individuals from prey category eaten
by each fish (ind./s)
fIn = zeros(length(Ntot),length(Ez),length(p1),length(L),length(vFilter)); % individuals from all categories eaten by each fish
(ind./s)
fi = zeros(length(Ntot),length(Ez),length(PreyC),length(p1),length(L),length(vFilter)); % absolute intake rate for each prey
category (J/s)
fI = zeros(length(Ntot),length(Ez),length(p1),length(L),length(vFilter)); % absolute intake rate for all prey (J/s)
fNI = zeros(length(Ntot),length(Ez),length(T),length(p1),length(L),length(vFilter)); % empty matrix for net specific energy
uptake for all prey combined (J/h/(g fish))
fNIOpt = zeros(length(Ntot),length(Ez),length(T),length(p1),length(L)); % net specific energy intake at optimal swimming speed
(J/h/(g fish))
vFind = zeros(length(Ntot),length(Ez),length(T),length(p1),length(L)); % index for optimal speed

vFilterOpt = zeros(length(Ntot),length(Ez),length(T),length(p1),length(L)); % optimal swimming speed of filter-feeding fish
(m/s)
fIOpt = zeros(length(Ntot),length(Ez),length(T),length(p1),length(L)); % absolute intake rate at optimal swimming speed (J/s)
fMOpt = zeros(length(Ntot),length(Ez),length(T),length(p1),length(L)); % metabolic rate of fish filter-feeding at optimal
swimming speed (J/h/(g fish))
fNiOpt = zeros(length(Ntot),length(Ez),length(PreyC),length(T),length(p1),length(L)); % net specific energy intake for each prey
catgory at optimal swimming speed (J/h/(g fish))
ffOpt = zeros(length(Ntot),length(Ez),length(PreyC),length(T),length(p1),length(L)); % volume cleared for prey category by fish
swimming at optimal speed (m^3/s)
fFOpt = zeros(length(Ntot),length(Ez),length(T),length(p1),length(L)); % volume cleared for all prey by fish swimming at optimal
speed (m^3/s)
feffOpt = zeros(length(Ntot),length(Ez),length(PreyC),length(T),length(p1),length(L)); % filtration efficiency for each prey
catgory
fEffOpt = zeros(length(Ntot),length(Ez),length(T),length(p1),length(L)); % filtration efficiency for all prey
fwiOpt = zeros(length(Ntot),length(Ez),length(PreyC),length(T),length(p1),length(L)); % daily consumption rate in weight of each
prey category by fish swimming at optimal speed (g/day/(g fish))
fwIOpt = zeros(length(Ntot),length(Ez),length(T),length(p1),length(L)); % daily consumption rate in weight by fish swimming at
optimal speed (g/day/(g fish))
fwpctOpt = zeros(length(Ntot),length(Ez),length(PreyC),length(T),length(p1),length(L)); % relative consumption of each prey
category by fish swimming at optimal speed (wet weight percentage)

% Loops

for N = 1:length(Ntot) % loop over different total prey densities (ind./m^3)
    for E = 1:length(Ez) % loop over different light intensities ( $\mu E/m^2/s$ )
        for vT = 1:length(T) % loop over different temperatures ( $^{\circ}C$ )

```

```

for vp = 1:length(p1) % loop over different proportions of prey category 1
  for vL = 1:length(L) % loop over different fish lengths (m)
    for vF = 1:length(vFilter) % loop over different swimming speeds (m/s)
      for preyC = 1:length(PreyC) % loop over different prey categories

        fin(N,E,preyC,vp,vL,vF) = vFilter(vF)*gAr(vL)*ft*Bf*Ntot(N)*p(prexC,vp)*Pe(prexC)*r; % individuals from prey category
eaten by each fish (ind./s) (Lovvorn, Baduini and Hunt, 2001)
        fIn(N,E,vp,vL,vF) = sum(fin(N,E,:,vp,vL,vF),3); % individuals from all categories eaten by each fish (ind./s)
        fi(N,E,preyC,vp,vL,vF) = fin(N,E,preyC,vp,vL,vF)*w(prexC)*d(prexC); % absolute intake rate for each prey category
(J/s)
        fI(N,E,vp,vL,vF) = sum(fi(N,E,:,vp,vL,vF),3); % absolute intake rate for all prey (J/s)
        fU = fI(N,E,vp,vL,vF)*3600/W(vL)*(1 - eg)*(1 - ex - sda); % mass-specific surplus energy intake (assimilated energy
minus excretion and specific dynamic action) (J/h/(g fish)) (Bachiller et al., 2018)
        fNI(N,E,vT,vp,vL,vF) = max((fU - fM(vT,vL,vF)), - Mroutine(vT,vL)); % net specific energy intake (J/h/(g fish))
        [fNIOpt(N,E,vT,vp,vL),vFind(N,E,vT,vp,vL)] = max(fNI(N,E,vT,vp,vL,:),[],6); % net specific energy intake at optimal
swimming speed (J/h/(g fish)); index for optimal speed

        vFilterOpt(N,E,vT,vp,vL) = vFilter(vFind(N,E,vT,vp,vL)); % optimal swimming speed of filter-feeding fish (m/s)
        fIOpt(N,E,vT,vp,vL) = fI(N,E,vp,vL,vFind(N,E,vT,vp,vL)); % absolute intake rate at optimal swimming speed (J/s)
        fMOpt(N,E,vT,vp,vL) = fM(vT,vL,vFind(N,E,vT,vp,vL)); % metabolic rate of fish filter-feeding at optimal swimming speed
(J/h/(g fish))
        fNiOpt(N,E,preyC,vT,vp,vL) = fi(N,E,preyC,vp,vL,vFind(N,E,vT,vp,vL))*3600/W(vL)*(1 - eg)*(1 - ex - sda) -
fMOpt(N,E,vT,vp,vL); % net specific energy intake for each prey category at optimal swimming speed (J/h/(g fish))
        ffOpt(N,E,preyC,vT,vp,vL) = fin(N,E,preyC,vp,vL,vFind(N,E,vT,vp,vL))/(Ntot(N)*p(prexC,vp)); % volume cleared for prey
category by fish swimming at optimal speed (m^3/s)
        fFOpt(N,E,vT,vp,vL) = fIn(N,E,vp,vL,vFind(N,E,vT,vp,vL))/Ntot(N); % volume cleared for all prey by fish swimming at
optimal speed (m^3/s)
        feffOpt(N,E,preyC,vT,vp,vL) = ffOpt(N,E,preyC,vT,vp,vL)/(vFilter(vFind(N,E,vT,vp,vL))*gAr(vL)); % filtration
efficiency for each prey category
        fEffOpt(N,E,vT,vp,vL) = fFOpt(N,E,vT,vp,vL)/(vFilter(vFind(N,E,vT,vp,vL))*gAr(vL)); % filtration efficiency for all
prey
        fwiOpt(N,E,preyC,vT,vp,vL) = fi(N,E,preyC,vp,vL,vFind(N,E,vT,vp,vL))*3600*24/d(prexC)/W(vL); % daily consumption rate
in weight of each prey category by fish swimming at optimal speed (g/day/(g fish))
        fwiOpt(N,E,vT,vp,vL) = sum(fwiOpt(N,E,:,vT,vp,vL),3); % daily consumption rate in weight by fish swimming at optimal
speed (g/day/(g fish))

      end

    for preyC = 1:length(PreyC) % loop over different prey categories

```

```

        fwpctOpt(N,E,preyC,vT,vp,vL) = fwiOpt(N,E,preyC,vT,vp,vL)/fwIOpt(N,E,vT,vp,vL)*100; % relative consumption of each
prey category by fish swimming at optimal speed (wet weight percentage)

        end % prey categories
        end % swimming speeds
        end % fish lengths
        end % proportions of prey category 1
        end % temperatures
        end % light intensities
end % prey densities

%% PLOTS

figure(1)
h1 = plot(Ntot,squeeze(bNIOpt(:,32,:,2,:,:)), 'LineWidth',2, 'Color',[0.91,0.234,0.325]); hold on;
h2 = plot(Ntot,squeeze(bNIOpt(:,32,:,1,:,:)), 'LineWidth',1, 'Color',[0.91,0.234,0.325]);
h3 = plot(Ntot,squeeze(bNIOpt(:,22,:,2,:,:)), 'LineWidth',2, 'Color',[0.7,0.18,0.25]);
h4 = plot(Ntot,squeeze(bNIOpt(:,22,:,1,:,:)), 'LineWidth',1, 'Color',[0.7,0.18,0.25]);
h5 = plot(Ntot,squeeze(fNIOpt(:,length(Ez),:,2,:)), '--', 'LineWidth',2, 'Color',[0.1,0.4,0.7]);
h6 = plot(Ntot,squeeze(fNIOpt(:,length(Ez),:,1,:)), '--', 'LineWidth',1, 'Color',[0.1,0.4,0.7]);
xlim([-1*10^4,11*10^4]);
ylim([-40,900]);
ax = gca; ax.XAxis.Exponent = 4;
xlabel('Prey density (ind. m^{-3})'); ylabel('Net intake rate (J h^{-1} g^{-1})');
legend([h1,h3,h5],{'Bite-feeding high light','Bite-feeding low light','Filter-
feeding'},'location','southeast','fontsize',9,'box','off');
set(gca,'box','off');
export_fig C:\Users\Admin\Documents\fig1.png -transparent -m2;

figure(2)
surf(log10(Ez),log10(Ntot),bNIOpt(:,:,:,dfvp,:,:),'FaceAlpha',0.8,'FaceColor',[0.81,0.21,0.29],'EdgeColor',[0.81,0.21,0.29]);
hold on;
surf(log10(Ez),log10(Ntot),fNIOpt(:,:,:,dfvp,:),'FaceAlpha',0.8,'FaceColor',[0.1,0.4,0.7],'EdgeColor',[0.1,0.4,0.7]);
ylim([0,log10(2) + 5]); zlim([-1,1200]);
yticks([0,1,2,3,4,5]);
xticklabels({'10^{-6}','10^{-4}','10^{-2}','10^{0}','10^{2}'});

```

```

yticklabels({'10^0','10^1','10^2','10^3','10^4','10^5'});
xlabel('Irradiance ( $\mu\text{E m}^{-3} \text{s}^{-1}$ )'); ylabel('Prey density (ind.  $\text{m}^{-3}$ )'); zlabel('Net intake rate ( $\text{J h}^{-1} \text{g}^{-1}$ )');
legend({'Bite-feeding','Filter-feeding'},'location','northeast','fontsize',9,'box','off');
set(gca, 'Color', 'none','LineWidth',1);
grid off
export_fig C:\Users\Admin\Documents\fig2.png -transparent -m2;

figure(3)
b1 = [transpose(p(:,1)*100),0,0];
b2 = [transpose(wpct(:,1)),0,0];
b3 = wpctEmp;
b4 = [reshape(bwpctOpt(36,22,::,dfvp,::),1,[]),0,0];
b5 = [reshape(fwpctOpt(36,22,::,dfvp,:),1,[]),0,0];
x = categorical({'WP2 samples (numbers)','WP2 samples (weight)','Stomach samples (weight)'...
    ,'Bite-feeding submodel (weight)','Filter-feeding submodel (weight)'});
x = reordercats(x,{'WP2 samples (numbers)','WP2 samples (weight)','Stomach samples (weight)'...
    ,'Bite-feeding submodel (weight)','Filter-feeding submodel (weight)'});
y = [b1; b2; b3; b4; b5];
bar(x,y,0.6,'stacked');
ylim([0,100]);
ytickformat('percentage');
legend({'Krill and amphipods','Calanoid copepods','Limacina retroversa','Others','Oithona',...
    ,'Crustacea remainders','Unidentified remainders'},'location','northeastoutside','fontsize',13,'box','off');
set(gcf,'position',[10,10,1000,600]);
set(gca,'fontsize',14);
export_fig C:\Users\Admin\Documents\fig3.png -transparent -m2;

```

APPENDIX 2 – MATLAB code for simulation of pilchard foraging

```
%% BITE-FEEDING AND FILTER-FEEDING
%*****

% The model compares net specific energy intake for fish bite-feeding and filter-feeding
% at varying light conditions and prey densities. The prey is divided into individual
% categories with different sets of parameter values, and swimming speeds are optimised
% to maximise net energy return. Values of R, which is the detection range of a visual
% predator, are calculated separately in Fortran and read from R-tables into Matlab.
% In this script version the model is calibrated using empirical data on pilchard
% (Sardinops sagax) bite-feeding and filter-feeding on single prey-types (van der Lingen,
% 1994; van der Lingen, 1995). Feeding trials with closed populations are simulated to
% compare predictions with experimental results.

close all;
clear all;

%% PARAMETERS

%% Parameters for environment / experimental conditions

Chla = 2; % concentration of chl a (mg/m^3)
BeamAtt = 0.066 + 0.39*Chla^0.57*0.93; % beam attenuation coefficient (m^-1) (Mobley, 1994)
E = logspace(-6,3,50); % range of ambient irradiances (µE/m^2/s)
Exp = 10^3; % either: default experimental irradiance (µE/m^2/s)
%Exp = logspace(-6,3,4); % or: range of experimental irradiances (µE/m^2/s) (for sensitivity analysis)
T = 17; % either: default ambient temperature (°C) (van der Lingen, 1994)
%T = [10,17,22]; % or: range of temperatures (°C) (for sensitivity analysis) (van der Lingen, 1995)
V = 1; % volume of water in experimental tank (m^3) (van der Lingen, 1994)
nFish1 = repmat(15,1,360); % total number of fish in experimental tank at each timestep (van der Lingen, 1994)
nFish2(:,1) = [repmat(3.08,1,60), repmat(0.75,1,60), repmat(0.45,1,60), repmat(0.45,1,60), repmat(0.45,1,60), ...
repmat(0.225,1,60)]; % average number of fish feeding on Calanus at each timestep (van der Lingen, 1994)
```

```

nFish2(:,2) = [repmat(12.5,1,60),repmat(9.83,1,60),repmat(4.35,1,60),repmat(0.75,1,60),repmat(0.45,1,60),...
              repmat(0.37,1,60)]; % average number of fish feeding on Artemia at each timestep (van der Lingen, 1994)
tmax = 60; % duration of feeding experiment (min) (van der Lingen, 1994)
ntstep = 360; % number of timesteps
dtstep = tmax/ntstep; % length of each timestep (min)
t1 = linspace(0,tmax,ntstep + 1); % time after food introduction (min) (for simulation)
t2 = linspace(0,tmax - 1,ntstep); % time after food introduction (min) (for simulation)
t3 = linspace(0,tmax,7); % time after food introduction (min) (sampling times in feeding trial)

% Loop choice

bnotime = 0; % 1 = run time-independent bite-feeding loop
fnotime = 0; % 1 = run time-independent filter-feeding loop
btime = 0; % 1 = run bite-feeding time loop
ftime = 1; % 1 = run filter-feeding time loop

%% Parameters for prey

PreyC = 1:2; % prey categories
N = logspace(0,6,50); % range of prey densities (ind./m^3)
Ctr = 0.3; % inherent contrast of prey (Utne-Palm, 1999)
pi = 4*atan(1); % value of pi
Fc = 0.8; % fraction of plan area of prey that is visible core area
Apscale = (pi/8)*(1.5*10^-3)^2*Fc; % image area of small prey (m^2) (for scaling)

% Parameters for prey category 1 (wild Calanus agulhensis adults)

N1xp(1) = 9*10^3; % initial prey density in experimental tank (at time of food introduction) (ind./m^3) (van der Lingen,
1994)
Nemp(:,1) = [9*10^3,1.5*10^3,3*10^2,5*10^2,3*10^2,4*10^2,2*10^2]; % observed prey density at each ten min during feeding trial
(ind./m^3) (van der Lingen, 1994)
l(1) = 2.48*10^-3; % mean length of prey (m) (van der Lingen, 1994)
w(1) = 6*(10.^(3.13*log10(10.^6*l(1))-8.18)/10.^6); % weight of prey ((g wet weight)/ind.) assuming that dry weight is 16% of
wet weight (Uye, 1982)
d(1) = 4500; % energy density of prey (J/(g wet weight)) (assumed to be similar to C. finmarchicus) (Davies, Ryan
and Taggart, 2012; Davis, 1993)
Pc = 0.72; % capture probability (fraction of attacked prey that fish succeeds in capturing)

```

```

Ar = (pi/8)*l(1)^2;           % plan area of prey (m^2) calculated as an ellipse with length l and width l/2 (Van Deurs, Jørgensen
and Fiksen, 2015)
Ap = Ar*Fc;                   % image area of prey (m^2)

% Parameters for prey category 2 (cultivated Artemia franciscana nauplii)

N1xp(2) = 7.85*10^5;          % initial prey density in experimental tank (at time of food introduction) (ind./m^3) (van der Lingen,
1994)
Nemp(:,2) = [7.9*10^5,1.45*10^5,4*10^4,1*10^4,9*10^3,8*10^3,7*10^3]; % observed prey density at each ten min during feeding
trial (ind./m^3) (van der Lingen, 1994)
l(2) = 4.87*10^-4;           % mean length of prey (m) (van der Lingen, 1994)
w(2) = 1.15*10^-5;           % weight of prey ((g wet weight)/ind.) assuming that dry weight is 20% of wet weight (Leger et al.,
1986)
d(2) = 4400;                 % energy density of prey (J/(g wet weight)) approximated from data on different Artemia nauplii (Leger
et al., 1986)
Pe = 0.9;                    % enter probability (probability that prey on the trajectory of the fish will enter the mouth)

%% Parameters for fish predator

L = 0.229;                   % either: default fish length (m) (van der Lingen, 1994)
%L = [0.22,0.23,0.24];      % or: range of fish lengths (m) (for sensitivity analysis)

vBite = linspace(0.26,0.51,10); % range of swimming speeds of bite-feeding fish (m/s) (van der Lingen, 1995)
vBiteEmp = [0.48,0.37,0.29,0.3,0.27,0.26,0.29]; % observed mean swimming speed at each ten min during bite-feeding trial (m/s)
(van der Lingen, 1994)
H = 1.5;                     % either: default handling time when capture probability is 1 (s/ind.)
%H = 1:6;                    % or: range of handling time values (s/ind.) (for sensitivity analysis)
Theta = 30;                  % half angle of reactive field (degrees) (Dunbrack and Dill, 1984; Giske and Aksnes, 1992)
Ke = 1;                       % half-saturation constant (irradiance at half the maximum processable level) ( $\mu\text{E}/\text{m}^2/\text{s}$ )
RsmallPrey = 1;              % detection distance in body lengths for small prey when light is not limiting (Varpe and Fiksen,
2010; Blaxter, 1966)

vFilter = linspace(0.15,0.67,10); % range of swimming speeds of filter-feeding fish (m/s) (van der Lingen, 1995)
vFilterEmp = [0.59,0.44,0.32,0.25,0.22,0.22,0.19]; % observed mean swimming speed at each ten min during filter-feeding trial
(m/s) (van der Lingen, 1994)
ft = 0.85;                   % fraction of time spent filtering (the duration of each filtering bout times the frequency) (van der
Lingen, 1994)
Bf = 0.95;                   % buccal flow as fraction of swimming speed

```

```

r = 0.99; % retention efficiency (maximum reached for prey classes) (van der Lingen, 1994)

vRoutine = 0.20; % routine swimming speed of non-feeding fish (m/s) (van der Lingen, 1995)
Mroutine = (0.2219*vRoutine/0.256 + 0.0047)*13560/1000; % metabolic rate of fish swimming at routine speed (J/h/(g fish)) (van
der Lingen, 1995)
eg = 0.16; % proportion of ingested energy egested (assumed to be similar to herring (Clupea harengus))
(Bachiller et al., 2018)
ex = 0.10; % proportion of assimilated energy excreted (assumed to be similar to C. harengus) (Bachiller et al.,
2018)
sda = 0.175; % proportion of assimilated energy expended in processing food (assumed to be similar to C. harengus)
(Bachiller et al., 2018)

% Initialising matrices

h = zeros(1,length(H)); % handling time for prey category (s/ind.)
prof = zeros(1,length(H)); % profitability of prey (J/s)
W = zeros(1,length(L)); % fish weight (g wet weight)
EM = zeros(1,length(L)); % visual capacity of fish scaled such that the detection distance in body lengths for small prey is 1
when light is not limiting (Varpe and Fiksen, 2010; Blaxter, 1966)
gAr = zeros(1,length(L)); % mouth gape area of fish (m^2)
bM = zeros(1,length(vBite)); % metabolic rate of bite-feeding fish (J/h/(g fish))
fM = zeros(1,length(vFilter)); % metabolic rate of filter-feeding fish (J/h/(g fish))

for vL = 1:length(L) % loop over different fish lengths (m)
    for vB = 1:length(vBite) % loop over different swimming speeds for bite-feeding (m/s)
        for vF = 1:length(vFilter) % loop over different swimming speeds for filter-feeding (m/s)
            for vH = 1:length(H) % loop over different handling time values (s/ind.)

                W(vL) = exp(-10.497 + 2.848*log(10^3*L(vL)) - 0.049); % fish weight (g wet weight) (Dorval et al., 2015)
                h(vH) = H(vH)/Pc; % handling time for prey category (s/ind.)
                prof(vH) = Pc*w(1)*d(1)/h(vH); % profitability of prey (energy gained per handling time) (J/s) (Visser and Fiksen, 2013)
                EM(vL) = (L(vL)*RsmallPrey)^2/(Ctr*Apscale); % visual capacity of fish eye (Varpe and Fiksen, 2010; Blaxter, 1966)
                gAr(vL) = 1.32*10^-6*(100*L(vL))^1.895; % mouth gape area of fish (m^2) (using regression for mackerel (Scomber
scombrus)) (MacKay, 1979)
                bM(vB) = (0.5711*vBite(vB)/0.256 - 0.2891)*13560/1000; % metabolic rate of bite-feeding fish (J/h/(g fish)) (van der
Lingen, 1995)
                fM(vF) = (0.4131*vFilter(vF)/0.256 - 0.2035)*13560/1000; % metabolic rate of filter-feeding fish (J/h/(g fish)) (van der
Lingen, 1995)
            end
        end
    end
end

```



```

    end % handling time
    end % swimming speeds filter-feeding
    end % swimming speeds bite-feeding
end % fish lengths

%% BITE-FEEDING MODEL (Calanus)

if bnotime == 1 % run loop below (intake rates at different prey densities and light intensities)

% Initialising matrices

R = zeros(length(E),length(L)); % visual range of fish (m)
B = zeros(length(E),length(L),length(vBite)); % search rate of fish (m3/s)
bin = zeros(length(N),length(E),length(L),length(vBite),length(H)); % individuals eaten by each fish during timestep
bi = zeros(length(N),length(E),length(L),length(vBite),length(H)); % absolute energy intake (J/s)
bNi = zeros(length(N),length(E),length(L),length(vBite),length(H)); % net specific energy intake (J/h/(g fish))
bNiOpt = zeros(length(N),length(E),length(L),length(H)); % net specific energy intake at optimal swimming speed (J/h/(g fish))
vBind = zeros(length(N),length(E),length(L),length(H)); % index for optimal speed

vBiteOpt = zeros(length(N),length(E),length(L),length(H)); % optimal swimming speed of fish searching for prey (m/s)
BOpt = zeros(length(N),length(E),length(L),length(H)); % search rate of fish swimming at optimal speed (m3/s)
biOpt = zeros(length(N),length(E),length(L),length(H)); % absolute energy intake at optimal swimming speed (J/s)
bfOpt = zeros(length(N),length(E),length(L),length(H)); % volume cleared for prey by fish swimming at optimal speed (m3/min)
bMOpt = zeros(length(N),length(E),length(L),length(H)); % metabolic rate of fish bite-feeding at optimal swimming speed (J/h/(g fish))
Nprof = zeros(length(L),length(H)); % net profitability of prey (net energy gained per handling time) (J/h/(g fish))

% Loop (time-independent)

for vN = 1:length(N) % loop over different prey densities (ind./m3)
    for vE = 1:length(E) % loop over different light intensities (μE/m2/s)
        for vL = 1:length(L) % loop over different fish lengths (m)
            for vB = 1:length(vBite) % loop over different swimming speeds (m/s)
                for vH = 1:length(H) % loop over different handling time values (s/ind.)
                    for preyC = 1 % loop over prey category

```

```

R(vE,vL) = getr(BeamAtt,Ctr,Ap,EM(vL),Ke,E(vE)); % visual range of fish (m), call SUBROUTINE GETR() (Aksnes and Utne,
1997)
B(vE,vL,vB) = vBite(vB)*pi*(R(vE,vL)*sind(Theta))^2; % search rate of fish (m^3/s) (Huse and Fiksen, 2010)
bin(vN,vE,vL,vB,vH) = N(vN)*B(vE,vL,vB)*Pc/(1 + N(vN)*B(vE,vL,vB)*h(vH)); % individuals eaten by each fish (ind./s)
bi(vN,vE,vL,vB,vH) = bin(vN,vE,vL,vB,vH)*w(preyc)*d(preyc); % absolute energy intake (J/s)
tSearcht = 1/(1 + N(vN)*B(vE,vL,vB)*h(vH)); % ratio of search time to total time (inverse of denominator)
bu = bi(vN,vE,vL,vB,vH)*3600/W(vL)*(1 - eg)*(1 - ex - sda); % mass-specific surplus energy intake (assimilated energy
minus excretion and SDA) (J/h/(g fish)) (Bachiller et al., 2018)
bNi(vN,vE,vL,vB,vH) = bu - bM(vB); % net specific energy intake (J/h/(g fish))
[bNiOpt(vN,vE,vL,vH),vBind(vN,vE,vL,vH)] = max(bNi(vN,vE,vL,:,vH),[],4); % net specific energy intake at optimal
swimming speed (J/h/(g fish)); index for optimal speed

vBiteOpt(vN,vE,vL,vH) = vBite(vBind(vN,vE,vL,vH)); % optimal swimming speed of fish searching for prey (m/s)
BOpt(vN,vE,vL,vH) = B(vE,vL,vBind(vN,vE,vL,vH)); % search rate of fish swimming at optimal speed (m^3/s)
biOpt(vN,vE,vL,vB,vH) = bi(vN,vE,vL,vBind(vN,vE,vL,vH),vH); % absolute energy intake at optimal swimming speed (J/s)
bfOpt(vN,vE,vL,vH) = bin(vN,vE,vL,vBind(vN,vE,vL,vH))/N(vN); % volume cleared for prey by fish swimming at optimal
speed (m^3/s)
bMOpt(vN,vE,vL,vH) = bM(vBind(vN,vE,vL,vH)); % total metabolic rate of fish bite-feeding at optimal swimming speed
(J/h/(g fish))
Nprof(vN,vE,vL,vH) = prof(vH)*3600/W(vL)*(1 - eg)*(1 - ex - sda) - bMOpt(vN,vE,vL,vH); % net profitability of prey (net
energy gained per handling time) (J/h/(g fish))

    end % prey category
    end % handling time
    end % swimming speeds
    end % fish lengths
    end % light intensities
end % prey densities

else % do not run loop above
end

if btime == 1 % run loop below (simulation of feeding experiment with closed populations)

% Initialising matrices

NOptxp1 = zeros(length(t2),length(Exp),length(L),length(H)); % prey density when fish swims at optimal speed (ind./m^3) (loop 1)
NOptxp2 = zeros(length(t2),length(Exp),length(L),length(H)); % prey density when fish swims at optimal speed (ind./m^3) (loop 2)

```

```

Rxp = zeros(length(Exp),length(L)); % visual range of fish (m)
Bxp = zeros(length(Exp),length(L),length(vBite)); % search rate of fish (m^3/s)
binxp = zeros(length(t2),length(Exp),length(L),length(vBite),length(H)); % individuals eaten by each fish during timestep
bixp = zeros(length(t2),length(Exp),length(L),length(vBite),length(H)); % absolute energy intake (J/s)
bNixp = zeros(length(t2),length(Exp),length(L),length(vBite),length(H)); % net specific energy intake (J/h/(g fish))
bNiOptxp = zeros(length(t2),length(Exp),length(L),length(H)); % net specific energy intake at optimal swimming speed (J/h/(g fish))
vBindxp = zeros(length(t2),length(Exp),length(L),length(H)); % index for optimal speed

vBiteOptxp1 = zeros(length(t2),length(Exp),length(L),length(H)); % optimal swimming speed of bite-feeding fish (m/s) (loop 1)
vBiteOptxp2 = zeros(length(t2),length(Exp),length(L),length(H)); % optimal swimming speed of bite-feeding fish (m/s) (loop 2)
BOptxp = zeros(length(t2),length(Exp),length(L),length(H)); % search rate of fish swimming at optimal speed (m^3/s)
biOptxp = zeros(length(t2),length(Exp),length(L),length(H)); % absolute energy intake at optimal swimming speed (J/s)
bfOptxp = zeros(length(t2),length(Exp),length(L),length(H)); % volume cleared for prey by fish swimming at optimal speed (m^3/min)
bMOptxp = zeros(length(t2),length(Exp),length(L),length(H)); % total metabolic rate of fish bite-feeding at optimal swimming speed (J/h/(g fish))
Nprof = zeros(length(L),length(H)); % net profitability of prey (net energy gained per handling time) (J/h/(g fish))

% Loop 1 over time (individual fish represents the average of the whole school)

for tstep = 1:ntstep % loop over different timesteps
    for vE = 1:length(Exp) % loop over different light intensities (µE/m^2/s)
        for vL = 1:length(L) % loop over different fish lengths (m)
            for vB = 1:length(vBite) % loop over different swimming speeds (m/s)
                for vH = 1:length(H) % loop over different handling time values (s/ind.)
                    for preyC = 1 % loop over prey category

                        NOptxp1(1, :, :, :) = N1xp(preyc); % initial prey density (ind./m^3)

                        Rxp(vE,vL) = getr(BeamAtt,Ctr,Ap,EM(vL),Ke,Exp(vE)); % visual range of fish (m), call SUBROUTINE GETR() (Aksnes and Utne, 1997)
                        Bxp(vE,vL,vB) = vBite(vB)*pi*(Rxp(vE,vL)*sind(Theta))^2; % search rate of fish (m^3/s) (Huse and Fiksen, 2010)
                        binxp(tstep,vE,vL,vB,vH) = NOptxp1(tstep,vE,vL,vH)*Bxp(vE,vL,vB)*Pc/(1 + NOptxp1(tstep,vE,vL,vH)*Bxp(vE,vL,vB)*h(vH));
                    % individuals eaten by each fish (ind./s)
                        bixp(tstep,vE,vL,vB,vH) = binxp(tstep,vE,vL,vB,vH)*w(preyc)*d(preyc); % absolute energy intake (J/s)
                        tSearchtxp = 1/(1 + NOptxp1(tstep,vE,vL,vH)*Bxp(vE,vL,vB)*h(vH)); % ratio of search time to total time
                end
            end
        end
    end
end

```

```

    buxp = bixp(tstep,vE,vL,vB,vH)*(1 - eg)*(1 - ex - sda); % mass-specific surplus energy intake (assimilated energy minus
excretion and SDA) (J/h/(g fish)) (Bachiller et al., 2018)
    bNixp(tstep,vE,vL,vB,vH) = buxp - bM(vB); % net specific energy intake (J/h/(g fish))
    [bNiOptxp(tstep,vE,vL,vH),vBindxp(tstep,vE,vL,vH)] = max(bNixp(tstep,vE,vL, :,vH), [],4); % net specific energy intake at
optimal swimming speed (J/h/(g fish)); index for optimal speed

    vBiteOptxp1(tstep,vE,vL,vH) = vBite(vBindxp(tstep,vE,vL,vH)); % optimal swimming speed of bite-feeding fish (m/s)
    BOptxp(tstep,vE,vL,vH) = Bxp(vE,vL,vBindxp(tstep,vE,vL,vH)); % search rate of fish swimming at optimal speed (m^3/s)
    biOptxp(tstep,vE,vL,vH) = bixp(tstep,vE,vL,vBindxp(tstep,vE,vL,vH),vH); % absolute energy intake at optimal swimming
speed (J/s)
    bMOptxp(tstep,vE,vL,vH) = bM(vBindxp(tstep,vE,vL,vH)); % total metabolic rate of fish bite-feeding at optimal swimming
speed (J/h/(g fish))
    bfOptxp(tstep,vE,vL,vH) = binxp(tstep,vE,vL,vBindxp(tstep,vE,vL,vH),vH)/NOptxp1(tstep,vE,vL,vH); % volume cleared for
prey by fish swimming at optimal speed (m^3/s)
    Nprof(vL,vH) = prof(vH)*3600/W(vL)*(1 - eg)*(1 - ex - sda) - bMOptxp(tstep,vE,vL,vH); % net profitability of prey (net
energy gained per handling time) (J/h/(g fish))

    if bNiOptxp(tstep,vE,vL,vH) > - Mroutine % if net intake rate is higher than routine metabolism...

        dNOptxp = binxp(tstep,vE,vL,vBindxp(tstep,vE,vL,vH),vH)*dtstep*60*nFish1(tstep)/V; % decrease in prey density during
timestep when fish swims at optimal speed (ind./m^3)
        NOptxp1(tstep + 1,vE,vL,vH) = max((NOptxp1(tstep,vE,vL,vH) - dNOptxp),0); % prey density at next timestep when fish
swims at optimal speed (ind./m^3)

    else

        NOptxp1(tstep + 1,vE,vL,vH) = NOptxp1(tstep,vE,vL,vH); % else, the fish has stopped feeding and prey density no longer
declines

    end

    end % prey category
    end % handling time
    end % swimming speeds
    end % fish lengths
    end % light intensities
end % timesteps

```

```

% Loop 2 over time (individual fish represents the average of only the feeding members of the school)

for tstep = 1:ntstep % loop over different timesteps
    for vE = 1:length(Exp) % loop over different light intensities ( $\mu\text{E}/\text{m}^2/\text{s}$ )
        for vL = 1:length(L) % loop over different fish lengths (m)
            for vB = 1:length(vBite) % loop over different swimming speeds (m/s)
                for vH = 1:length(H) % loop over different handling time values (s/ind.)
                    for preyC = 1 % loop over prey category

                        NOptxp2(1, :, :, :) = N1xp(prexC); % initial prey density (ind./m3)

                        Rxp(vE, vL) = getr(BeamAtt, Ctr, Ap, EM(vL), Ke, Exp(vE)); % visual range of fish (m), call SUBROUTINE GETR() (Aksnes and
                        Utne, 1997)
                        Bxp(vE, vL, vB) = vBite(vB)*pi*(Rxp(vE, vL)*sind(Theta))^2; % search rate of fish (m3/s) (Huse and Fiksen, 2010)
                        binxp(tstep, vE, vL, vB, vH) = NOptxp2(tstep, vE, vL, vH)*Bxp(vE, vL, vB)*Pc/(1 + NOptxp2(tstep, vE, vL, vH)*Bxp(vE, vL, vB)*h(vH));
                    % individuals eaten by each fish (ind./s)
                        bixp(tstep, vE, vL, vB, vH) = binxp(tstep, vE, vL, vB, vH)*w(prexC)*d(prexC); % absolute energy intake (J/s)
                        tSearchtxp = 1/(1 + NOptxp2(tstep, vE, vL, vH)*Bxp(vE, vL, vB)*h(vH)); % ratio of search time to total time
                        buxp = bixp(tstep, vE, vL, vB, vH)*(1 - eg)*(1 - ex - sda); % mass-specific surplus energy intake (assimilated energy minus
                        excretion and SDA) (J/h/(g fish)) (Bachiller et al., 2018)
                        bNixp(tstep, vE, vL, vB, vH) = buxp - bM(vB); % net specific energy intake (J/h/(g fish))
                        [bNiOptxp(tstep, vE, vL, vH), vBindxp(tstep, vE, vL, vH)] = max(bNixp(tstep, vE, vL, :, vH), [], 4); % net specific energy intake at
                        optimal swimming speed (J/h/(g fish)); index for optimal speed

                        vBiteOptxp2(tstep, vE, vL, vH) = vBite(vBindxp(tstep, vE, vL, vH)); % optimal swimming speed of bite-feeding fish (m/s)
                        BOptxp(tstep, vE, vL, vH) = Bxp(vE, vL, vBindxp(tstep, vE, vL, vH)); % search rate of fish swimming at optimal speed (m3/s)
                        biOptxp(tstep, vE, vL, vH) = bixp(tstep, vE, vL, vBindxp(tstep, vE, vL, vH), vH); % absolute energy intake at optimal swimming
                        speed (J/s)
                        bMOptxp(tstep, vE, vL, vH) = bM(vBindxp(tstep, vE, vL, vH)); % total metabolic rate of fish bite-feeding at optimal swimming
                        speed (J/h/(g fish))
                        bfOptxp(tstep, vE, vL, vH) = binxp(tstep, vE, vL, vBindxp(tstep, vE, vL, vH), vH)/NOptxp2(tstep, vE, vL, vH); % volume cleared for
                        prey by fish swimming at optimal speed (m3/s)
                        Nprof(vL, vH) = prof(vH)*3600/W(vL)*(1 - eg)*(1 - ex - sda) - bMOptxp(tstep, vE, vL, vH); % net profitability of prey (net
                        energy gained per handling time) (J/h/(g fish))

                    if bNiOptxp(tstep, vE, vL, vH) > - Mroutine % if net intake rate is higher than routine metabolism...

```

```

        dNOptxp = binxp(tstep,vE,vL,vBindxp(tstep,vE,vL,vH),vH)*dtstep*60*nFish2(tstep,1)/V; % decrease in prey density during
timestep when fish swims at optimal speed (ind./m^3)
        NOptxp2(tstep + 1,vE,vL,vH) = max((NOptxp2(tstep,vE,vL,vH) - dNOptxp),0); % prey density at next timestep when fish
swims at optimal speed (ind./m^3)

    else

        NOptxp2(tstep + 1,vE,vL,vH) = NOptxp2(tstep,vE,vL,vH); % else, the fish has stopped feeding and prey density no longer
declines

    end

    end % prey category
    end % handling time
    end % swimming speeds
    end % fish lengths
    end % light intensities
end % timesteps

else % do not run loop above
end

%% FILTER-FEEDING MODEL (Artemia)

if fnotime == 1 % run loop below (intake rates at different prey densities and light intensities)

% Initialising matrices

fin = zeros(length(N),length(E),length(L),length(vFilter)); % individuals eaten by each fish (ind./s)
fi = zeros(length(N),length(E),length(L),length(vFilter)); % absolute energy intake (J/s)
fNi = zeros(length(N),length(E),length(L),length(vFilter)); % net specific energy intake (J/h/(g fish))
fNiOpt = zeros(length(N),length(E),length(L)); % net specific energy intake at optimal swimming speed (J/h/(g fish))
vFind = zeros(length(N),length(E),length(L)); % index for optimal speed

vFilterOpt = zeros(length(N),length(E),length(L)); % optimal swimming speed of filter-feeding fish (m/s)
fiOpt = zeros(length(N),length(E),length(L)); % absolute energy intake at optimal swimming speed (J/s)

```

```

ffOpt = zeros(length(N),length(E),length(L)); % volume cleared for prey by fish swimming at optimal speed (m^3/s)
feffOpt = zeros(length(N),length(E),length(L)); % filtration efficiency
fMOpt = zeros(length(N),length(E),length(L)); % metabolic rate of fish filter-feeding at optimal swimming speed (J/h/(g fish))

% Loop (time-independent)

for vN = 1:length(N) % loop over different prey densities (ind./m^3)
    for vE = 1:length(E) % loop over different light intensities (μE/m^2/s)
        for vL = 1:length(L) % loop over different fish lengths (m)
            for vF = 1:length(vFilter) % loop over different swimming speeds (m/s)
                for preyC = 2 % loop over prey category

                    fin(vN,vE,vL,vF) = vFilter(vF)*gAr(vL)*ft*Bf*N(vN)*Pe*r; % individuals eaten by each fish (ind./s) (Lovvorn, Baduini and
Hunt, 2001)
                    fi(vN,vE,vL,vF) = fin(vN,vE,vL,vF)*w(preyc)*d(preyc); % absolute energy intake (J/s)
                    fu = fi(vN,vE,vL,vF)*3600/W(vL)*(1 - eg)*(1 - ex - sda); % mass-specific surplus energy intake (assimilated energy minus
excretion and specific dynamic action) (J/h/(g fish)) (Bachiller et al., 2018)
                    fNi(vN,vE,vL,vF) = fu - fM(vF); % net specific energy intake (J/h/(g fish))
                    [fNiOpt(vN,vE,vL),vFind(vN,vE,vL)] = max(fNi(vN,vE,vL,:),[],4); % net specific energy intake at optimal swimming speed
(J/h/(g fish)); index for optimal speed

                    vFilterOpt(vN,vE,vL) = vFilter(vFind(vN,vE,vL)); % optimal swimming speed of filter-feeding fish (m/s)
                    fiOpt(vN,vE,vL) = fi(vN,vE,vL,vFind(vN,vE,vL)); % absolute energy intake at optimal swimming speed (J/s)
                    ffOpt(vN,vE,vL) = fin(vN,vE,vL,vFind(vN,vE,vL))/N(vN); % volume cleared for prey by fish swimming at optimal speed
(m^3/s)
                    feffOpt(vN,vE,vL) = ffOpt(vN,vE,vL)/(vFilter(vFind(vN,vE,vL))*gAr(vL)); % filtration efficiency
                    fMOpt(vN,vE,vL) = fM(vFind(vN,vE,vL)); % metabolic rate of fish filter-feeding at optimal swimming speed (J/h/(g fish))

                end % prey category
            end % swimming speeds
        end % fish lengths
    end % light intensities
end % prey densities

else % do not run loop above
end

```

```

if ftime == 1 % run loop below (simulation of feeding experiment with closed populations)

% Initialising matrices

NOptxp1 = zeros(length(t2),length(Exp),length(L)); % prey density when fish swims at optimal speed (ind./m^3) (loop 1)
NOptxp2 = zeros(length(t2),length(Exp),length(L)); % prey density when fish swims at optimal speed (ind./m^3) (loop 2)

finxp = zeros(length(t2),length(Exp),length(L),length(vFilter)); % individuals eaten by each fish (ind./s)
fixp = zeros(length(t2),length(Exp),length(L),length(vFilter)); % absolute energy intake (J/s)
fNixp = zeros(length(t2),length(Exp),length(L),length(vFilter)); % net specific energy intake (J/h/(g fish))
fNiOptxp = zeros(length(t2),length(Exp),length(L)); % net specific energy intake at optimal swimming speed (J/h/(g fish))
vFindxp = zeros(length(t2),length(Exp),length(L)); % index for optimal speed

vFilterOptxp1 = zeros(length(t2),length(Exp),length(L)); % optimal swimming speed of filter-feeding fish (m/s) (loop 1)
vFilterOptxp2 = zeros(length(t2),length(Exp),length(L)); % optimal swimming speed of filter-feeding fish (m/s) (loop 2)
fiOptxp = zeros(length(t2),length(Exp),length(L)); % absolute energy intake at optimal swimming speed (J/s)
fMOptxp = zeros(length(t2),length(Exp),length(L)); % metabolic rate of fish filter-feeding at optimal swimming speed (J/h/(g fish))
ffOptxp = zeros(length(t2),length(Exp),length(L)); % volume cleared for prey by fish swimming at optimal speed (m^3/s)
feffOptxp = zeros(length(t2),length(Exp),length(L)); % filtration efficiency

% Loop 1 over time (individual fish represents the average of the whole school)

for tstep = 1:ntstep % loop over different timesteps
    for vE = length(Exp) % loop over different light intensities (µE/m^2/s)
        for vL = 1:length(L) % loop over different fish lengths (m)
            for vF = 1:length(vFilter) % loop over different swimming speeds (m/s)
                for preyC = 2 % loop over prey category

                    NOptxp1(1, :, :) = N1xp(preyc); % initial prey density (ind./m^3)

                    finxp(tstep, vE, vL, vF) = vFilter(vF) * gAr(vL) * ft * Bf * NOptxp1(tstep, vE, vL) * Pe * r; % individuals eaten by each fish (ind./s)
                    (Lovvorn, Baduini and Hunt, 2001)
                    fixp(tstep, vE, vL, vF) = finxp(tstep, vE, vL, vF) * w(preyc) * d(preyc); % absolute energy intake (J/s)
                    fuxp = fixp(tstep, vE, vL, vF) * 3600 / W(vL) * (1 - eg) * (1 - ex - sda); % mass-specific surplus energy intake (assimilated
                    energy minus excretion and specific dynamic action) (J/h/(g fish)) (Bachiller et al., 2018)
                    fNixp(tstep, vE, vL, vF) = fuxp - fM(vF); % net specific energy intake (J/h/(g fish))

```



```

    [fNiOptxp(tstep,vE,vL),vFindxp(tstep,vE,vL)] = max(fNixp(tstep,vE,vL,:),[],4); % net specific energy intake at optimal
swimming speed (J/h/(g fish)); index for optimal speed

    vFilterOptxp1(tstep,vE,vL) = vFilter(vFindxp(tstep,vE,vL)); % optimal swimming speed of filter-feeding fish (m/s)
    fiOptxp(tstep,vE,vL) = fixp(tstep,vE,vL,vFindxp(tstep,vE,vL)); % absolute energy intake at optimal swimming speed (J/s)
    fMOptxp(tstep,vE,vL) = fM(vFindxp(tstep,vE,vL)); % metabolic rate of fish filter-feeding at optimal swimming speed
(J/h/(g fish))
    ffOptxp(tstep,vE,vL) = finxp(tstep,vE,vL,vFindxp(tstep,vE,vL))/NOptxp1(tstep,vE,vL); % volume cleared for prey by fish
swimming at optimal speed (m^3/s)
    feffOptxp(tstep,vE,vL) = ffOptxp(tstep,vE,vL)/(vFilter(vFindxp(tstep,vE,vL))*gAr(vL)); % filtration efficiency

    if fNiOptxp(tstep,vE,vL) > - Mroutine % if net intake rate is higher than routine metabolism...

        dNOptxp = finxp(tstep,vE,vL,vFindxp(tstep,vE,vL))*dtstep*60*nFish1(tstep)/V; % decrease in prey density during timestep
when fish swims at optimal speed (ind./m^3)
        NOptxp1(tstep + 1,vE,vL) = max((NOptxp1(tstep,vE,vL) - dNOptxp),0); % prey density at next timestep when fish swims at
optimal speed (ind./m^3)

    else

        NOptxp1(tstep + 1,vE,vL) = NOptxp1(tstep,vE,vL); % else, the fish has stopped feeding and prey density no longer
declines

    end

    end % prey category
    end % swimming speeds
    end % fish lengths
    end % light intensities
end % timesteps

% Loop 2 over time (individual fish represents the average of only the feeding members of the school)

for tstep = 1:ntstep % loop over different timesteps
    for vE = length(Exp) % loop over different light intensities (μE/m^2/s)
        for vL = 1:length(L) % loop over different fish lengths (m)
            for vF = 1:length(vFilter) % loop over different swimming speeds (m/s)
                for preyC = 2 % loop over prey category

```

```

NOptxp2(1, :, :) = N1xp(preyc); % initial prey density (ind./m^3)

    finxp(tstep, vE, vL, vF) = vFilter(vF)*gAr(vL)*ft*Bf*NOptxp2(tstep, vE, vL)*Pe*r; % individuals eaten by each fish (ind./s)
(Lovvorn, Baduini and Hunt, 2001)
    finxp(tstep, vE, vL, vF) = finxp(tstep, vE, vL, vF)*w(preyc)*d(preyc); % absolute energy intake (J/s)
    fuxp = finxp(tstep, vE, vL, vF)*3600/W(vL)*(1 - eg)*(1 - ex - sda); % mass-specific surplus energy intake (assimilated
energy minus excretion and specific dynamic action) (J/h/(g fish)) (Bachiller et al., 2018)
    fNixp(tstep, vE, vL, vF) = fuxp - fM(vF); % net specific energy intake (J/h/(g fish))
    [fNiOptxp(tstep, vE, vL), vFindxp(tstep, vE, vL)] = max(fNixp(tstep, vE, vL, :), [], 4); % net specific energy intake at optimal
swimming speed (J/h/(g fish)); index for optimal speed

    vFilterOptxp2(tstep, vE, vL) = vFilter(vFindxp(tstep, vE, vL)); % optimal swimming speed of filter-feeding fish (m/s)
    fiOptxp(tstep, vE, vL) = finxp(tstep, vE, vL, vFindxp(tstep, vE, vL)); % absolute energy intake at optimal swimming speed (J/s)
    fMOptxp(tstep, vE, vL) = fM(vFindxp(tstep, vE, vL)); % metabolic rate of fish filter-feeding at optimal swimming speed
(J/h/(g fish))
    ffOptxp(tstep, vE, vL) = finxp(tstep, vE, vL, vFindxp(tstep, vE, vL))/NOptxp2(tstep, vE, vL); % volume cleared for prey by fish
swimming at optimal speed (m^3/s)
    feffOptxp(tstep, vE, vL) = ffOptxp(tstep, vE, vL)/(vFilter(vFindxp(tstep, vE, vL))*gAr(vL)); % filtration efficiency

    if fNiOptxp(tstep, vE, vL) > - Mroutine % if net intake rate is higher than routine metabolism...

        dNOptxp = finxp(tstep, vE, vL, vFindxp(tstep, vE, vL))*dtstep*60*nFish2(tstep, 2)/V; % decrease in prey density during
timestep when fish swims at optimal speed (ind./m^3)
        NOptxp2(tstep + 1, vE, vL) = max((NOptxp2(tstep, vE, vL) - dNOptxp), 0); % prey density at next timestep when fish swims at
optimal speed (ind./m^3)

    else

        NOptxp2(tstep + 1, vE, vL) = NOptxp2(tstep, vE, vL); % else, the fish has stopped feeding and prey density no longer
declines

    end

    end % prey category
    end % swimming speeds
    end % fish lengths
    end % light intensities

```

```

end % timesteps

else % do not run loop above
end

%% PLOTS

figure(1)
plot(t1,NOptxp1(:, :, :, :), 'LineWidth', 2, 'Color', [0.91 0.234 0.325]); hold on;
plot(t1,NOptxp2(:, :, :, :), 'LineWidth', 1, 'Color', [0.91 0.234 0.325]); hold on;
err = [5000, 1500, 180, 250, 250, 250, 180];
errorbar(t3, Nemp(:, 1), err, 'o', 'Color', [0.8500 0.3250 0.0980], 'MarkerFaceColor', [0.9290 0.6940 0.1250]);
xlim([-3, 62]);
ylim([-1*10^3, 15*10^3]);
ax = gca;
ax.YAxis.Exponent = 3;
xlabel('Time after food introduction (min)'); ylabel('Observed and predicted prey density (ind. m-3)');
legend({'Predicted (whole school)', 'Predicted (only feeding fish)', 'Observed'}, 'Location', 'northeast', 'FontSize', 8);
set(gca, 'box', 'off');
export_fig C:\Users\Admin\Documents\fig10.png -transparent -m2;

figure(2)
h1 = plot(t2, vBiteOptxp1(:, :, :, :)*100, 'LineWidth', 2, 'Color', [0.91 0.234 0.325]); hold on
plot(t2, vBiteOptxp2(:, :, :, :)*100, 'LineWidth', 1, 'Color', [0.91 0.234 0.325]); hold on
err = [0.07, 0.06, 0.08, 0.05, 0.07, 0.07, 0.07]*100;
h2 = errorbar(t3, vBiteEmp*100, err, 'o', 'Color', [0.8500 0.3250 0.0980], 'MarkerFaceColor', [0.9290 0.6940 0.1250]);
xlim([-3, 62]);
ylim([0, 70]);
xlabel('Time after food introduction (min)'); ylabel('Observed and predicted swimming speed (cm s-1)');
legend([h1, h2], {'Predicted', 'Observed'}, 'Location', 'northeast', 'FontSize', 8);
set(gca, 'box', 'off');
export_fig C:\Users\Admin\Documents\fig11.png -transparent -m2;

figure(3)
plot(t1, NOptxp1(:, :, :), '--', 'LineWidth', 2, 'Color', [0.1 0.4 0.7]); hold on;
plot(t1, NOptxp2(:, :, :), '--', 'LineWidth', 1, 'Color', [0.1 0.4 0.7]); hold on;
err = [5.5*10^4, 2.5*10^4, 2*10^4, 10^4, 9*10^3, 8*10^3, 8*10^3];

```

```

errorbar(t3,Nemp(:,2),err,'o','Color',[0.4940 0.1840 0.5560],'MarkerFaceColor',[0.9 0.7 1]);
xlim([-3,62]);
ylim([-40*10^3,900*10^3]);
ax = gca;
ax.YAxis.Exponent = 3;
xlabel('Time after food introduction (min)'); ylabel('Observed and predicted prey density (ind. m^{-3})');
legend({'Predicted (whole school)','Predicted (only feeding fish)','Observed'},'location','northeast','fontsize',9,'box','off');
set(gca,'box','off');
export_fig C:\Users\Admin\Documents\fig12.png -transparent -m2;

figure(4)
plot(t2,vFilterOptxp1(:, :, :)*100,'--','LineWidth',2,'Color',[0.1 0.4 0.7]); hold on
plot(t2,vFilterOptxp2(:, :, :)*100,'--','LineWidth',1,'Color',[0.1 0.4 0.7]); hold on
err = [0.06,0.07,0.05,0.02,0.03,0.07,0.04]*100;
errorbar(t3,vFilterEmp*100,err,'o','Color',[0.4940 0.1840 0.5560],'MarkerFaceColor',[0.9 0.7 1]);
xlim([-3,62]);
ylim([0,70]);
xlabel('Time after food introduction (min)'); ylabel('Observed and predicted swimming speed (cm s^{-1})');
legend({'Predicted (whole school)','Predicted (only feeding fish)','Observed'},'location','northeast','fontsize',9,'box','off');
set(gca,'box','off');
export_fig C:\Users\Admin\Documents\fig13.png -transparent -m2;

```

APPENDIX 3 – References MATLAB scripts

- Agersted, M. D. and Nielsen, T. G. (2014) 'Krill diversity and population structure along the sub-Arctic Godthåbsfjord, SW Greenland', *Journal of Plankton Research*. doi: 10.1093/plankt/fbt139.
- Aksnes, D. L. and Utne, A. C. W. (1997) 'A revised model of visual range in fish', *Sarsia*. doi: 10.1080/00364827.1997.10413647.
- Bachiller, E., Utne, K. R., Jansen, T. and Huse, G. (2018) 'Bioenergetics modeling of the annual consumption of zooplankton by pelagic fish feeding in the Northeast Atlantic', *PLoS ONE*. doi: 10.1371/journal.pone.0190345.
- Bagøien, E., Melle, W. and Kaartvedt, S. (2012) 'Seasonal development of mixed layer depths, nutrients, chlorophyll and *Calanus finmarchicus* in the Norwegian Sea - A basin-scale habitat comparison', *Progress in Oceanography*. doi: 10.1016/j.pocean.2012.04.014.
- Becker, G. A. and Pauly, M. (1996) 'Sea surface temperature changes in the North Sea and their causes', *ICES Journal of Marine Science*. doi: 10.1006/jmsc.1996.0111.
- Bednaršek, N., Mozina, J., et al. (2012) 'The global distribution of pteropods and their contribution to carbonate and carbon biomass in the modern ocean', *Earth System Science Data*. doi: 10.5194/essd-4-167-2012.
- Bednaršek, N., Tarling, G. A., et al. (2012) 'Population dynamics and biogeochemical significance of *Limacina helicina antarctica* in the Scotia Sea (Southern Ocean)', *Deep-Sea Research Part II: Topical Studies in Oceanography*. doi: 10.1016/j.dsr2.2011.08.003.
- Choquet, M. et al. (2018) 'Can morphology reliably distinguish between the copepods *Calanus finmarchicus* and *C. glacialis*, or is DNA the only way?', *Limnology and Oceanography: Methods*. doi: 10.1002/lom3.10240.
- Collette, B. B. and Nauen, C. E. (1983) 'FAO Species Catalogue: Vol. 2 Scombrids of the World', *FAO Fisheries Synopsis No. 125*.
- Davis, N. D. (1993) 'Caloric Content of Oceanic Zooplankton and Fishes for Studies of Salmonid Food Habits and Their Ecologically Related Species', *North Pacific Anadromous Fish Commission*.
- Davies, K. T. A., Ryan, A. and Taggart, C. T. (2012) 'Measured and inferred gross energy content in diapausing *Calanus* spp. in a Scotian shelf basin', *Journal of Plankton Research*. doi: 10.1093/plankt/fbs031.
- Davis, N. D., Meyers, K. W. and Ishida, Y. (1998) 'Caloric value of high-seas salmon prey organisms and simulated salmon ocean growth and prey consumption', *North Pacific Anadromous Fish Commission Bulletin* 1: 146–162.
- Davis, C. S. and Wiebe, P. H. (1985) 'Macrozooplankton biomass in a warm-core Gulf Stream ring: time series changes in size structure, taxonomic composition, and vertical distribution.', *Journal of Geophysical Research*. doi: 10.1029/JC090iC05p08871.
- Van Deurs, M., Jørgensen, C. and Fiksen, O. (2015) 'Effects of copepod size on fish growth: A model based on data for North Sea sandeel', *Marine Ecology Progress Series*. doi: 10.3354/meps11092.
- Dorval, E. et al. (2015) 'Changes in growth and maturation parameters of Pacific sardine *Sardinops sagax* collected off California during a period of stock recovery from 1994 to 2010', *Journal of Fish Biology*. doi: 10.1111/jfb.12718.
- Dunbrack, R. L. and Dill, L. M. (1984) 'Three-Dimensional Prey Reaction Field of the Juvenile Coho Salmon (*Oncorhynchus kisutch*)', *Canadian Journal of Fisheries and Aquatic Sciences*. doi: 10.1139/f84-139.
- Elliott, J. M. and Davison, W. (1975) 'Energy equivalents of oxygen consumption in animal energetics', *Oecologia*. doi: 10.1007/BF00345305.
- Giske, J. and Aksnes, D. L. (1992) 'Ontogeny, season and trade-offs: Vertical distribution of the mesopelagic fish *maurolicus muelleri*', *Sarsia*. doi: 10.1080/00364827.1992.10413510.
- Glass, C. W., Wardle, C. S. and Mojsiewicz, W. R. (1986) 'A light intensity threshold for schooling in the Atlantic mackerel, *Scomber scombrus*', *Journal of Fish Biology*. doi: 10.1111/j.1095-8649.1986.tb05000.x.
- Hirche, H. J. et al. (1994) 'The Northeast Water polynya, Greenland Sea - III. Meso- and macrozooplankton distribution and production of dominant herbivorous copepods during spring', *Polar Biology*. doi: 10.1007/BF00239054.
- Huse, G. and Fiksen, Ø. (2010) 'Modelling encounter rates and distribution of mobile predators and prey', *Progress in Oceanography*. doi: 10.1016/j.pocean.2009.09.011.
- James, D. A. et al. (2012) 'A generalized model for estimating the energy density of invertebrates', *Freshwater Science*. doi: 10.1899/11-057.1.
- Johnstone, A. D. F., Wardle, C. S. and Almatar, S. M. (1993) 'Routine respiration rates of Atlantic mackerel, *Scomber scombrus* L., and herring, *Clupea harengus* L., at low activity levels', *Journal of Fish Biology*. doi: 10.1111/j.1095-8649.1993.tb00314.x.
- Kulka, D. W. and Corey, S. (1982) 'Length and Weight Relationships of Euphausiids and Caloric Values of *Meganycitphanes Norvegica* (M. Sars) in the Bay of Fundy', *Journal of Crustacean Biology*. doi: 10.2307/15

48004.

- Leger, P. *et al.* (1986) 'The use and nutritional value of *Artemia* as a food source', *Oceanogr.Mar.Biol.Ann.Rev.* doi: 10.1673/031.011.14601.
- Lovvorn, J. R., Baduini, C. L. and Hunt, G. L. (2001) 'Modeling underwater visual and filter feeding by planktivorous shearwaters in unusual sea conditions', *Ecology*. doi: 10.1890/0012-9658(2001)082[2342:MUVAFF]2.0.CO;2.
- MacKay, K.T. (1979) 'Synopsis of biological data of the northern population Atlantic mackerel (*Scomber scombrus*)' *Fisheries and Marine Service Technical Report #885*, St. Andrews, NB.
- Macy, W. K., Sutherland, S. J. and Durbin, E. G. (1998) 'Effects of zooplankton size and concentration and light intensity on the feeding behavior of Atlantic mackerel *Scomber scombrus*', *Marine Ecology Progress Series*. doi: 10.3354/meps172089.
- Mobley, C. D. (1994) *Light and Water : Radiative Transfer in Natural Waters, Light and Water : Radiative Transfer in Natural Waters*. doi: 10.1002/9781118622179.
- Molina, R. E., Manrique, F. A. and Velasco, H. E. (1996) 'Filtering apparatus and feeding of the pacific mackerel (*Scomber japonicus*) in the Gulf of California', *California Cooperative Oceanic Fisheries Investigations Reports*.
- Muus, B.J. and Nielsen, J.G. (1999) *Sea fish. Scandinavian Fishing Year Book*, Hedehusene, Denmark. 340 p.
- Nøttestad, L., Diaz, J., Penã, H., Søiland, H., Huse, G. and Fernø, A. (2016) 'Feeding strategy of mackerel in the Norwegian Sea relative to currents, temperature, and prey', *ICES Journal of Marine Science*. doi: 10.1093/icesjms/fsv239.
- Pepin, P., Koslow, J. A. and Pearre Jr., S. (1988) 'Laboratory Study of Foraging by Atlantic Mackerel, *Scomber scombrus*, on Natural Zooplankton Assemblages', *Canadian Journal of Fisheries and Aquatic Sciences*. doi: 10.1139/f88-106.
- Percy, J. A. and Fife, F. J. (1981) 'The Biochemical Composition and Energy Content of Arctic Marine Macrozooplankton', *ARCTIC*. doi: 10.14430/arctic2533.
- Radach, G. and Pätsch, J. (1997) 'Climatological annual cycles of nutrients and chlorophyll in the North Sea', *Journal of Sea Research*. doi: 10.1016/S1385-1101(97)00048-8.
- Schaafsma, F. L. *et al.* (2018) 'Review: the energetic value of zooplankton and nekton species of the Southern Ocean', *Marine Biology*. doi: 10.1007/s00227-018-3386-z.
- Sirenko, B.I., Clarke, C., Hopcroft, R.R., Huettmann, F., Bluhm, B.A. and Gradinger, R. (eds) (2019) '*The Arctic Register of Marine Species (ARMS) compiled by the Arctic Ocean Diversity (ArcOD)*'. Accessed at <http://www.marinespecies.org/arms> on 2019-09-22.
- Stewart, D. J. *et al.* (2009) 'An Energetics Model for Lake Trout, *Salvelinus namaycush*: Application to the Lake Michigan Population', *Canadian Journal of Fisheries and Aquatic Sciences*. doi: 10.1139/f83-091.
- Utne, K. R. *et al.* (2012) 'Estimating the consumption of *Calanus finmarchicus* by planktivorous fish in the Norwegian Sea using a fully coupled 3D model system', *Marine Biology Research*. doi: 10.1080/17451000.2011.642804.
- Utne-Palm, A. C. (1999) 'The effect of prey mobility, prey contrast, turbidity and spectral composition on the reaction distance of *Gobiusculus flavescens* to its planktonic prey', *Journal of Fish Biology*. doi: 10.1006/jfbi.1999.0961.
- Uye, S. ichi (1982) 'Length-weight relationships of important zooplankton from the Inland Sea of Japan', *Journal of the Oceanographical Society of Japan*. doi: 10.1007/BF02110286.
- Varpe, Ø. and Fiksen, Ø. (2010) 'Seasonal plankton-fish interactions: Light regime, prey phenology, and herring foraging', *Ecology*. doi: 10.1890/08-1817.1.
- Varpe, Ø., Fiksen, Ø. and Slotte, A. (2005) 'Meta-ecosystems and biological energy transport from ocean to coast: The ecological importance of herring migration', *Oecologia*. doi: 10.1007/s00442-005-0219-9.
- Visser, A. W. and Fiksen, O. (2013) 'Optimal foraging in marine ecosystem models: Selectivity, profitability and switching', *Marine Ecology Progress Series*. doi: 10.3354/meps10079.